Designing Productive Assembly System Configurations Based on Hierarchical Subassembly Decomposition with Application to Automotive Battery Packs

by

Sha Li

A dissertation submitted in partial fulfillment
of the requirements for the degree of
Doctor of Philosophy
(Mechanical Engineering)
in The University of Michigan
2012

DEDICATION

To my family

ACKNOWLEDGEMENTS

I would like to first thank my advisor, Professor Jack Hu, for recruiting and mentoring me. Without his encouragement and discovery, I would not be able to apply for and get admitted to the world class engineering school at the University of Michigan. Without his guidance and support, I would not be able to accomplish what I have done in graduate school. His great vision, vast knowledge, invaluable inspiration and inquisitive questions have given me wisdom and strength to continue my research. His enormous patience and persistent confidence in me supported me when my progress stalled. Going through graduate school with him as an advisor have been a valuable process which will benefit me for a long time to come.

I would also like to thank all my committee members for all their help. In particular, Professor Panos Y. Papalambros and Professor Judy Jin for their insights and suggestions on my dissertation; for being a great help throughout my faculty search application process; Dr. Hui Wang for not only providing guidance to me on the big picture, but also working with me in detailed programming side by side; Dr. Jeffrey Abell for giving me opportunities to work as an intern three times at General Motors, which help me gain many industry experiences and conduct application-based research. In addition, I want to thank my mentor at General Motors, Yhu-Tin Lin, for providing me his industrial insights, experience and expertise to my research.

I would like to thank all the group members in the Hu lab, past and present. They have made my graduate school life so much more enjoyable. I want to thank them all for their help and support, the great insights and valuable discussions.

Lastly and most importantly, I want to thank my family for their unconditional love and support. I want to thank my parents for always believing in me no matter what decisions I made. I want to thank my beloved husband, Wei, for always understanding and comforting me in the hard times; sharing my joy in the great times.

Thank you, my Lord, for everything you entrust me. The most important thing I have learned during these years in graduate school is that: No matter what, we have GOD with us. So love your family, love your friends and love life!

TABLE OF CONTENTS

LIST OF FIGURES

LIST OF TABLES

ABSTRACT

This thesis develops a systematic method to design assembly systems with hybrid configurations by considering the assembly hierarchy associated with product designs and their varieties and applies it for automotive battery packs. With the growing concern of fossil fuel depletion and climate change, high power and capacity lithium-ion batteries are being widely adopted in personal transportation systems. A large size battery pack usually has a hierarchical composition of components assembled in some repetitive patterns. A lot of battery designs are emerging on the market. They require different processes and equipment from cell to module assembly, but similar processes and equipment from module to pack assembly. Conventional assembly system with a serial configuration has limitations in coping with increasing demand and fast development of the battery products. There is a strong need to develop assembly systems with complex, non-serial (hybrid) configurations to deal with the challenges, e.g. a system layout with multiple branch lines that converge to a common assembly line. Such configurations could be asymmetric and allows for pre-assembly of different components on multiple lines simultaneously, thereby potentially enhancing the system throughput and reconfigurability, while effectively dealing with product variety.

Previous research has been focused on sequential task sequence generation but did not address the impact of product assembly hierarchy on configuration. Limited work exists addressing the line balancing problem on complex configuration. There is also a lack of research on non-serial system configuration design for both known and future product variants. Existing methods for designing complex system configuration do not consider equipment selection.

Based on graph theory and combinatorial mathematics, a new algorithm for analyzing the liaison topographic patterns in products is developed to identify optimal assembly/subassembly decompositions that link product designs to system configurations. Compared with the sequential method for system design, the integrated approach of concurrent assembly process planning, system balancing, equipment selection, and system configuration design leads to higher throughput performances. Meanwhile, a method is developed to model the impact of product variety on system configuration design by considering stochastic product mix changes. This research enhances the understanding of the complex interactions among product designs, product varieties, and assembly system configurations.

CHAPTER 1

INTRODUCTION

1.1 Motivation

In recent years, due to the concerns of fossil fuel depletion [1] and the environment, there is a demand for the development of fuel efficient and environmentally friendly personal transportation systems. Battery-powered electrical vehicles become one option. Among all battery technologies lithium-ion battery has several advantages over others because of its characteristics of high power and energy density, long cycle life and low environmental impact, which make li-ion battery attractive for automobile applications [2].

Cost-effective manufacturing of lithium-ion batteries for electrical and hybrid electrical vehicles (EV/HEV) has not yet been fully developed. Efficient, flexible, and reliable battery assembly automation is needed for the following two reasons: 1) A variety of new battery pack designs and their changing demand rates require the assembly system to be flexible and reconfigurable [3]; 2) The high current and voltage in battery cells, modules and packs require automatic assembly and material handling.

Conventional assembly systems were mostly developed with a serial configuration. Such configurations have limitations in coping with increasing demand

and fast development of the battery products. There is a strong need to develop assembly systems with non-serial configurations to deal with the challenges.

1.2 Assembly system design for automotive battery packs

Compared with lead-acid and nickel-metal hydride batteries, Li-ion batteries offer significantly higher energy density, lighter weight and longer cycle life, which are crucial to the operation of EVs [4].

For sufficient power and driving range, each EV needs hundreds or even thousands of battery cells assembled together into a large-sized battery pack. As shown in Figure 1-1, a large-size Li-ion battery pack is assembled together using modules with each module consisting of multiple cells that are electrically and mechanically connected for a specific electric power and energy capacity. Assembly in this way facilitates easy scale-up of battery packs and simplifies the control of battery functions. However, as shown in Figure 1-2, Figure 1-3, and Figure 1-4, battery assembly has to deal with multiple issues: (a) different battery cell types, such as prismatic or cylindrical cells, (b) different serial-parallel electrical connections, and (c) existence of the auxiliary members for thermal management as well as mechanical structure rigidity [5]. Automotive battery packs require the assembly of many cells in hierarchical, repetitive patterns as shown in Figure 1-5 [6]. Such a product design pattern impacts the design of assembly systems including assembly task design, assembly sequence planning, and equipment selection to accomplish the tasks. Variable rates of production are required in cell/component assembly, module assembly and pack assembly. Most of the current EV battery packs are believed to be assembled manually, which is slow, costly, and may produce inconsistent modules or stacks. The high current and voltage in battery cells, modules and packs also pose hazardous risk to human operators and manufacturing facility since the incoming cells are at their 40%~50% state-of-charge level and cannot be fully discharged before assembly [7-8]. Therefore a battery module/pack assembly system for integrating multiple cell components together should have high speed and be responsive, flexible and reliable to the needs and for various types of batteries with different designs.

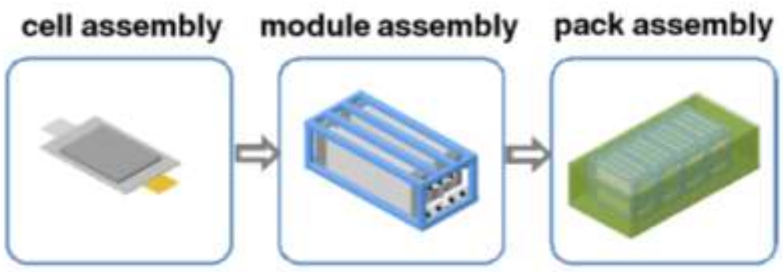

Figure 1-1 Battery cell, module and pack assembly

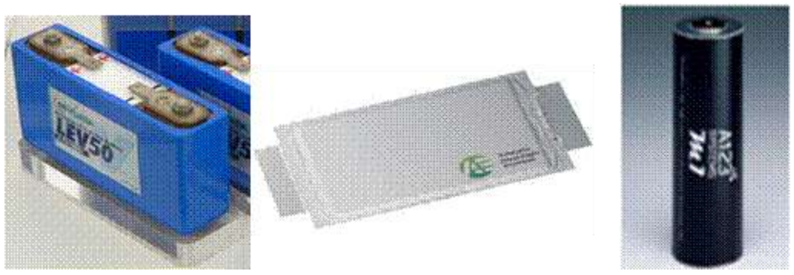

Figure 1-2 Different battery cell types [5]

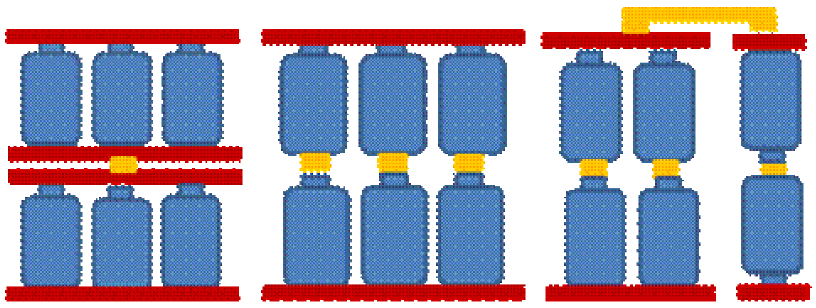

Figure 1-3 Different electrical connections (From left to right: first parallel, then serial; first serial, then parallel; hybrid (mixed serial & parallel)) [5]

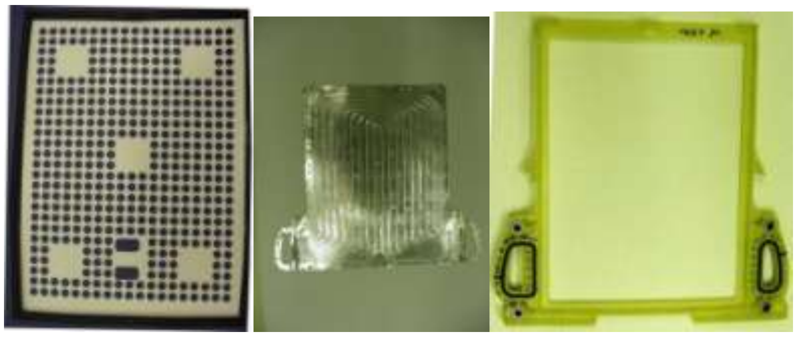

Figure 1-4 Auxiliary members: battery foam, cooling plate, battery frame [5]

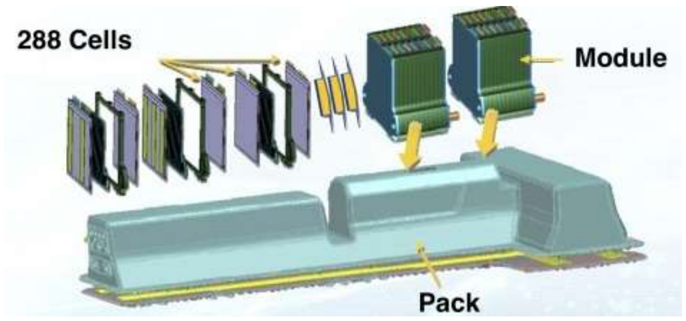

Figure 1-5 Battery cell and ancillary members and an example of battery stacking pattern (adopted from GM volt battery pack) [6]

In recent years, plenty of patents have been granted on the designs of module/pack configurations, thermal management system, and electrical connection. However, most of them are related to improving battery functions rather than addressing manufacturing issues. Li et al [5] conducted a review of available battery module/pack designs and investigated their implications to the automation of battery assembly. The associated assembly cost, efficiency, flexibility, quality issues were considered as well.

A lithium-ion battery pack usually has a hierarchical structure consisting of several modules with each module consisting of multiple battery cells and ancillary members, such as frames, cooling fins, and compression foams, as shown in Figure 1-5 [6]. Kurfer *et al* [9] investigated the stacking process of high-energy lithium-ion cells.

Tornow and Raatz [10] proposed a conceptual design for assembly (DFA) method for electric vehicle battery systems. However, systematic approaches do not yet exist for addressing the relationship between battery module/pack configurations and battery assembly processes.

Traditionally, an assembly system adopts a symmetric configuration such as a serial line, a parallel system, a serial system with parallel stations and a parallel system with serial stations (Figure 1-6). There also exist more complex configurations such as an asymmetric hybrid configuration with subassembly branch lines (Figure 1-7). Under this configuration, different tasks are independently performed at the different branches, i.e., preassembling different components into subassemblies at different branches. Then the different subassemblies are fed to an assembly station which processes the finished modules. Such a system could also have parallel stations which process identical tasks as in the traditional assembly system for scalability requirements. High-volume production of diverse battery products requires the assembly system with complex (hybrid) configurations in the future because of the unique features of battery assembly process: cell-module assembly requires different process and equipment among different battery products, while module to pack assembly is quite similar across different products, which allows sharing of some branches in the assembly system. Such a hybrid configuration could be more adaptive to product variety and potentially improve system throughput. The system can also be very conveniently reconfigured by adding or removing branches. But very little research has addressed such complex assembly system design problem including task/sequence generation, configuration design, line balancing and equipment selection [11].

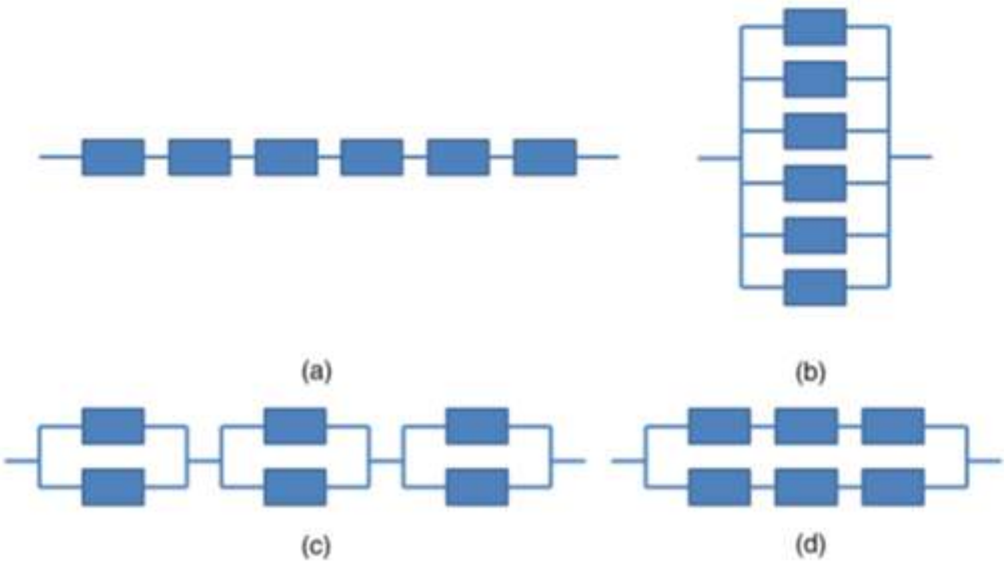

Figure 1-6 Symmetric configurations (squares represent machines)

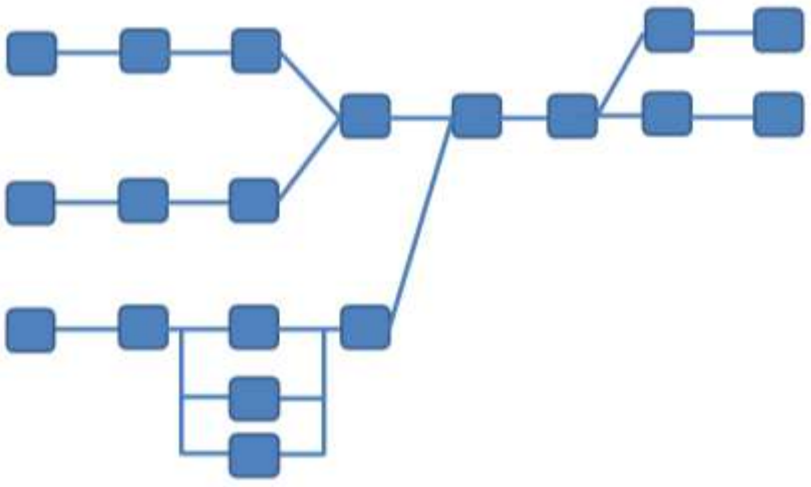

Figure 1-7 An example of an asymmetric configuration

Currently, the industrial assembly system design starts from process planning which includes assembly task identification and sequence generation. Then the assembly system configuration is generated. However, since the process planning and system configuration generation influence each other, the traditional sequential procedure may lead to suboptimal system solutions. This interaction can be illustrated with an example of automotive battery assembly. Figure 1-8 shows two possible ways of assembling four battery components into a module. Figure 1-8(a) shows the sequential way: the first two components are assembled first and the other components are loaded and assembled sequentially. Figure 1-8(b) shows a hybrid line where two components can be pre-assembled into subassemblies which in turn are assembled with the other subassembly to form the final product. By allowing for concurrent tasks and operations, hybrid configurations may be more suitable for dealing with products assembled in a hierarchy and potentially enhance the system throughput. However, if the process planning in Figure 1-8(a) were chosen at the beginning, the branch line layout would never be derived and the system throughput might never reach the optimal level.

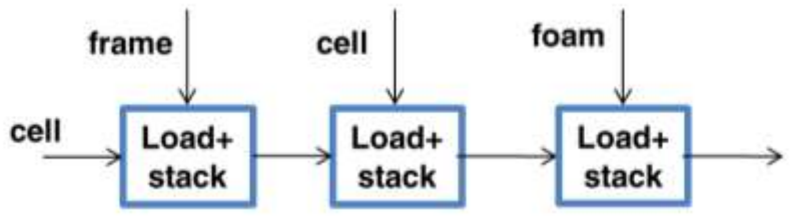

(a)

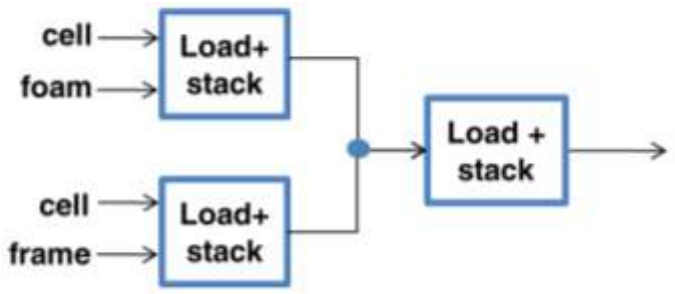

(b)

Figure 1-8 Two possible ways of assembly process planning and configuration generation given product design

Another common practice is that the system configuration is implemented for current generations of products under a fixed demand requirement without considering the needs of generational changes. The changes can be 1) in the demand due to changes of customer preference; 2) in the variety due to advances of new technology. When the changes happen, the original system could be costly to reconfigure, resulting in the system being discarded. By taking the available but limited information of future products into consideration at the time of assembly system deployment, the time of product launch can be significantly shortened and the responsiveness and competitiveness of companies to dynamic market demands can be greatly enhanced. For example, a company's current strategy is to produce 100% type 1 first generation of battery packs to be employed in the electric vehicles (Figure 1-9). But the engineers also have some preliminary designs (Product type 2) for their second generation of battery packs. Figure 1-9 shows the possible system configuration options for multiple generations of products. The serial configuration (Figure 1-9(a)) may be the most cost effective way for assembling current generation product (product type 1) by adding one component at a time, but its reconfiguration effort and cost could be significant in order to produce both types of products. Assume that the hybrid configuration (Figure 1-9(b)), which involves subassembly branches, is adopted at the current production plan to produce product 1, then it may take less effort to convert the configuration to a system that is adaptable to both product 1 and product 2 (Figure 1-9(c)) than a serial configuration.

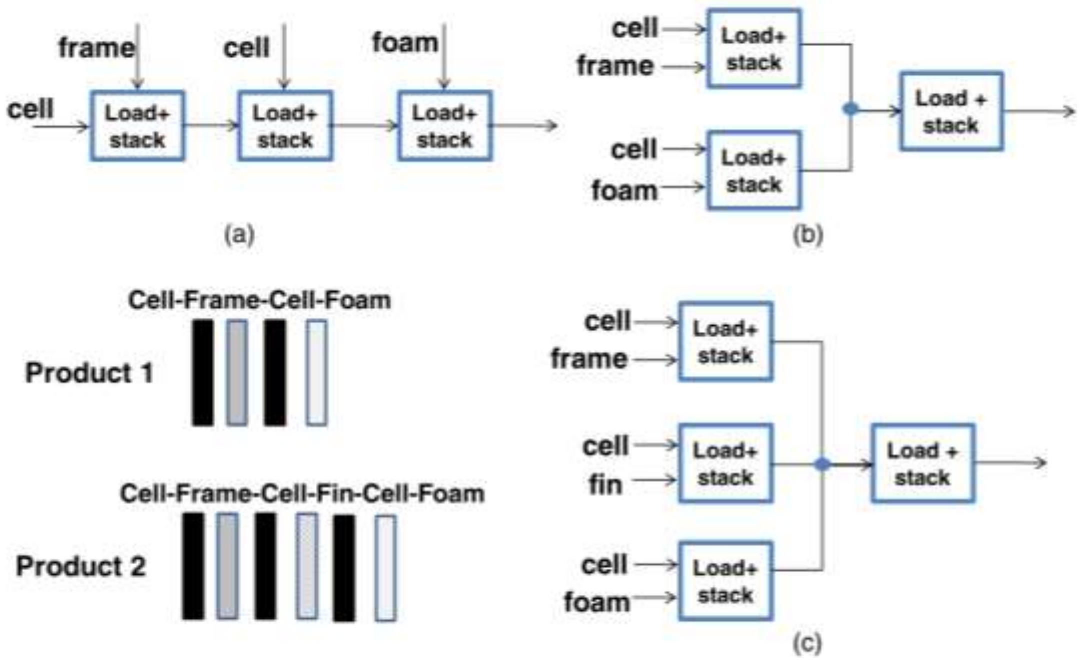

Figure 1-9 System configuration options for multiple generations of products

In balancing the assembly line with more than one product types, one major challenge is the "drift" problem caused by task variations associated with different products. Drift is defined as the deviation of system processing time from the nominal cycle time [12-13]. To more effectively deal with increased product variety, the assembly system can be set up with more complex, non-serial configurations, e.g., systems with multiple subassembly branch lines that converge to an assembly station. Such complex configurations allow for pre-assembly of different components on multiple lines simultaneously, thereby may potentially enhance the system productivity and reduce drift. However, there is a lack of research on non-serial system configuration design for product variety and the effect of such design on drift.

1.3 Research objective

The research objective of this thesis is to develop methods and algorithms for designing productive assembly system configurations by simultaneously considering product assembly hierarchy, product evolution, task and sequence generation, task assignment, and equipment selection for non-serial configurations. Figure 1-10 shows the inputs and outputs of such algorithms. The inputs are product design patterns, product varieties (denoted by P_1, P_2, … , P_N) and evolution. The outputs are system configuration design and equipment selection.

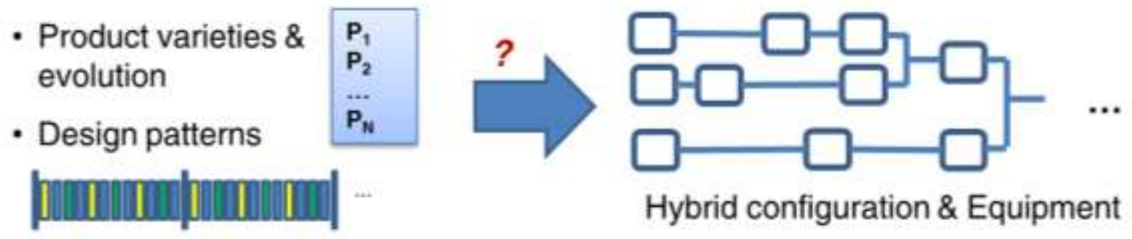

• Product varieties & evolution
• Design patterns
P1
P2
...
PN
?
Hybrid configuration & Equipment

Figure 1-10 Research objective

The specific research tasks are proposed below:

(1) *Subassembly decomposition method based on analysis of product liaison topographic patterns*

This research aims to 1) analyze the topographic patterns in general product design, including non-serially linked products, and to translate design information of products into the assembly/subassembly operations for assembly configuration generation [14]; and 2) develop a recursive algorithm to generate feasible subassembly pairs for serially linked products, such as automotive batteries, to enable efficient design and optimization of manufacturing system configuration [15]. The computational method provides a new and efficient way to enumerate all candidate tasks and sequences and enable the ensuing optimization process to result in the right solution.

(2) *Methodologies of joint process planning, system configuration selection, system balancing, and equipment selection*

The hierarchical composition of product design is utilized in generating system configurations with equipment selection for optimal assembly system design [16]. A nested framework is proposed to model the relationship between the product design and system configuration. The generated configurations are embedded in an optimal assembly system design problem for simultaneous equipment selection and task assignment to minimize equipment investment cost.

(3) *System configuration design for a product family*

A new method is developed for designing assembly system configurations for multiple products [14]. Unlike the system configuration for a family of products with delayed differentiation, the proposed configuration has diverse subassemblies in the upstream as required by the various battery components and has common assemblies in the downstream. The method enables efficient assembly of products with hierarchical structures.

(4) *Software development and industrial implementation: Battery Assembly System Configurator*

A software package for system configuration, *Battery Assembly System Configurator*, is developed to integrate functions of process planning and optimal system configuration generation given product information of the current and possible future generations of battery packs [17]. The system is being tested at an industrial site.

1.4 Dissertation organization

The thesis is organized as shown in Figure 1-11, in a multiple manuscript format. Chapter 2 first discusses the hierarchical subassembly decomposition method for complex configuration generation. A systematic approach is developed to translate product design patterns into assembly/subassembly operations that allow for parallel assembly sequences and adding more than one part at a time. In Chapter 3, a new method is developed and implemented for automatic system configuration generation with machine selection considering the hierarchical composition of battery components for a single product type. Chapter 4 presents a systematic method for designing system configurations for a family of products. Chapter 5 introduces the implementation of discussed methods: a math-based tool, *Assembly System Configurator*, for designing flexible battery assembly processes and systems.

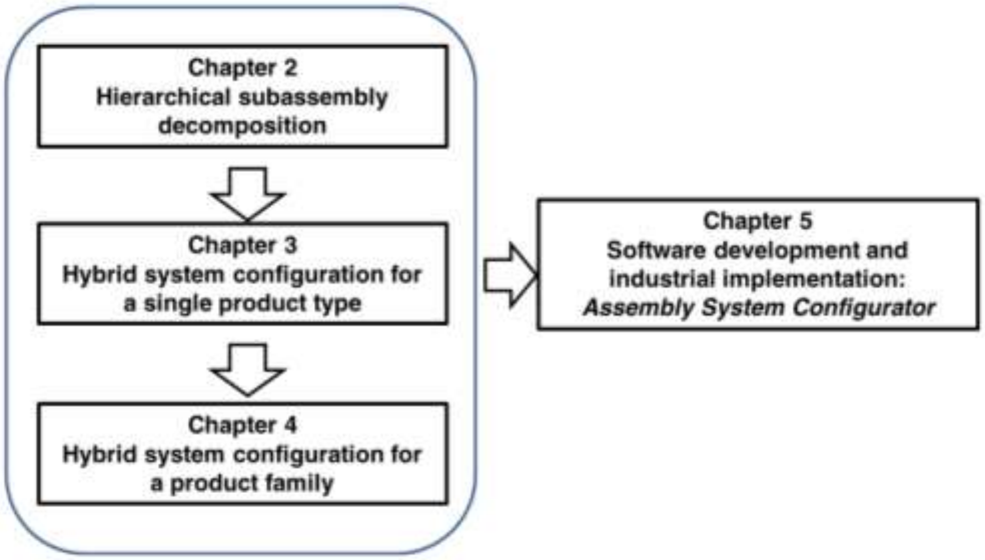
Chapter 2
Hierarchical subassembly decomposition
Chapter 3
Hybrid system configuration for a single product type
Chapter 4
Hybrid system configuration for a product family
Chapter 5
Software development and industrial implementation:
Assembly System Configurator

Figure 1-11 Organization of the dissertation

CHAPTER 2

AUTOMATIC HIERARCHICAL SUBASSEMBLY DECOMPOSITION FOR COMPLEX CONFIGURATION GENERATION

A computational method is developed to generate candidate assembly/subassembly operations automatically based on the analysis of liaison topographic patterns. The system configuration generation algorithms start with the identification of assembly layers. Then a recursive algorithm is developed to generate feasible subassembly groupings, assembly sequences, and configurations including hybrid configurations. The algorithm adopts the transformation of a typical system layout diagram into a string of characters or numbers representing assembly components and sequences of operations. The computational method provides a new and efficient way to enumerate all candidate system configurations and enable the ensuing optimization process to generate the right solution. This enables efficient design and optimization of manufacturing system configurations.

2.1 Introduction

In most manufactured products, their components are linked to each other following certain topographic patterns. Therefore, in production, assembly machines or workstations need to be arranged in proper processing sequence or flow on the factory floor such that individual components can be assembled efficiently. A system configuration represents the realization of this arrangement of machines and material flow among them.

As reviewed in Chapter 1, a lithium battery pack usually has a hierarchical structure consisting of several modules, while a module is composed of battery cells and ancillary members, such as frames, cooling fins, and compression foams. These components are usually assembled or stacked together in a certain pattern, such as frame-cell-foam-cell-cooling fin. In order to fulfill a vehicle's power requirement, this stacking pattern is repeated a number of times to form a module (Figure 1-5).

In production, an assembly workstation typically deals with unloading each individual component from its container and then loading it onto another component or a partially completed subassembly or stack. Figure 2-1 illustrates a few schematic diagrams of possible system configurations for the assembly operation: (a) a serial configuration, where each component is loaded and assembled at each station sequentially by an individual robot or material handling machine into a stacking pallet on a moving conveyor belt; (b) parallel configurations, where each robot is capable of picking and placing all components to complete a stack assembly; (c) a hybrid configuration with subassembly lines, where some components can be pre-stacked into subassemblies by one or more robots in branch lines, which are eventually merged to the main line according to the assembly sequence. A hybrid configuration is defined as a non-serial system layout, which has multiple branch lines and/or parallel stations. Conceivably, there are many other ways to design the system configurations by pre-stacking adjacent components into different subassemblies, which can be further assembled with other adjacent components or subassemblies into a larger module. As shown in Figure 2-1, a given product design pattern Frame-Cell-Foam-Cell-Fin could yield various subassembly groupings or assembly hierarchies and sequences such as ((((Frame-Cell)Foam)Cell)Fin) (Figure 2-1(a)), (Frame-Cell-Foam-Cell-Fin) (Figure 2-1(b))and ((Frame-Cell)(Foam-Cell)Fin) (Figure 2-1(c)) where the parenthesis represents a grouping of components into an assembly/subassembly task. The configuration in Figure 2-1(c) is a branched line, which is different from a parallel line (Figure 2-1(b)). Parallel line shares the same upstream resources, therefore, the components need to be split and fed into multiple parallel machines (Figure 2-1(b)). The subassembly branches in Figure 2-1(c) are independent and the components do not need to be split.

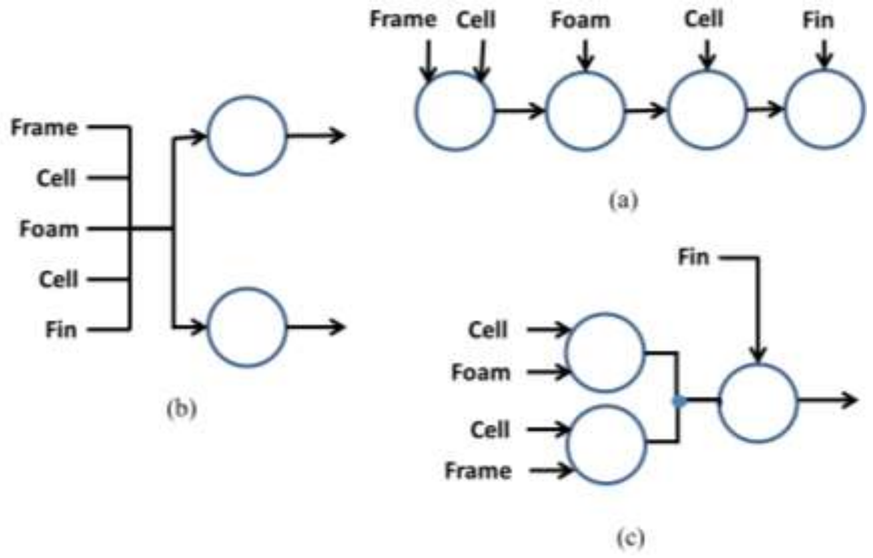

Figure 2-1 Varieties of system configurations: (a) serial, (b) parallel, (c) hybrid

Identifying all the candidate assembly/subassembly groupings and sequences is critical to system configuration design. Traditional assembly sequence generation methods focused on sequential task sequences. Among them, Bourjault [18] presented the first algorithm to generate all feasible assembly sequences. Building on Bourjault's method, Whitney [19] increased the size of the problem to accommodate assemblies with much higher number of components by asking two questions of precedence. A number of approaches, such as algorithms and graph based methods, have been used to generate the assembly sequences [20-23]. Methods were also developed to derive the assembly sequences from the disassembly sequences [24-25]. Traditional sequential task sequence based approach does not consider parallel subassembly tasks. By allowing for concurrent tasks and adding more than one part at a time, hybrid configurations are more suitable for dealing with products assembled in a hierarchy.

In essence, identifying the number of candidate assembly/subassembly groupings and sequences is an enumeration problem. The enumeration problem has been studied and applied to assembly sequence generation, manufacturing system configuration, as well as supply chain configurations. To facilitate enumeration problem solving, Webbink and Hu [26] enumerated system configurations by using parentheses to group a string of "1" characters, e.g., ((11)1) as shown in Figure 2-2. Each "1" character denotes a workstation and each pair of parentheses represents a path of processing line in a parallel-serial system configuration. Their work, however, does not distinguish the assembly sequences of ((11)1) and (1(11)), for instance, because all components are treated generically the same. Similar parentheses and alphanumerical coding are employed to create groups of product components or subassemblies in a supply chain configuration investigation by Wang et al. [27]. This method of transforming a diagrammatic system configuration into a binary string with parentheses is conveniently adopted in this study.

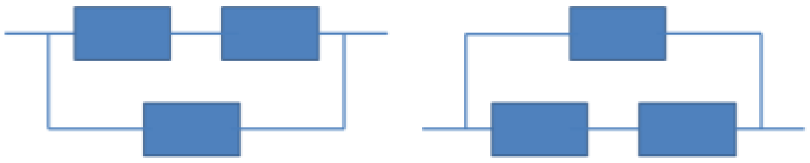

Figure 2-2 Layout diagrams of ((11)1)

De Fazio and Whitney [19] proposed the "liaison" concept for assembly sequence generation. A "liaison" is the connection between components, which represents the physical contact or joining between components. Each pair of connected components is assigned a liaison number. The enumeration problem is to identify the liaison or assembly sequences through a state-transition diagram arranged in an inverted tree form and determined by certain precedence rules. However, the work doesn't handle more than two components in one assembly workstation.

Likewise, Abell [28] developed a recursive algorithm to enumerate all possible sequences for robotic material handling systems in a general *m*-machine layout. The algorithm examines the system state space and generates all possible material handling sequences while eliminating redundant sequences. Still, enumeration of multiple part sequences is not considered.

Given a predetermined topographic pattern in product design, assembly/subassembly decomposition is to translate design information of products into the assembly/subassembly operations/tasks and to group assembly operations into a combination of single-operation and multi-operation machines arranged in series, parallel or mixed patterns. Therefore, the assembly/subassembly decomposition in this chapter is, mathematically speaking, a partition problem in combinatorics [29] or one of Stanley's Twelvefold Way of combinatorics [30], but with the assembly requirements of allowing more than two components in one station and parallel subassembly grouping, which had not been addressed before.

This chapter starts with an overview of the proposed method, and then explains the enumeration of assembly/subassembly grouping in detail. Hierarchical representations of assembly sequence are introduced. A recursive algorithm for assembly sequence generation is developed. The binary data tree or structure employed in representing the recursive algorithms of assembly/subassembly generation resembles that of integer partitions in combinatorics [29,31]. Furthermore, the computational method also includes a filtering function to accommodate other assembly constraints, such as "some adjacent components may or may not be preassembled", which could significantly reduce the number of candidate system layouts for practical handling. Lin [15] calculated the total number of candidate system configurations which helps validate the computational assembly/subassembly decomposition method that ensues in this chapter.

2.2 Method overview

In this chapter, a recursive method is developed in conjunction with a graph search algorithm to generate candidate assembly/subassembly groupings and sequences. The method can be described as follows.

Step 1: Identify branches (assembly layers) in the product liaison. Given a topographic pattern in product design (Figure 2-3), wherein nodes represent components/parts and lines between nodes represent relations (physical contact or joining) between components, the branches can be determined by two possible ways: 1) to use given engineering knowledge to determine the base module etc. For example, the predetermined unit/module/pack grouping; 2) to identify the graph diameter that is the longest path between two vertices in a graph as the first branch (assembly layer). Figure 2-4(a) shows the identification of longest path as assembly layer 1.

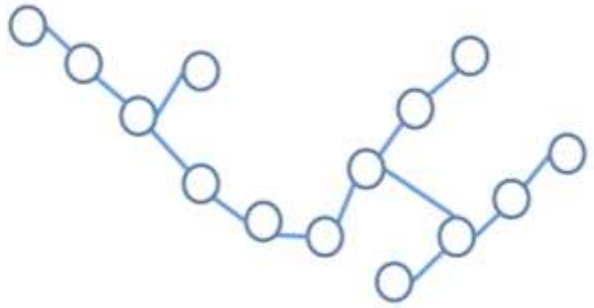

Figure 2-3 Liaison graph for a general product design

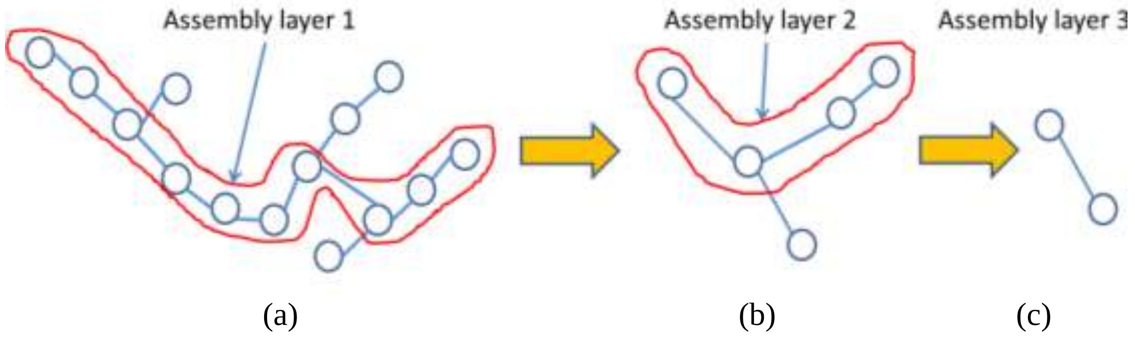

Figure 2-4 Assembly layer/branch identification

Step 2: Replace the identified branch with a node and return to Step 1, until there is only one assembly layer left (Figure 2-4(b)(c)).

Step 3: Apply subassembly decomposition algorithm to each assembly layer. The detailed algorithm will be discussed in section 2.3.

The procedure of identifying the longest path in a graph can be described as follows. First, a connection matrix is constructed. According to graph theory, the relationship showed in a liaison graph can be mapped one-to-one into a connection matrix $M = [m_{ij}]$ (Figure 2-5), where m_{ij}=1 when components i and j are directly connected and m_{ij}=0 when no connection exists between two components i and j or self-relationship. Second, start from any node (denoted by r) in the product liaison graph and perform depth-first search (DFS) algorithm [32] to identify the farthest node to r, denoted as v by $D_{T_r}(r, V(T_r)) = \max_{s \in child(r)} \{D_{T_s}(s, V(T_s)) + m(r,s)\}$, where T_r is the subtree rooted at vertex $r \in V$, which is the subgraph induced on vertex r and all its descendants; and child(r) is the set of children of v and *m(r,s)* is the distance associated with the arc connecting nodes r and s, which can be calculated using connection matrix. Then perform the DFS again to identify the fastest node(s) from the node v, denoted as v'. At last, the longest branch is obtained between v and v' (Figure 2-6).

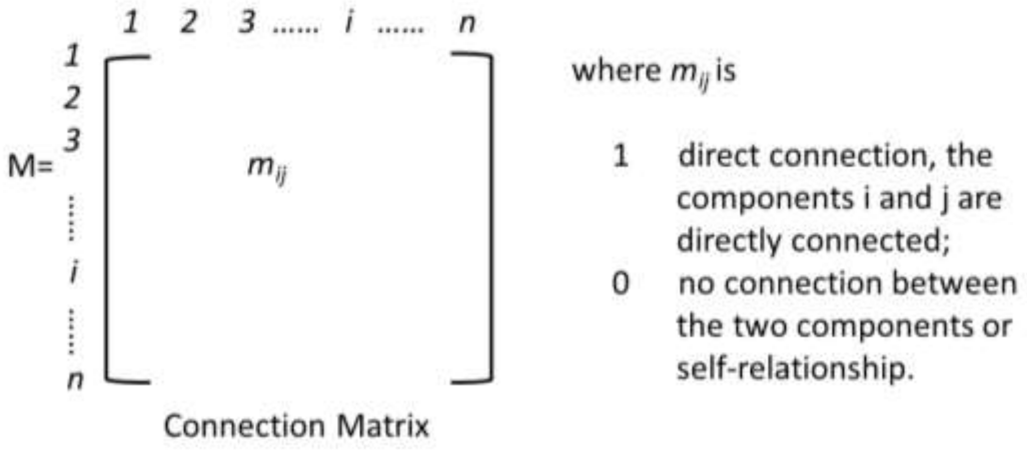

M=
1 2 3 ...... i ...... n
m_{ij}
Connection Matrix
where m_{ij} is
1 direct connection, the components i and j are directly connected;
0 no connection between the two components or self-relationship.

Figure 2-5 Connection matrix

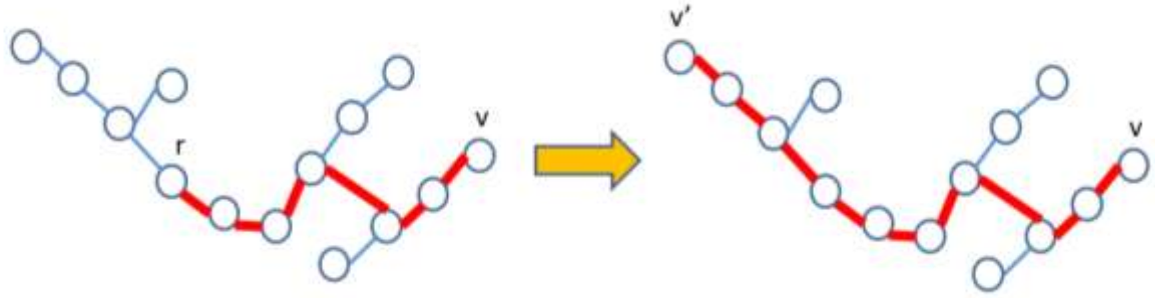

Figure 2-6 Depth-first search (DFS) algorithm to identify the longest path

2.3 Subassembly decomposition

2.3.1 Enumeration of subassembly grouping

Given an assembly of *n* elements $\{a_1, a_2, a_3, \ldots a_n\}$, the parenthesis operator, (.), is used to group two or more adjacent elements together, such as $(a_k a_{k+1})$, into a candidate subassembly. The subassembly can be further grouped with other elements, single or groups, to create larger groups, e.g., grouping of (a_1a_2) and a_3 leads to $((a_1a_2)a_3)$; and grouping of (a_4a_5) and (a_6a_7) yields $((a_4a_5)(a_6a_7))$. Thus, the generation of each set of subassembly combinations is the result of grouping elements at different levels, which is called hierarchical grouping in this chapter. The subassembly decomposition problem is to enumerate all the non-repetitive ways of hierarchically grouping *n* elements.

Denote $P(n)$ as the enumeration problem with *n* elements. The following steps summarize the subassembly grouping procedure.

Step 1: Enumerate all the non-repetitive cases for grouping two elements, such as $\{(a_1a_2)a_3 \ldots a_n\}$, $\{a_1(a_2a_3)\ldots a_n\}\ldots$ $\{a_1a_2a_3\ldots(a_{n-1}a_n)\}$. Only two elements are merged at a time, multiple two-element grouping, $\{(a_1a_2)a_3\ldots(a_{n-1}a_n)\}$ for example, is not allowed. Under each case, the grouped elements are treated as a subassembly and the enumeration problem degenerates into a $P(n\text{-}1)$ problem since there are n-1 elements left;

Step 2: Enumerate all the non-repetitive cases for grouping three elements, such as $\{(a_1a_2a_3)\ldots a_n\}$, … $\{a_1\ldots\ a_{n-3}\ (a_{n-2}a_{n-1}a_n)\}$. Under each case, the grouped elements are treated as a subassembly and the enumeration problem degenerates into a $P(n\text{-}2)$ problem since there are n-2 elements;

…

Step n-1: Enumerate the non-repetitive cases for grouping all n elements. Apparently, there is only one possible scenario, i.e., $(a_1, a_2, a_3, \ldots a_n)$.

It can be seen that solving a $P(n)$ problem involves n-1 steps. The *i*th step has two problems: (*i*) to enumerate all the non-repetitive cases for grouping i+1 elements and (*ii*) to solve a $P(n\text{-}i)$ problem. The idea is to decompose a complex problem $P(n)$ into n-1 degenerated problems in n-1 steps, and each degenerated problem is further decomposed into a number of simpler enumeration problems in hierarchical order or structure.

Similar to Whitney's assembly sequence generation methods [19], each letter $(a_1\ldots a_n)$ denotes a component and the aforementioned grouping represents any of certain user-defined relations between parts called "liaisons". From the inside-out grouping order, the assembly sequences are generated accordingly.

Table 2-1 Comparison between assembly sequences and physical representation of the enumerations

Case	Assembly Sequence	Physical Representation	Liaison Diagram	#of Liaisons
1	1→2→3	*(((AB)C)D)*	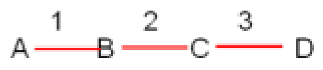	3
2	3→2→1	*(A(B(CD)))*		
3	2→1→3	*((A(BC))D)*		
4	3→1→2	*((AB)(CD))*		
5	1→3→2	*((AB)(CD))*		
6	2→3→1	*(A((BC)D))*		
7	[12]→3	*((ABC)D)*	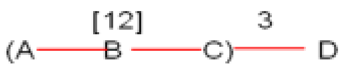	1
8	1→ [23]	*((AB)CD)*	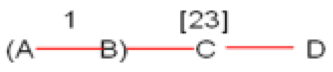	
9	[23] →1	*(A(BCD))*	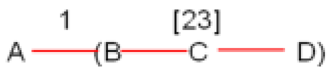	
10	3→ [12]	*(AB(CD))*	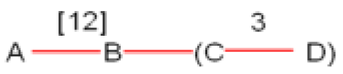	
11	2→ [13]	*(A(BC)D)*	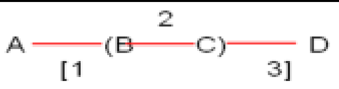	
12	[13] →2	*((AB)(CD))*	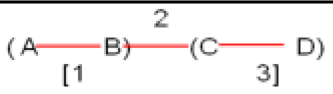	
13	[123]	*(ABCD)*	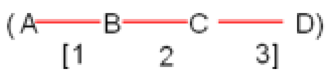	0

Table 2-1 shows an example of assembling four components {*A, B, C, D*} together. Compared with Whitney's assembly sequence generation methods, the differences can be summarized as the following:

- There is no sequence differentiation between parallel groups, thus enabling parallel subassembly grouping, sequences and configurations (See case 4 &5 in Table 2-1).
- Assembly grouping is hierarchical and considered at all levels. Not only components pairs can be assembled, groups of components, called subassemblies, can also be assembled (See case 7-13 in Table 2-1).

The enumeration process consists of the two major tasks below that will be addressed in the following sections:

- A data structure must be defined to facilitate assembly sequence representation and manipulation.
- An algorithm must be devised to generate all non-repetitive groupings given *i* elements. For example, in step 1, the same enumeration grouping $\{(a_1a_2)a_3\ldots(a_{n-1}a_n)\}$ exists when solving the $P(n-1)$ problem under the cases $\{(a_1a_2)a_3\ldots a_n\}$ and $\{a_1a_2a_3\ldots(a_{n-1}a_n)\}$.

2.3.2 Hierarchical representation of assembly sequence

To enable computational assembly sequence generation, it is more efficient to use numbers and numerical operations. By the fact that only neighboring components are grouped, the enumeration problem can be formulated as merging or adding the numerals in an identity array in various ways. For example, an identity array {1, 1, 1}, with each "1" denotes a component, can be merged into (1+1) +1, 1+ (1+1), or (1+1+1). The summed numbers within one set of parentheses stand for the components to be grouped. Table 2-2 shows the enumerations for grouping an identity array {1, 1, 1, 1} with four 1's in sequence corresponding to components *A*, *B*, *C*, and *D*, respectively. Compared with Table 2-1, since there is no sequence differentiation between parallel groups (Cases 4, 5 & 12 in Table 2-1 are the same), there are eleven possible assembly sequences generated based on our enumeration algorithm.

Table 2-2 Enumeration for Four Elements {*A*, *B*, *C*, *D*}

Enumeration index	Enumeration of number merging	Physical interpretation
1	(1+1)+1+1	*((AB)CD)*
2	((1+1)+1)+1	*(((AB)C)D)*
3	(1+1)+(1+1)	*((AB)(CD))*
4	1+(1+1)+1	*(A(BC)D)*
5	(1+(1+1))+1	*((A(BC))D)*
6	1+((1+1)+1)	*(A((BC)D))*
7	1+1+(1+1)	*(AB(CD))*
8	1+(1+(1+1))	*(A(B(CD)))*
9	(1+1+1)+1	*((ABC)D)*
10	1+(1+1+1)	*(A(BCD))*
11	(1+1+1+1)	*(ABCD)*

It can be seen that the numerical grouping can be represented in a hierarchical structure whereby the numbers are added at different recursive steps to be discussed later. An example of the hierarchy is given in Figure 2-7, where Figure 2-7(a) shows a sequence of grouping numbers under a data tree structure and Figure 2-7(b) shows a simplified structure by dropping redundant 1's. For clarity of illustration, the data tree structure of Figure 2-7(a) is used in the following description. The "+" sign can be omitted in all the representations of data structure and arrays since it is the only operator involved.

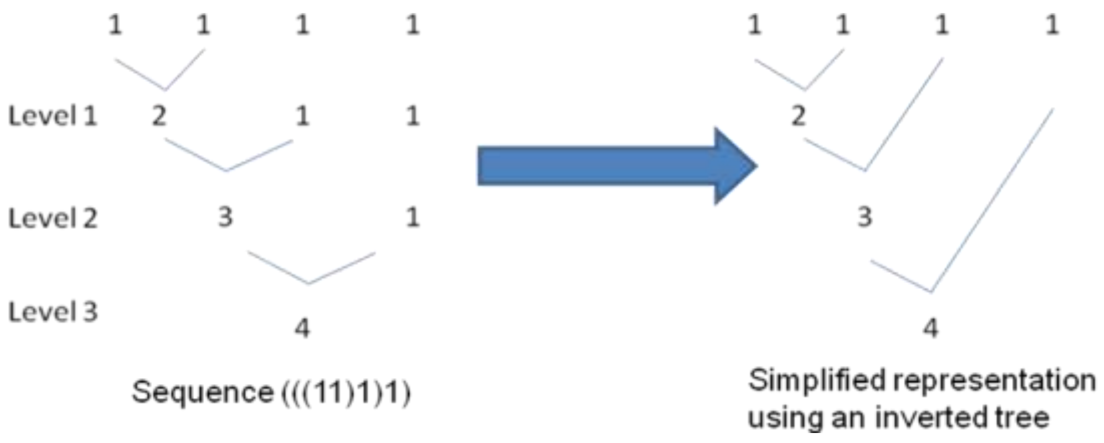

(a) (b)

Figure 2-7 Hierarchical representations of sequence (((11)1)1)

The hierarchical data structure can be characterized with a few parameters. Denote *m* as an index of the recursive steps. There are three recursive steps in Figure 2-7. In the recursive step *m* = 1, 2, 3, an internal array ***c***(*m*) is defined to represent the intermediate enumeration result, such as ***c***(1) = [2 1 1], ***c***(2) = [3 1]. The length of the internal array ***c***(*m*) is denoted as *n*(*m*) and *n*(0) = *n*. As shown in Figure 2-8, the window size parameter *win*(*m*) specifies the number of components to be grouped in the internal array ***c***(*m*), and the end position parameter *ep*(*m*) denotes the location of the last component in the grouping window of the internal array ***c***(*m*). Figure 2-9 shows the examples of using these parameters to represent the hierarchical data structure.

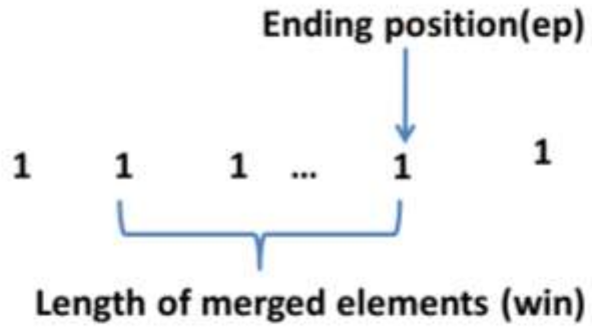

Figure 2-8 Parameters *ep*(*m*): end position (the location of the last component in the grouping window) and *win*(*m*): window size (number of components to be grouped)

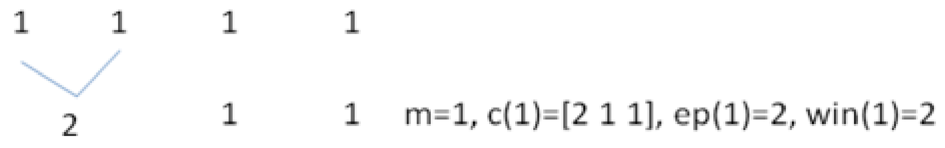

(a) Sequence ((11)11)

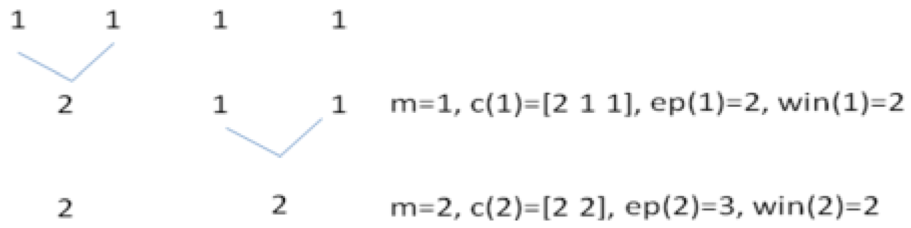
1 1 1 1
2 1 1
m=1, c(1)=[2 1 1], ep(1)=2, win(1)=2
2 2
m=2, c(2)=[2 2], ep(2)=3, win(2)=2

(b) Sequence ((11)(11))

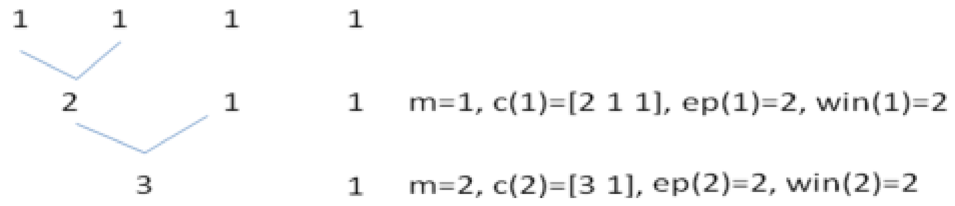
1 1 1 1
2 1 1
m=1, c(1)=[2 1 1], ep(1)=2, win(1)=2
3 1
m=2, c(2)=[3 1], ep(2)=2, win(2)=2

(c) Sequence (((11)1)1)

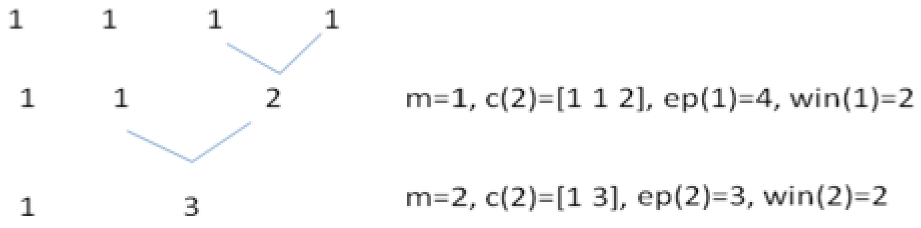
1 1 1 1
1 1 2
m=1, c(2)=[1 1 2], ep(1)=4, win(1)=2
1 3
m=2, c(2)=[1 3], ep(2)=3, win(2)=2

(d) Sequence (1(1(11)))

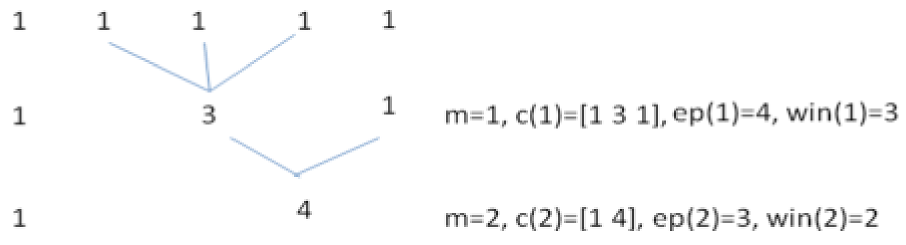
1 1 1 1 1
1 3 1
m=1, c(1)=[1 3 1], ep(1)=4, win(1)=3
1 4
m=2, c(2)=[1 4], ep(2)=3, win(2)=2

(e) Sequence (1((111)1))

Figure 2-9 Examples of characterizing hierarchical data structure with parameters

2.3.3 Recursive algorithm for assembly sequence generation

As mentioned above, there are *n*-1 steps involved in solving problem *P*(*n*) with each step using the same window size *win*(1), where *win*(1)=2,3,…*n* respectively. The increment in *win*(1) can be achieved by using a computational loop with respect to *win*(1). In step *win*(1)-1, one needs to solve two problems (*i*) the problem of enumerating all the non-repetitive cases for grouping *win*(1) elements, and (*ii*) the *P*(*n*(1)-*win*(1)+1) enumeration problem in the recursive step *m*=2 following the same procedures.

In the *m*th (*m*≥2) recursive step, one can have *n*(*m*)=*n*(*m*-1)-*win*(*m*-1)+1 and *win*(*m*)=2,3…*n*(*m*). The increment in *win*(*m*) can be achieved by using a computational loop of *win*(*m*). There are *n*(*m*)-1 steps involved to solve problem *P*(*n*(*m*)). In step *win*(*m*)-1, one needs to solve (*i*) the problem of enumerating all the non-repetitive cases for grouping *win*(*m*) elements and (*ii*) problem *P*(*n*(*m*)-*win*(*m*)+1) in the (*m*+1)th recursive step. The recursion continues until *n*(*m*)-*win*(*m*)+1<1, i.e., *n*(*m*)<*win*(*m*).

The problem (*i*) in the *m*th recursive step can be solved by moving a grouping window with a fixed length *win*(*m*) from left to right along the internal array *c*(*m*) as shown in Figure 2-10. Assume that the leftmost window ends at *ep0*(*m*). There are *n*(*m*)-*ep0*(*m*)+1 ways (windows) of groupings *win*(*m*) elements in the internal array *c*(*m*). The rightmost window ends at *n*(*m*).

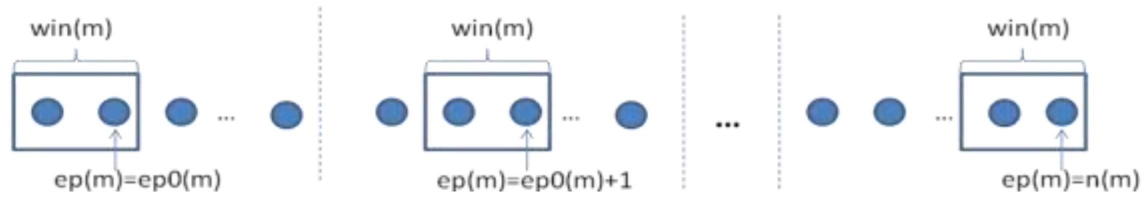

Figure 2-10 Shift of grouping window in enumeration process (*i*)

It is critical to determine the end position *ep0*(*m*) of the leftmost window. A proper selection of *ep0*(*m*) can effectively eliminate the repetitive enumerations. In Figure 2-11(a), the enumeration (*i*) when *ep*(*m*-1)=2 and (*ii*) when *ep*(*m*-1)>3 yield the same assembly sequence in the *m*th recursive step. Therefore, in enumeration (ii), the value of *ep0*(*m*) cannot be arbitrary. To avoid such a repetitive enumeration, selection of *ep0*(*m*) should ensure that in the *m*th recursive step, the enumeration starts from the group that is created in the (*m*-1)th recursive step. Such a group is generated by merging numbers with a window with a size of *win*(*m*-1) ending at the *ep*(*m*-1)th element in the internal array *c*(*m*-1). Since the position of the group in the internal array *c*(*m*) is *ep*(*m*-1)-*win*(*m*-1)+1, it can be concluded that *ep0*(*m*)=*ep*(*m*-1)-*win*(*m*-1)+1 as shown in Figure 2-11(b).

Hence, in the *m*th recursive step, the enumeration problem (*i*) is to explore all the possible combinations of the parameters *ep*(*m*) and *win*(*m*), which can be handled by a double-loop for the two parameters in computer programming.

All the generated assembly sequences can be converted into the string format with parentheses from the hierarchical structure parameters *c*(*m*), *ep*(*m*), *win*(*m*), and *n*(*m*) via a number decoding procedure as follows,

1) Replace each greater than 1 numeral in *c*(*m*) with string concatenation of 1's and add characters "2" before the string and "3" after the string to represent the left parenthesis and the right parenthesis respectively, e.g., 3 becomes concatenating string "2", "1", "1", "1", and "3".
2) Convert the strings to a cell or a number, e.g., "21113" is changed to 21113.

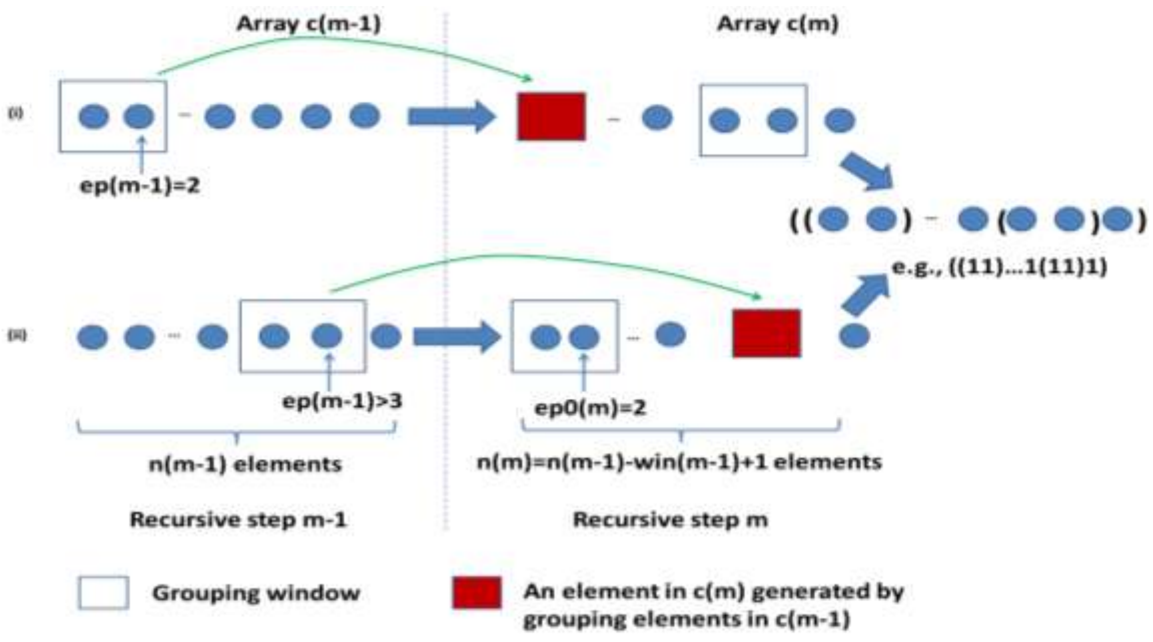

(a) Repetitive enumeration exists when (*i*) *ep*(*m*-1)=2 and (*ii*) *ep*(*m*-1)>3 yield the same assembly sequence in the *m*th recursive step

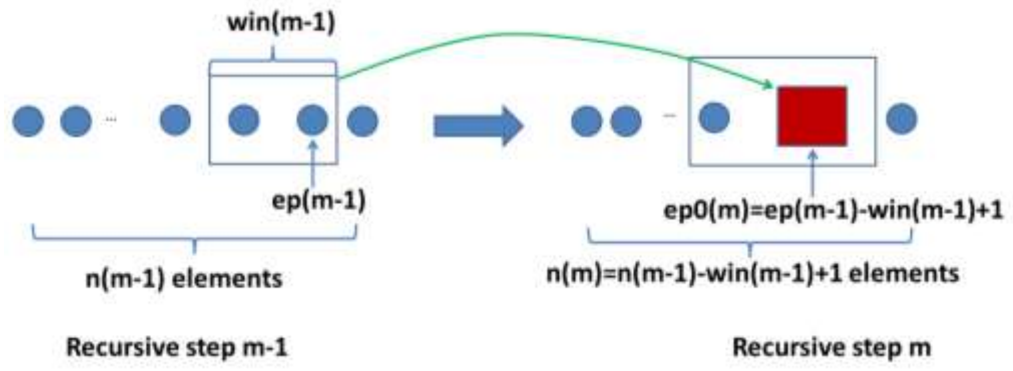

(b) Non-repetitive enumeration can be assured when the end position *ep0*(*m*)=*ep*(*m*-1)-*win*(*m*-1)+1

Figure 2-11 Determination of *ep0*(*m*)

3) Convert number to string, e.g., 21113 to (111), where 2 is replaced by "(" and 3 is replaced by ")". Lastly, all the 1's can be replaced by "a", "b", "c", etc. sequentially.

Remark: The decoding procedures as outlined above can only process very limited number of elements (up to 7 elements). This is due to the limitations of 32-bit or 64-bit operating system in dealing with integer numbers. As *n* grows, the length of the intermediate integer numbers significantly increases. However, any integer number that is larger than 2^{32} or 2^{64} will be automatically rounded by a computer, thus rendering the results inaccurate. To solve this problem, a cell data type can be adopted by which the computer treats a string as a single cell and decoding from a large integer is no longer necessary. For example, each element of a regular string array can only be one character such as "(", "*a*", "*b*", or ")" etc. This storage requires a large array size to store a string and is not efficient for the enumeration. If a cell array is employed, a string "(*abc*)" can be saved as one single element in the array. Such storage syntax is similar to storing an integer number in a regular array and can greatly facilitate the enumeration.

The flowchart of the developed algorithms is given in Figure 2-12, where a function mergeN() is defined to implement the recursion. The algorithm involves initialization, a double-loop of *win*(*m*) and *ep*(*m*) to solve problem (*i*), recursion with respect to *m* to solve problem (*ii*), decoding of numbers with strings as illustrated above, and a filtering algorithm to be discussed next.

As an example to illustrate the algorithm, Table 2-3 lists intermediate values of *ep0*(*m*), *ep*(*m*), *win*(*m*), and *c*(*m*), *m* =1, 2 for a *P*(4) problem of enumerating four elements {1,1,1,1}. The parameter values for *m* = 3 are not listed because it is a straightforward data merging with *c*(3) = 4, *ep0*(3) =1, and *ep*(3) = *win*(3) = 2. It is noted, unlike the algorithms for counting the number of sequence, the enumeration algorithms generate all the sequence with *n* elements for all the possible numbers of groups. If needed, the sequence for a specific number of groups can be segregated by the recursive step *m* in the computational output.

2.3.4 Filtering algorithm for sequence reduction

In certain assembly scenarios, some components must or must not be assembled together. These extra precedence constraints should be compared with the enumerated assembly sequences to screen out the infeasible ones. For example, one may specify that only elements *a* and *b* must be assembled together. Then strings such as (*a*(*bc*)*d*) and (*ab*(*cd*)) are not selected. On the other hand, if elements *a* and *b* must not be co-assembled, strings that contain "(*ab*)" are not permissible output.

Note that the filtering algorithm strictly matches the strings and great care must be exercised when some constraints are applied. For example, if the constraint is that *a* and *b* must be assembled together, the pass should be pass = *ab* (dropping the parentheses).

The filtering of the enumerated assembly sequences given precedence constraints can be achieved by operations of string comparisons. Users will specify a number of component combinations that must be assembled together and are saved in a string array called pass. The algorithm will determine if "pass" are contained in the inspected assembly sequences. A string will be output once a match is found. Similarly, those component combinations that must not be co-assembled are saved on in a string called block. Those strings that do not contain "block" will be output. The flow chart of the filtering algorithm is shown in Figure 2-13.

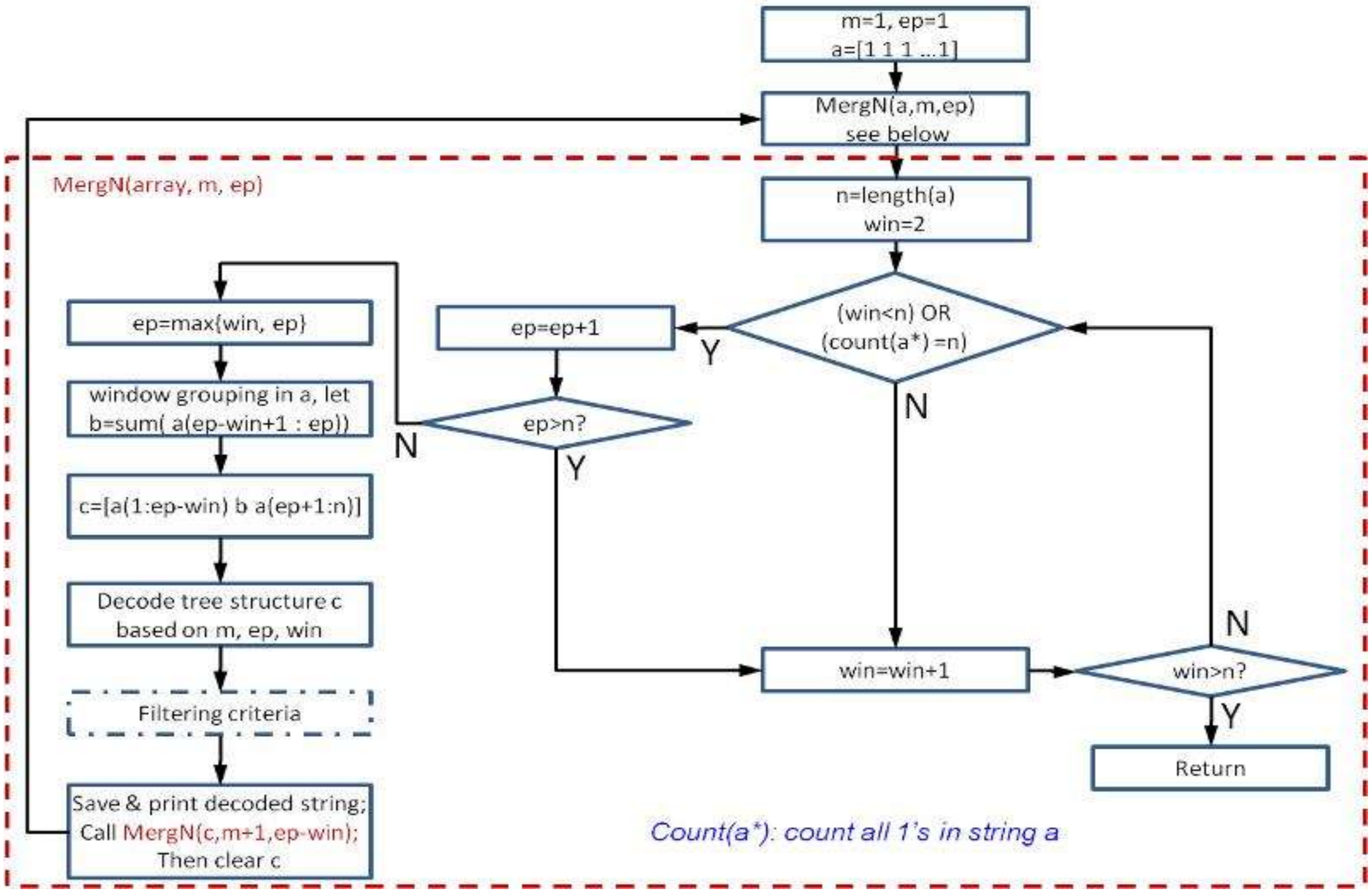

Figure 2-12 Flowchart of enumeration algorithms

Table 2-3 Intermediate values for a **P**(4) enumeration problem for {1,1,1,1}

Output string	c(1)	c(2)	ep0(1)	ep0(2)	ep(1)	ep (2) (for the merged array)	win(1)	win(2) (for the merged array)
((11)11)	2 1 1	4	1	NA	2	NA	2	NA
(((11)1)1)	2 1 1	3 1	1	1	2	2	2	2
((11)(11))	2 1 1	2 2	1	1	2	3	2	2
(1(11)1)	1 2 1	4	1	NA	3	NA	2	NA
((1(11))1)	1 2 1	3 1	1	2	3	2	2	2
(1((11)1))	1 2 1	1 3	1	2	3	3	2	2
(11(11))	1 1 2	4	1	NA	4	NA	2	NA
(1(1(11)))	1 1 2	1 3	1	3	4	3	2	2
((111)1)	3 1	4	1	NA	3	NA	3	NA
(1(111))	1 3	4	1	NA	4	NA	3	NA
(1111)	4	NA	1	NA	4	NA	4	NA

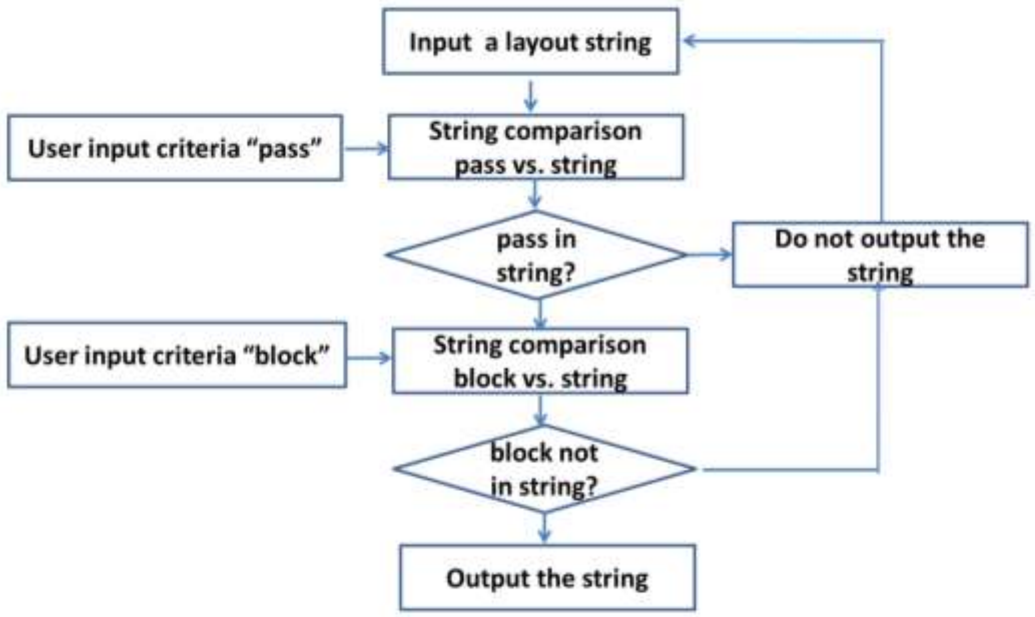
Input a layout string
User input criteria "pass"
String comparison pass vs. string
pass in string?
Do not output the string
User input criteria "block"
String comparison block vs. string
block not in string?
Output the string

Figure 2-13 Flowchart of filtering algorithm

The reduction of possible assembly sequences given precedence constraints can be dramatic. Table 2-4 compares the enumeration results for 5 elements {*A*, *B*, *C*, *D*, *E*} before and after applying three filtering criteria (constraints), i.e., pass=(*AB*), block(1)=(*CD*), and block(2)=((*BC*)*DE*). It can be seen that without precedence constraints, the total number of sequences is 45, while given precedence constraints, the total number of assembly sequences become 8.

Table 2-4 Reduction of assembly sequence enumerations:

(a) without precedence constraints

((AB)CDE)	(A((BC)D)E)	(ABC(DE))
(((AB)C)DE)	((A((BC)D))E)	(AB(C(DE)))
((((AB)C)D)E)	(A(((BC)D)E))	(A(B(C(DE))))
(((AB)C)(DE))	(A(BC)(DE))	(A(BC(DE)))
((AB)(CD)E)	(A((BC)(DE)))	((ABC)DE)
(((AB)(CD))E)	((A(BC)D)E)	(((ABC)D)E)
((AB)((CD)E))	(A((BC)DE))	((ABC)(DE))
((AB)C(DE))	(AB(CD)E)	(A(BCD)E)
((AB)(C(DE)))	(A(B(CD))E)	((A(BCD))E)
(((AB)CD)E)	((A(B(CD)))E)	(A((BCD)E))
((AB)(CDE))	(A((B(CD))E))	(AB(CDE))
(A(BC)DE)	(AB((CD)E))	(A(B(CDE)))
((A(BC))DE)	(A(B((CD)E)))	((ABCD)E)
(((A(BC))D)E)	((AB(CD))E)	(A(BCDE))
((A(BC))(DE))	(A(B(CD)E))	(ABCDE)

(b) with precedence constraints (filtering)

((AB)CDE)
(((AB)C)DE)
((((AB)C)D)E)
(((AB)C)(DE))
((AB)C(DE))
((AB)(C(DE)))
(((AB)CD)E)
((AB)(CDE))

2.4 Discussion

In this work, the system configurations are generated and evolved including not only traditional serial/parallel lines but also hybrid lines with branches. Webbink and Hu [26] proposed an automated distribution method to enumerate all the possibilities of different combinations of stations which are of serial or parallel configuration. Then the configurations are matched with assembly sequences generated by Whitney's enumeration methods [19]. Webbink and Hu's work assigned serial sequences to each routes (material flow path) of the system with hybrid configurations. Figure 2-14 shows an example of system configuration where all the different routes can produce the final product (ABCD). The first route allows for loading and assembling components one at a time; the second route allows assembling A and B first, then loading and assembling C, D sequentially onto AB; the third route assembles A, B and C together first, and then assembles D onto ABC. Lines that are in parallel may perform the same task sequence but in different steps. For example, the parallel lines, which are shared by route 1 & 2, both perform assembly task sequence (AB). In route 1, the task sequence needs two steps while in route 2, it needs only one step.

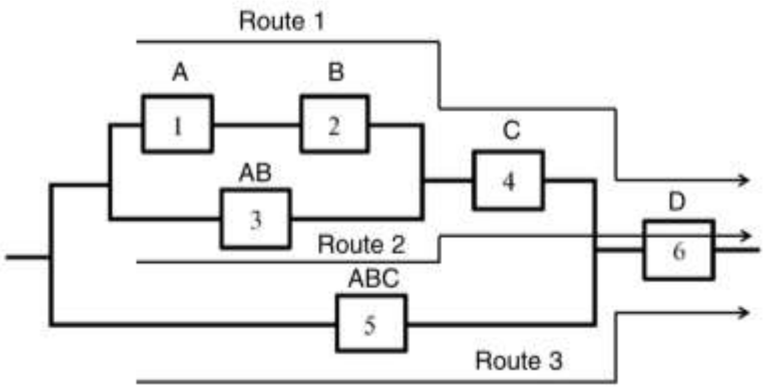

Figure 2-14 Example system configuration (A, B, C, D are components)

Webbink’s work didn’t consider hybrid lines with branches, where tasks on the different branches of the lines are independent subassembly tasks. If the assembly/subassembly groupings generated by this research are used to expand each route in Webbink’s work, more configurations can be generated. Table 2-5 shows an example of the configuration generation and evolvement given assembly/subassembly groupings and sequences in Table 2-2.

2.5 Conclusion

In this chapter, a new hierarchical subassembly decomposition method is developed by utilizing hierarchical data structure and recursive decomposition algorithms to enumerate all non-redundant assembly/subassembly groupings. The computational sequence generation is enabled by a transformation scheme devised to convert a typical diagram of assembly system configuration into a string of characters or numerals representing assembly components and sequences of operations. User-defined filtering functions are also considered in the enumeration algorithms for handling additional system requirements or constraints, which could reduce the number of assembly/subassembly groupings significantly. The efficient, exhaustive computational sequence generation method provides enough candidate systems for special considerations and ensures that a truly optimal system can be identified.

The above algorithm is verified using a combinatorial approach [15] to count the number of candidate system configurations without physically generating them. The number of configurations not only helps validate the computational sequence generation algorithms, but also provides a quick assessment of the scope of the problem. Both the

Table 2-5 An example of configuration generation and evolvement

Assembly grouping	Initial configuration	Configuration evolvement examples
((AB)CD)	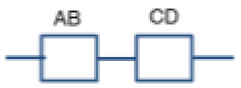	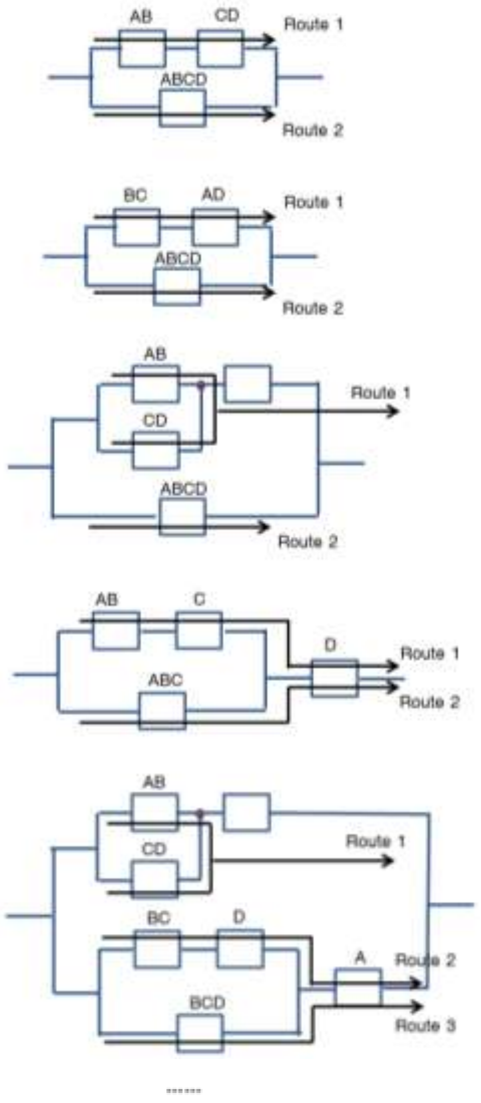 AB CD Route 1 ABCD Route 2 BC AD Route 1 ABCD Route 2 AB Route 1 CD ABCD Route 2 AB C D Route 1 ABC Route 2 AB Route 1 CD BC D A Route 2 BCD Route 3 ……
(((AB)C)D)	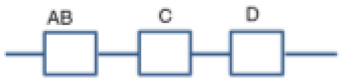	
((AB)(CD))	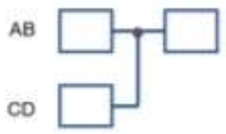	
(A(BC)D)	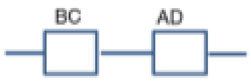	
((A(BC))D)	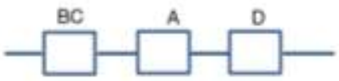	
(A((BC)D))	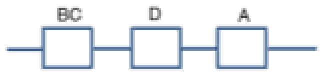	
(AB(CD))	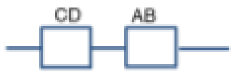	
(A(B(CD)))	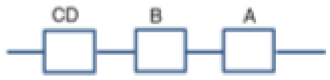	
((ABC)D)	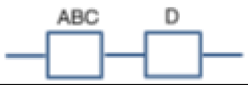	
(A(BCD))	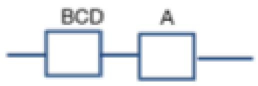	
(ABCD)	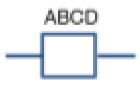	

algorithms for system sequence generation and counting the number of system configurations have been tested and validated.

CHAPTER 3

AUTOMATIC GENERATION OF ASSEMBLY SYSTEM CONFIGURATION WITH EQUIPMENT SELECTION FOR AUTOMOTIVE BATTERY MANUFACTURING

High power and high capacity lithium-ion batteries are being adopted for electrical and hybrid electrical vehicles (EV/HEV) applications. An automotive Li-ion battery pack usually has a hierarchical composition of components assembled in repetitive patterns. Such a product assembly hierarchy may facilitate automatic configuration of assembly systems including assembly task grouping, sequence planning, and equipment selection. This chapter utilizes such a hierarchical composition in generating system configurations with equipment selection for optimal assembly system design. A recursive algorithm is developed to generate feasible assembly sequences and the initial configurations including hybrid configurations. The generated configurations are embedded in an optimal assembly system design problem for simultaneous equipment selection and task assignment by minimizing equipment investment cost. The complexity of the computational algorithm is also discussed.

3.1 Introduction

Lithium-ion batteries are gaining more attention in electrical and hybrid electrical vehicles (EV/HEV) because they offer significantly higher energy density as well as lighter weight and longer cycle life compared with lead acid and nickel-metal hydride batteries [2]. A lithium-ion battery pack usually has a hierarchical structure consisting of several modules, while a module is composed of battery cells and ancillary members which are assembled or stacked together in a certain pattern (Figure 1-5). Prismatic pouch cells or prismatic cells with case enclosure are usually stacked in one direction, vertical or horizontal, while cylindrical cells are assembled in tubular or grid patterns (Figure 3-1) [5].

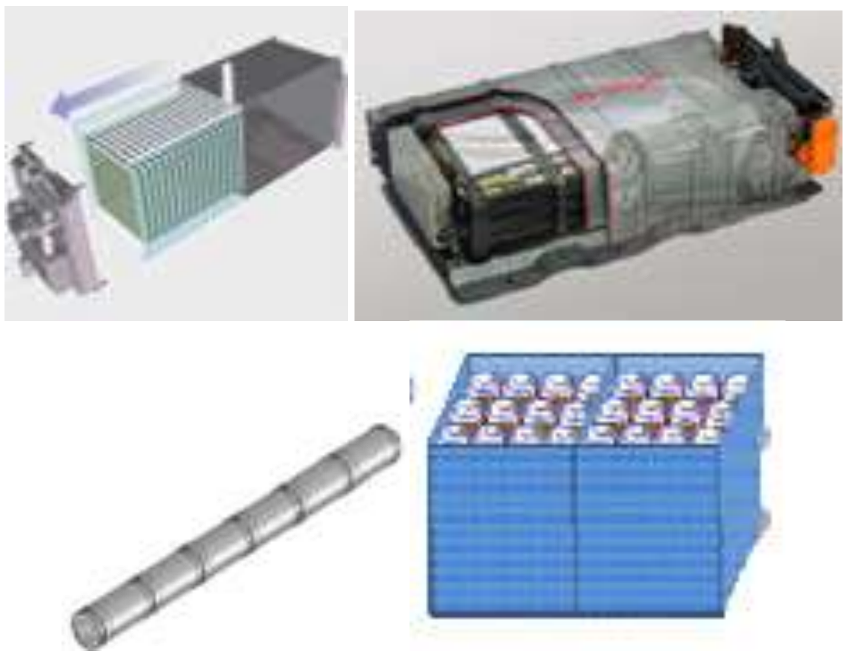
Figure 3-1 Different stacking patterns for battery cells [5]

The design of an assembly system often begins with assembly sequence generation [33-34]. The challenge to assembly sequence generation is that there are many ways of assembling the components for a given stacking pattern in battery packs. For example, components can be added one at a time, leading to serial sequences. Alternatively, all the components can be assembled in one station with flexible machines, resulting in a parallel operation. Various hybrid assembly sequences can also be obtained by preassembling different number of components into subassemblies which in turn are assembled with other components or subassemblies. Figure 3-2 illustrates a set of five candidate assembly sequences in assembling a section of a battery module.

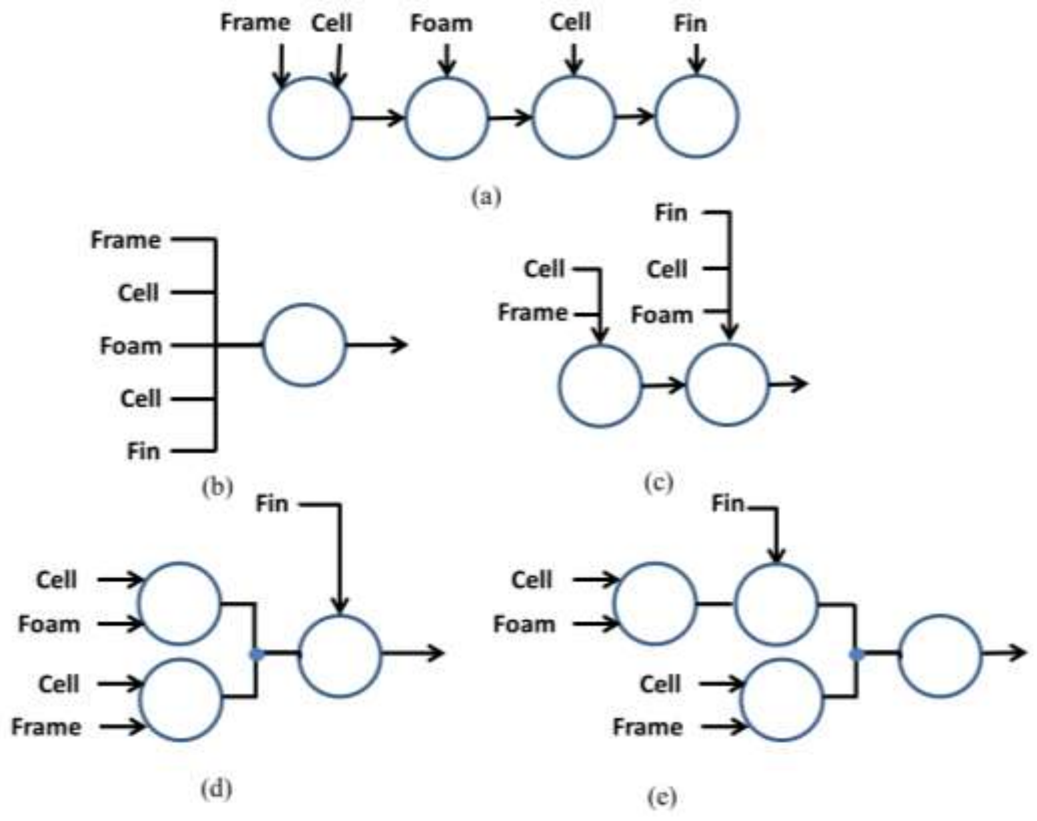

Figure 3-2 Different examples of assembly sequences (a) components are loaded and stacked in a serial sequence; (b) components are stacked simultaneously in one station; (c), (d) and (e) components are stacked into subassemblies and then stacked with other components or subassemblies (circles represent tasks for loading and stacking)

Traditional assembly sequence generation methods focused on sequential task sequences. Among them, Bourjault [18] presented the first algorithm to generate all feasible assembly sequences. Building on Bourjault’s method, Whitney [19] increased the size of the problem to accommodate assemblies with much higher number of components numbers by asking two questions of precedence. A number of approaches, such as algorithms and graph based methods, have been used to generate the assembly sequences [20-23]. Methods were also developed to derive the assembly sequences from the disassembly sequences [24-25].

Based on the sequential task sequences, the assembly system commonly adopts a dedicated serial configuration for mass production of limited product variants (Figure 1-6 (a)). Other configurations were also considered including parallel configurations, serial systems with parallel machines, or parallel lines with machines in serial (Figure 1-6(b)(c)(d)) [35]. Significant amount of research has been done investigating the effects of system configurations on performance [36-41]. On assembly system design, Webbink and Hu [26] proposed an automated distribution method to enumerate all the possibilities of different combinations of stations which are of serial or parallel configuration. In this work, the hybrid configuration is generated by assigning the sequential task sequences to each route in the system. The optimization is thus reduced to the conventional line balancing problem of assigning a sequential task sequence to a serial line in each route. Ko and Hu [42] presented a new method for designing complex configurations by linking manufacturing requirements to configuration structure. The balancing of assembly systems with the complex configurations focused on specific configurations for delayed product differentiation (Figure 3-3).

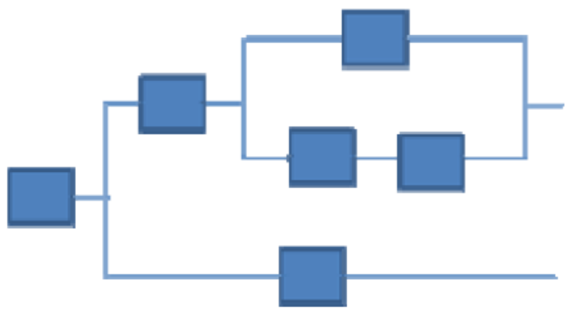

Figure 3-3 An example of manufacturing system configuration for delayed product differentiation [42]

Equipment selection is another problem in assembly system design. When equipment selection is considered with line balancing, such a problem is called an assembly line design problem (ALDP) [43]. Pinto *et al*. [44] studied a method of simultaneously considering manufacturing process alternatives and assembly line balancing (ALB) to minimize total costs. Graves and Lamar [45] and Graves and Holmes Redfield [46] considered an assembly line for one or multi-products with the stations being chosen from a set of non-identical station types with different equipment choices. Bukchin and Tzur [47] considered stations being provided with several equipment alternatives while minimizing the overall equipment cost. Most equipment selection has been implemented on serial configurations.

Traditional sequential task sequence based approach does not consider parallel subassembly tasks. In addition, there is a lack of method for simultaneous equipment selection and complex configuration generation. This paper describes a new method for designing assembly systems by integrating automatic configuration generation with equipment selection considering product hierarchy. Based on an automatic enumeration algorithm for generating assembly tasks and sequences derived from the assembly hierarchy [15], a two loop nested optimization algorithm is developed to determine the optimal hybrid system configuration along with equipment selection. By allowing for concurrent tasks and adding more than one part at a time, hybrid configurations are more suitable for dealing with products assembled in a hierarchy.

The remainder of the chapter is organized as follows. Section 3.2 introduces the method of automatic system configuration with equipment selection. An overview of methodology is discussed first and then the enumeration algorithm and balancing and equipment selection model are introduced. Section 3.3 presents an example of system design given a battery configuration. Section 3.4 draws the conclusions.

3.2 System configuration generation with machine selection

3.2.1 Methodology overview

The overall procedure for the system configuration generation is shown in Figure 3-4. Taking product designs as inputs, the outer loop algorithm first enumerates all feasible assembly tasks and the corresponding sequences $\boldsymbol{T}_1$, $\boldsymbol{T}_2 \ldots \boldsymbol{T}_k$. For each sequence, one task is assigned to one machine each, thus creating an initial configuration (config_k^0) generated from the assembly sequence. The initial configuration will be evolved and updated following the inner-loop optimization procedures that explore all candidate machines and feasible ways of task-machine assignments (Figure 3-5(a)). Different from past research that focuses on assigning tasks to machines in serial configuration (Figure 3-5(b)), this method considers complex configurations that may possess superior throughput performance and reconfigurability. After a configuration is chosen, the performance responses, e.g., throughput Th_i*, and its associated cost C_i* for the optimal configuration are generated and the responses Th_i* and costs C_i* are compared over all the task sequences to determine the global optimal configuration in the outer loop optimization. When the number of the enumerated task sequences grows large, the exhaustive search is not computationally feasible. Genetic algorithm or computer experiment approaches are employed to approximate the near-optimum. The outer-loop optimization is the hierarchical subassembly decomposition method which has already been discussed in chapter 2.

3.2.2 Model for balancing and equipment selection

Enumeration in the outer loop generates the candidate assembly tasks/task groups, sequences, and initial configurations. The inner loop evolves each configuration by assigning the tasks to the selected machines. This section describes a mathematical model for the inner loop optimization including task-machine assignment, workload balancing and machine type and number selection in assembly systems. A simplified formulation is described in chapter 5 in order to speed up the optimization.

<u>Decision variables</u>

Define a task-machine assignment variable, which represents whether or not a task is assigned to a machine, as

$$x_{i,j,k} = \begin{cases} 1 & \text{if task } i \text{ is assigned to the } k\text{th machine of the } j\text{th machine type} \\ 0 & \text{otherwise} \end{cases}$$

Also define $y_{i,j}$, which represents whether or not a machine type is utilized for task i, as

$$y_{i,j} = \begin{cases} 1, \text{if task i is assigned to machine type j, i.e. } M_{i,j} \neq 0 \\ 0, \qquad \text{otherwise, i.e. } M_{i,j} = 0 \end{cases}$$

where $M_{i,j} = \sum_{k=1}^{K_j} x_{i,j,k}$

K_j are quantities for the machine type j

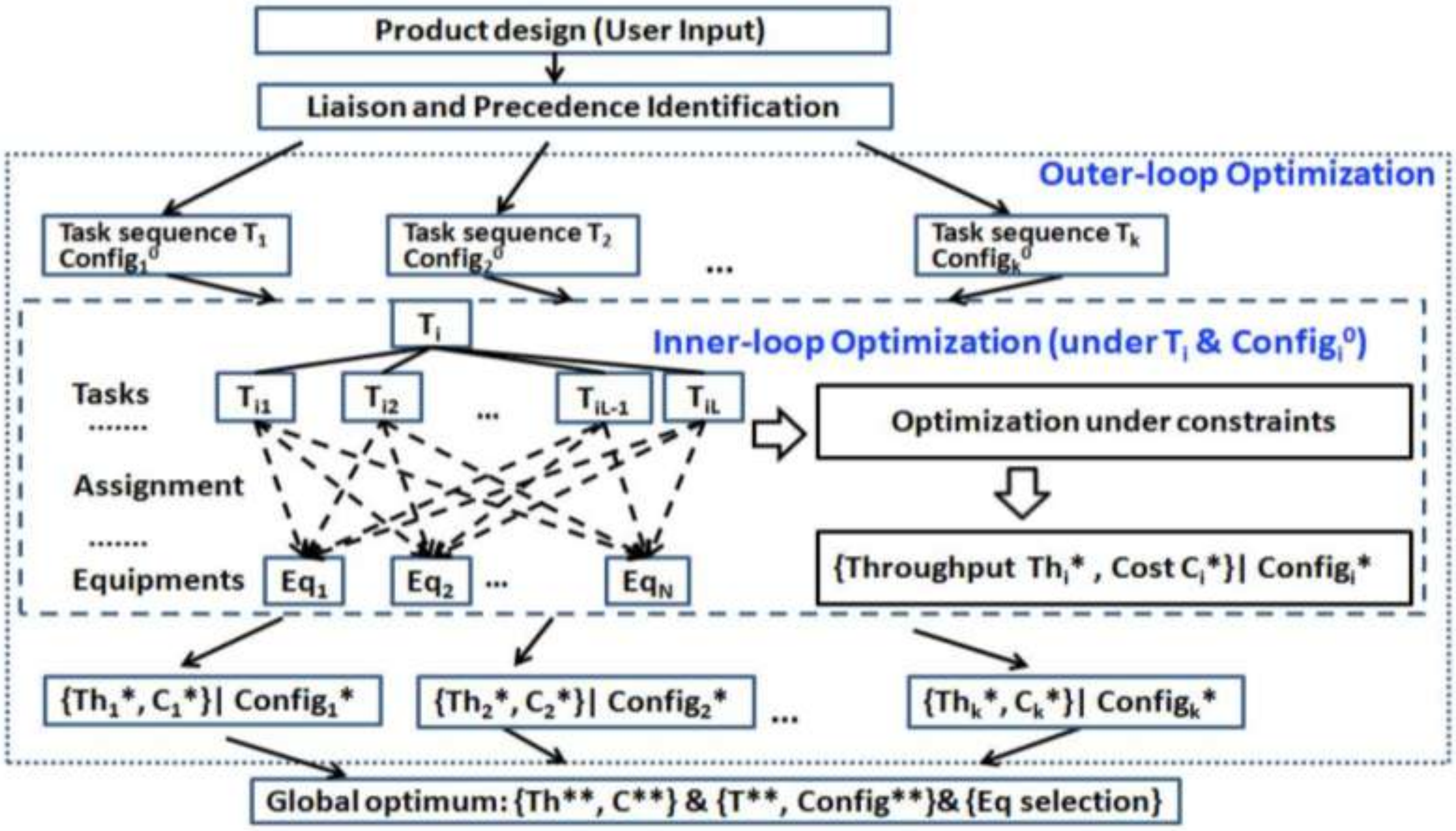
Product design (User Input)
Liaison and Precedence Identification
Outer-loop Optimization
Task sequence T1 Config1^0
Task sequence T2 Config2^0
...
Task sequence Tk Configk^0
Ti
Inner-loop Optimization (under Ti & Configi^0)
Tasks
Ti1
Ti2
TiL-1
TiL
Assignment
Equipments
Eq1
Eq2
EqN
Optimization under constraints
{Throughput Thi* , Cost Ci*}| Configi*
{Th1*, C1*}| Config1*
{Th2*, C2*}| Config2*
{Thk*, Ck*}| Configk*
Global optimum: {Th**, C**} & {T**, Config**}& {Eq selection}

Figure 3-4 The nested procedure for combinatorial optimization

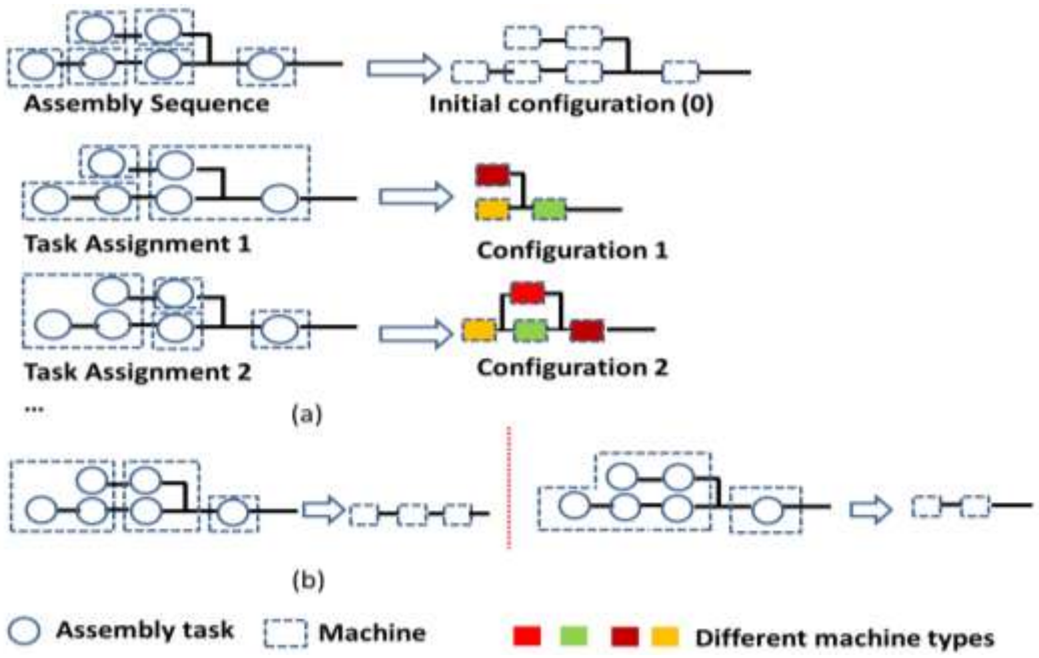

Figure 3-5 Assignment of tasks to machines with certain configuration

The variable $y_{i,j}$ is derived from $x_{i,j,k}$, i.e.,

$$y_{i,j} = \cup_{k=1}^{K_j} x_{i,j,k} \text{ or } \begin{cases} \sum_{k=1}^{K_j} x_{i,j,k} \le M_{i,j} y_{i,j}, & \forall \text{ machine type } j \\ \sum_{k=1}^{K_j} x_{i,j,k} \ge y_{i,j}, & \forall \text{ machine type } j \end{cases}$$

where the first inequality ensures that $y_{i,j}$ is 1 if task *i* is assigned to at least one machine of machine type *j*; and the second ensures that $y_{i,j}$ is 0 if task *i* is not assigned to machine type *j*.

<u>Objective function</u>

The objective in this model is to balance an assembly system by minimizing the equipment investment cost while ensuring the throughput requirement, i.e.,

$$\min \quad G = \sum_{i=1}^{I} \sum_{j=1}^{J} \sum_{k=1}^{K_j} c_{ij} x_{ijk} \tag{1}$$

where $c_{i,j}$ is the operating cost of assigning task i to machine type j. The purchasing cost of each machine type is assumed not to be considered here.

<u>Constraints</u>

1) Task assignment constraint

This constraint requires task i to be assigned to only one type of machine, i.e.,

$$\sum_{j=1}^{J} y_{i,j} = 1 \tag{2}$$

Note: It is feasible that different types of machines can perform the identical operations at the same time and pace. However, this way will pose challenges to logistics, wiring, and machine set up.

2) Task-machine matching constraint

Certain engineering experiences may require a set of tasks not to be assigned to certain machine type, i.e.,

$$y_{m,n} = 0, (m,n) \in TM - \text{set that task m cannot be assigned to machine type } n \tag{3}$$

3) Assembly constraint

This constraint specifies the material flows between tasks. The upstream assembly or subassemblies have to be finished before the downstream tasks can be processed. For example, in battery assembly, one module consists of four units and one unit consists of eight cells. If it takes one minute to produce a module, then unit stacking should not exceed one fourth minute and cell loading should not exceed 1/32 minute. Denote $g_i(\cdot_I)$ as the function of such material flow relationship between task i and the final task I. This constraint ensures that the throughput of component i satisfies the demand of final products and can be represented by

$$M_i / \sum_{j=1}^{J} t_{ij} y_{ij} \geq M_I / g_i (\sum_{j=1}^{J} t_{Ij} y_{Ij}), \quad \forall i < I \tag{4}$$

where $\sum_{j=1}^{J} t_{ij} y_{ij}$ is the processing time for task *i* and M_i is the number of machines used for task i and $M_i = \sum_{j=1}^{J} \sum_{k=1}^{K_j} x_{ijk}$

4) Cost constraint

This constraint requires that the total equipment cost does not exceed the budget limit and can be represented by

$$\sum_{i=1}^{I} \sum_{j=1}^{J} \sum_{k=1}^{K_j} c_{ij} x_{ijk} \leq G_0 \tag{5}$$

5) Throughput constraint

This constraint requires the system throughput to meet the production demand, i.e., the throughput of the bottleneck operation satisfies

$$M_B / t_B \geq Th_0 \tag{6}$$

6) Task zoning constraint

Some tasks must be assigned to the same machine, and the other tasks cannot be assigned to the same machine. These constraints are known as positive and negative zoning constraints in [48-50]. For example, tasks requiring similar manufacturing process or a very expensive machine may be assigned to one machine in order to reduce equipment cost. Tasks requiring different types of manufacturing processes or having certain safety requirements usually cannot be assigned to the same machine. The following two equations represent positive and negative constraints, respectively.

$$\begin{aligned} & x_{u,j,k} = x_{v,j,k}, (u,v) \in ZS\text{--set of tasks that must be assigned to the same machine} \\ & x_{u,j,k} + x_{v,j,k} \leq 1, k = 1, \ldots K_j, (u,v) \in ZD\text{--set of tasks that cannot be on the same machine} \end{aligned} \tag{7}$$

Inner-loop optimization model selection

In the formulations (2)-(7), the upper bound K_j of the quantities for the machine type *j* is assumed to be given. To determine the optimal K_j, a model selection procedure is developed as shown in Figure 3-6. First, a set of initial values of upper limits K_1, K_2, …, K_j … are assigned to each machine type when implementing the inner loop optimization. For the inner loop optimization, the genetic algorithm (GA) is adopted. Then the values of the upper limits are increased and the inner-loop optimization is implemented again. The new configuration is compared with the previous one. Keep increasing the values for the upper limits and update the solution until the resultant configurations do not change (converge) as the $\{K_j\}$ increases.

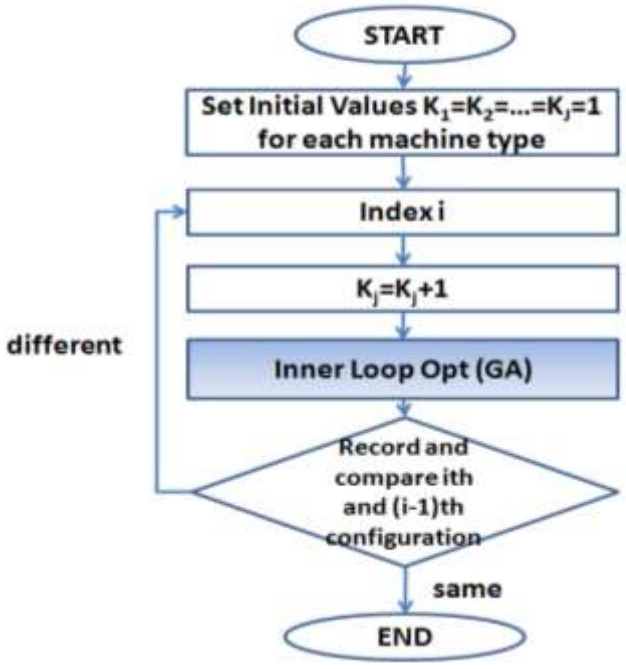
START
Set Initial Values $K_1=K_2=…=K_j=1$ for each machine type
Index i
$K_j=K_j+1$
Inner Loop Opt (GA)
Record and compare ith and (i-1)th configuration
different
same
END

Figure 3-6 Procedure for inner-loop optimization model selection

Solution Method

Genetic algorithm is a directed search algorithm based on the mechanics of biological evolution. Most of the time a solution can be identified if initial solutions are close to it and the solution could be local optimal. Exhaustive search method has also been used to find the optimal solution (Figure 3-7). It takes longer time so pre-filtering criteria could be needed in order to reduce possible enumeration.

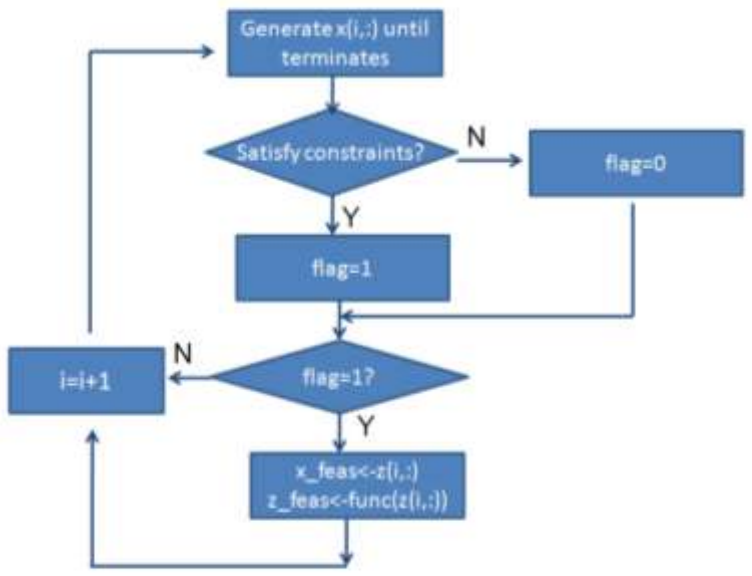

Figure 3-7 Exhaustive search method

The following constraints have been linearized to use binary integer search method.

$$y_{i,j} = \cup_{k=1}^{K_j} x_{i,j,k} \text{ or } \begin{cases} \sum_{k=1}^{K_j} x_{i,j,k} \le M_{i,j} y_{i,j}, & \forall \text{ machine type } j \\ \sum_{k=1}^{K_j} x_{i,j,k} \ge y_{i,j}, & \forall \text{ machine type } j \end{cases} \rightarrow$$

$$y_{i,j} = \cup_{k=1}^{K_j} x_{i,j,k} \text{ or } \begin{cases} \sum_{k=1}^{K_j} x_{i,j,k} \le B y_{i,j}, & \forall \text{ machine type } j, \textit{where } B = K_j \\ \sum_{k=1}^{K_j} x_{i,j,k} \ge y_{i,j}, & \forall \text{ machine type } j \end{cases} \quad (8)$$

Binary integer search is a linear programming based branch and bound algorithm. The algorithm creates a search tree by repeatedly adding constraints to the problem (branching) (Figure 3-8). Different nodes represent different variable combinations. The objective function is estimated during the binary integer search in order to find the optimal solution.

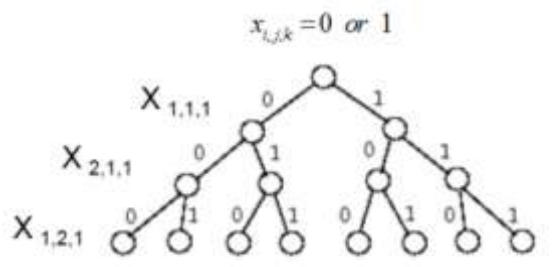

Figure 3-8 Binary integer search tree

Computational complexity

The proposed exhaustive search method in the outer-loop optimization to solve the combinatorial optimization problem of assembly sequence enumeration may face computational challenges when k is large. A recursive formulation is discussed in Lin *et al*. [15] for counting the number of total enumerations. For such huge number of enumerations, solutions can be found as follows: (1) the precedence constraints (filtering criteria) will significantly reduce k by eliminating infeasible sequences; (2) grouping some of the components, such as identical components, into subassemblies first, then the enumeration algorithm is applied in different assembly levels, and redundant enumerations can thus be avoided; (3) if the reduced k still poses challenges to computation, other searching methods such as genetic algorithm, simulated annealing, or Kriging method should be adopted based on a number of representative solutions and responses to obtain an approximation of the global optimum.

3.3 Case study

This section demonstrates the configuration generation and equipment selection method using a case study of battery module assembly.

3.3.1 Problem description and results

As shown in Figure 3-9, a repetitive pattern in a battery module is the frame-cell-foam-cell-cooling fin. Such a pattern repeats a number of times (*N*) in the module. Non-repetitive components are added to the two ends of the repetitive pattern stack to form the module.

Let *A, B, C, D, E* denote the cell and ancillary components. The repetitive pattern is *B*-*A*-*D*-*A*-*C* with the non-repetitive components *E*-*A*-*C* at one end and *A*-*E* at the other end. Also assume that the first cell *A* and foam *D* has to be assembled together. Table 3-1

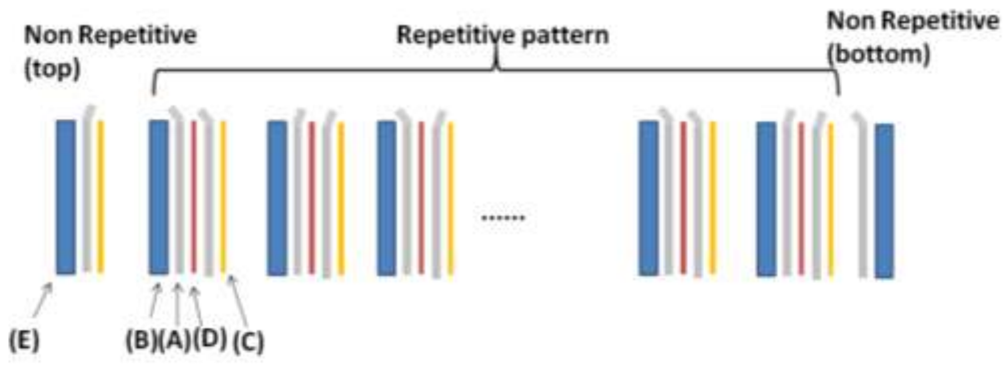

Figure 3-9 An example of assembly of battery module

shows the enumeration results for the repetitive pattern. Table 3-2 shows only the first 10 enumeration results for the whole module due to the page limitation. If there are no constraints applied, there are 197 possible sequences generated in total [15].

Table 3-1 Enumeration results for the repetitive pattern (*R*)

Case#	1	2	3	4
Sequence	*(B(AD)AC)*	*((B(AD))AC)*	*(((B(AD))A)C)*	*((B(AD))(AC))*
Case#	5	6	7	8
Sequence	*(B((AD)A)C)*	*((B((AD)A))C)*	*(B(((AD)A)C))*	*(B(AD)(AC))*
Case#	9	10	11	
Sequence	*(B((AD)(AC)))*	*((B(AD)A)C)*	*(B((AD)AC))*	

Table 3-2 First 10 enumeration results for the module ("*R*" represents repetitive pattern)

Case#	1	2	3
Seq.	*((EA)CRAE)*	*(((EA)C)RAE)*	*((((EA)C)R)AE)*
Case#	4	5	6
Seq.	*(((((EA)C)R)A)E)*	*((((EA)C)R)(AE))*	*(((EA)C)(RA)E)*
Case#	7	8	9
Seq.	*((((EA)C)(RA))E)*	*(((EA)C)((RA)E))*	*(((EA)C)R(AE))*
Case#	10		
Seq.	*(((EA)C)(R(AE)))*		

To illustrate the inner-loop optimization, consider case #5 of the repetitive pattern and case #9 of the whole module pattern. Table 3-3 lists the assembly tasks for repetitive (L591-L593) and non-repetitive pattern (L594-L596) assemblies and the final assembly (L597), where in L_{ijk}, *i* is the index for certain combinations of repetitive pattern, *j* is the index for module pattern and *k* is the index of assembly tasks involved in the *ij*th pattern. The task sequence is shown in Figure 3-10. Other task information such as processing time and machine operating cost is given in Table 3-4. Since task L597 requires *N* repetitive patterns, the processing time of tasks L591-L593 are *N* times the processing time of performing one repetitive pattern at each single machine. The zoning constraints require tasks for repetitive (L591-L593) and non-repetitive pattern (L594-L596) and the final assembly (L597) not to be assigned to the same machine. Since tasks L594 and L596 are essentially the same, they must be assigned to the same machine.

Table 3-3 Assembly tasks of repetitive pattern #5 & module #9

Task #	Description
L591	Assembly of components A & D
L592	Assembly of components (AD) & A
L593	Assembly of components (ADA) & B & C
L594	Assembly of components E & A
L595	Assembly of components (EA) & C
L596	Assembly of components A & E
L597	Assembly of components (EAC) & R & (AE)

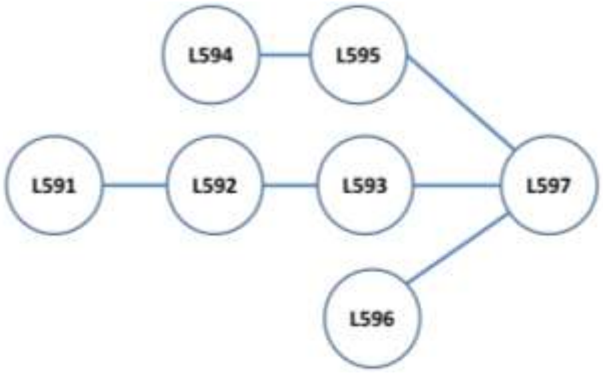

Figure 3-10 Task sequence graph for battery module assembly

Assume that there are two machines available for each machine type due to the budget constraint. Figure 3-11 shows the initial configuration and the configuration after the inner loop optimization. For example, tasks L591 and L592 can be processed in one machine type and task L593 in another machine type. Tasks L594-L596 can be processed in one machine with the same machine type as tasks L591&L592. Task L597 is assigned to a third type machine, which stacks repetitive pattern and non-repetitive pattern together.

For the outer-loop, one needs to find the optimal configurations for other assembly sequences. Figure 3-12 gives the optimal configuration generated by repetitive pattern case #8 and module assembly case #9. It has been found that repetitive pattern cases #1, #2, #3, #5, #6, #7, #10, #11 (Table 3-1) and case #9 of the whole module (Table 3-2) yield the same configurations (Figure 3-11(b)) in the inner-loop optimization while repetitive pattern cases #4, #8, and #9 (Table 3-1) and case #9 of the whole module (Table 3-2) yield the same configurations (Figure 3-12). The configuration in Figure 3-11(b) is superior since it is cheaper (The cost difference is $470,000) while maintaining the same throughput as the configuration in Figure 3-12. Similar procedure shall be applied for other cases of the whole module pattern in Table 3-2.

3.3.2 Discussion

In the above example, the difference between processing time of the final stacker and previous tasks for stacking repetitive patterns is not drastic. In the generated configurations, repetitive patterns and non-repetitive patterns are processed on two branch lines, respectively; and assembled in one machine in the final station. The processing time for non-repetitive pattern is 15~35 seconds per product, which is significantly smaller than the processing time for other stations (130~280 seconds per product). To minimize the cost, tasks for stacking non-repetitive patterns could be assigned to minimum number of machines without violating throughput constraint and zoning constraint.

Table 3-4 Task information for the example problem

Task (i)	Machine Type (j)	Processing Time ($t_{i,j}$)	Machine Cost ($c_{i,j}$)	Zoning Constr.	
				ZS	ZD
L591	Ejecting + Elevator	$t_{1,1}$=120 (sec)	$c_{1,1}$=10		L594-L597
	Gantry Robot	$t_{1,2}$=158.44	$c_{1,2}$=30		
	Articulate Robot	$t_{1,3}$=180	$c_{1,3}$=50		
L592	Ejecting + Elevator	$t_{2,1}$=160	$c_{2,1}$=10		L594-L597
	Gantry Robot	$t_{2,2}$=196.86	$c_{2,2}$=30		
	Articulate Robot	$t_{2,3}$=210	$c_{2,3}$=50		
L593	Ejecting + Elevator	$t_{3,1}$=200	$c_{3,1}$=10		L594-L597
	Gantry Robot	$t_{3,2}$=255	$c_{3,2}$=20		
	Articulate Robot	$t_{3,3}$=280	$c_{3,3}$=50		
L594	Ejecting + Elevator	$t_{4,1}$=15	$c_{4,1}$=10	L596	L591-L593 &L597
	Gantry Robot	$t_{4,2}$=19.03	$c_{4,2}$=30		
	Articulate Robot	$t_{4,3}$=25	$c_{4,3}$=50		
L595	Ejecting + Elevator	$t_{5,1}$=25	$c_{5,1}$=10		L591-L593 &L597
	Gantry Robot	$t_{5,2}$=30.61	$c_{5,2}$=20		
	Articulate Robot	$t_{5,3}$=35	$c_{5,3}$=50		
L596	Ejecting + Elevator	$t_{6,1}$=15	$c_{6,1}$=10	L594	L591-L593 &L597
	Gantry Robot	$t_{6,2}$=19.03	$c_{6,2}$=30		
	Articulate Robot	$t_{6,3}$=25	$c_{6,3}$=50		
L597	Ejecting + Elevator	$t_{7,1}$=150	$c_{7,1}$=100		L591-L596
	Gantry Robot	$t_{7,2}$=180	$c_{7,2}$=60		
	Articulate Robot	$t_{7,3}$=260	$c_{7,3}$=50		

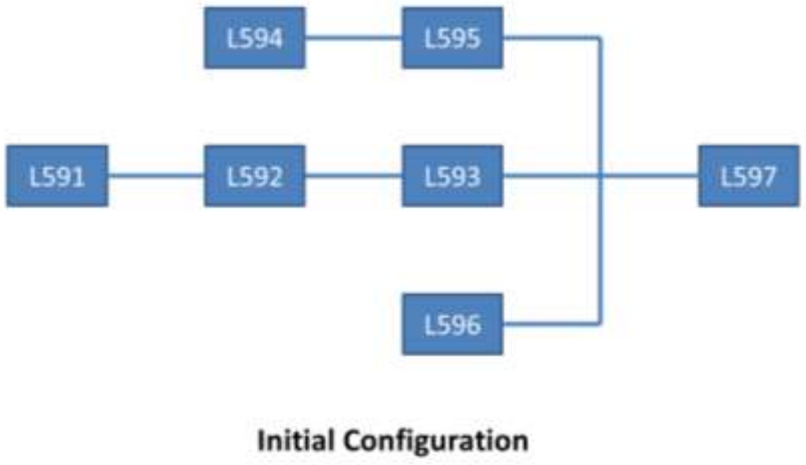

(a)

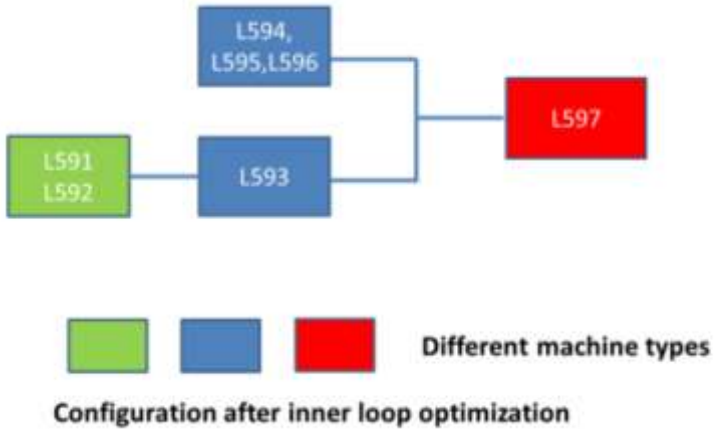

(b)

Figure 3-11 System configuration before and after optimization for R#5 and Module#9

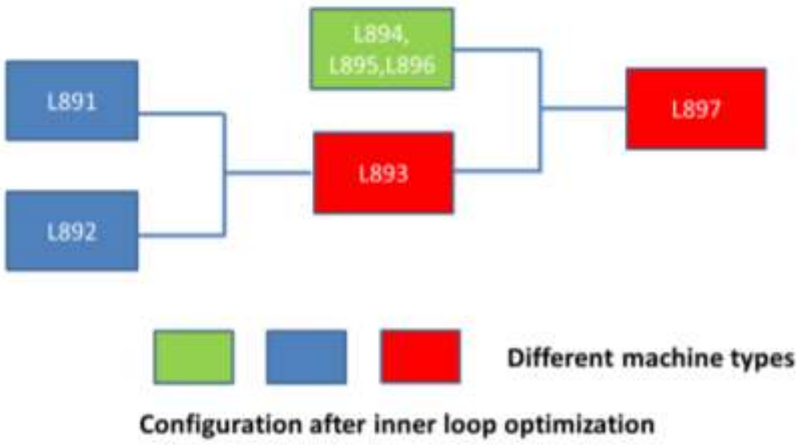

Figure 3-12 System configuration before and after optimization for R#8 and Module#9

If the difference between processing time of final stacker and previous tasks is big, e.g., the final stacking task L597 has significantly longer processing time than all its prior tasks, the final stacker becomes the bottleneck of the whole system. As a result, the inner-loop optimization for all the assembly sequences generates a similar configuration, i.e., tasks prior to the final stacking are assigned to the minimum number of machines and final stacking has two or more machines in parallel (to satisfy the demand). Figure 3-13 shows an example of the configuration after balancing and equipment selection for repetitive pattern case #5 and case #9 of the whole module, given processing time of 5~30 seconds per product for all the stations prior to final stacker and 100~200 seconds per product for the final stacking station. The throughput requirement is increased to 40JPH compared with around 15JPH requirement in the above example.

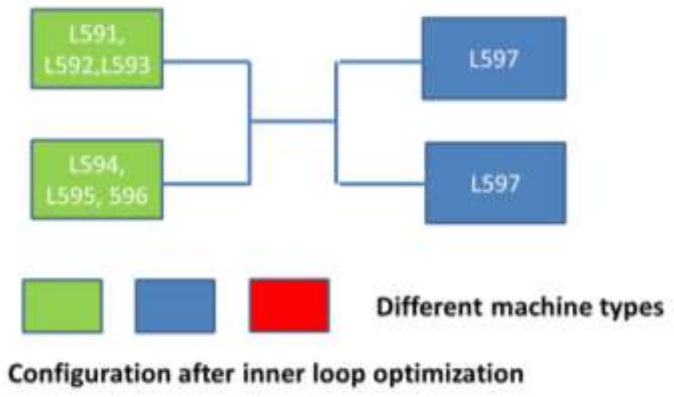

Figure 3-13 Different configuration when processing time between stations are significantly different and throughput requirement is increased

3.4 Conclusion

This chapter develops a new approach for designing optimal assembly system with complex configurations by jointly considering product design hierarchy, line balancing, and equipment selection for a single product type. The system initial configurations are automatically generated making use of the hierarchical and repetitive composition of product designs. A two loop nested optimization algorithm with inner loop and outer loop has been developed to explore all the possible assembly design solutions based on the initial configurations. The outer loop iterates task grouping and sequence generation and compares the performance responses among various configurations. The inner loop explores all the feasible ways of task-machine assignments and machine selection (type & quantity). Compared with the previous research on assembly system configuration generation, the novel contributions of this work are the generation of assembly system configurations considering product assembly hierarchy on non serial task sequences, and the two loop nested optimization of task and assembly sequence generation, equipment selection, and task-machine assignment and balancing.

Future research includes design of material flow path and control logic based on the generated configuration, hybrid system configuration design for multiple products with hierarchical assembly, and manufacturing system reconfiguration.

3.5 Nomenclature

i	Index of tasks; i=1, 2...I;
j	Index of machine types; j=1, 2...J;
k	Label of machine for each type; k=1,2...K_J;
$x_{i,j,k}$	Decision variable;
$y_{i,j}$	Decision variable;
$t_{i,j}$	Processing time of each task i for the jth machine type;
c_{ij}	Operating cost of performing task i on machine type j;
C_0	Machine budget;
$M_{i,j}$	Number of machine j used for task i;
M_i	Total number of machines used for task i;
Th_0	Throughput requirement;
$g_i(\cdot_I)$	Function of material flow relationship between task i and the final task I; $g_i(\cdot_I)$=1;
TM	Set of task machine pairs for matching constraint;
ZS	Set of task pairs for positive zoning constraint;
ZD	Set of task pairs for negative zoning constraint.

CHAPTER 4

ASSEMBLY SYSTEM CONFIGURATION DESIGN FOR A PRODUCT FAMILY

Traditionally, mixed-model assembly systems with a serial configuration are used to manufacture families of products. Task variations associated with different models cause “drift” in such an assembly line. “Drift” is defined as the deviation of system processing time from the nominal cycle time. To more effectively deal with increased product variety, the assembly system can be set up with more complex, non-serial configurations, e.g., systems with multiple subassembly branch lines that converge to an assembly line. Such complex configurations allow for pre-assembly of different components on multiple lines simultaneously, thereby may potentially enhance the system productivity and reduce drift. This chapter establishes a systematic method for designing non-serial system configurations for a family of products. A new mathematical definition for “drift” is introduced and a cumulative sum (CUSUM) analysis is proposed to model the “drift”. Then the “drift” modeling is embedded in an optimal assembly system design problem for task assignment to minimize cost and drift. The method is developed based on a product family with tree type liaisons (no cycle in component connections). A case study of battery pack manufacturing is conducted to demonstrate the method. Conditions are identified when non-serial configuration with branches outperforms conventional mixed-model line in drift reduction.

4.1 Introduction

Nowadays, a nearly endless variety of products is available on the market that can meet almost each customer's specific preferences and needs. In order to keep pace with the fast development of technology and satisfy customers' needs while maintaining a reasonable cost, manufacturers tend to produce product variety through the sharing of components. Many companies are developing product platforms and designing product families in order to provide a sufficient variety of products for the market while achieving low cost. Usually, a product family is defined as a group of related products that are derived from a product platform to satisfy a variety of market needs but is characterized by some common features, components, modules or subsystems [51]. Accordingly, a product platform can be defined as "a set of common components, modules, or parts from which a stream of derivative products can be efficiently developed and launched [52]."

Three types of product platforms have been observed in industry examples:

- *Integral platform*: In the integral platform, all the products in the family share a single part, such as the telecommunications ground network for interplanetary spacecraft [53].
- *Modular platform*: In the modular platform, products are customized by adding, removing or replacing one or more functional modules [51]. For example, *Sony*'s more than 250 models of its Walkmans® are built on key modules [54].
- *Scalable platform*: The scalable platform can be a subset of the modular platform, in which products are developed by scaling the components or modules to satisfy the market needs [51]. For example, *Boeing*'s many

airplanes are “stretched” or “shrunk” according to different applications for transferring passengers and carrying cargo [55].

No matter which product platform a product family is developed from, a product family is composed of common components or modules and variant components or modules. Any given product within a family may have a unique component or module, which is a special case of a variant component or module. Figure 4-1 shows a product family architecture (PFA) [11]. Such an approach enabled high product variety at near mass production cost. Figure 4-2 shows a battery product family example, including one common plate module, two variant repetitive patterns and one unique interconnect cover module.

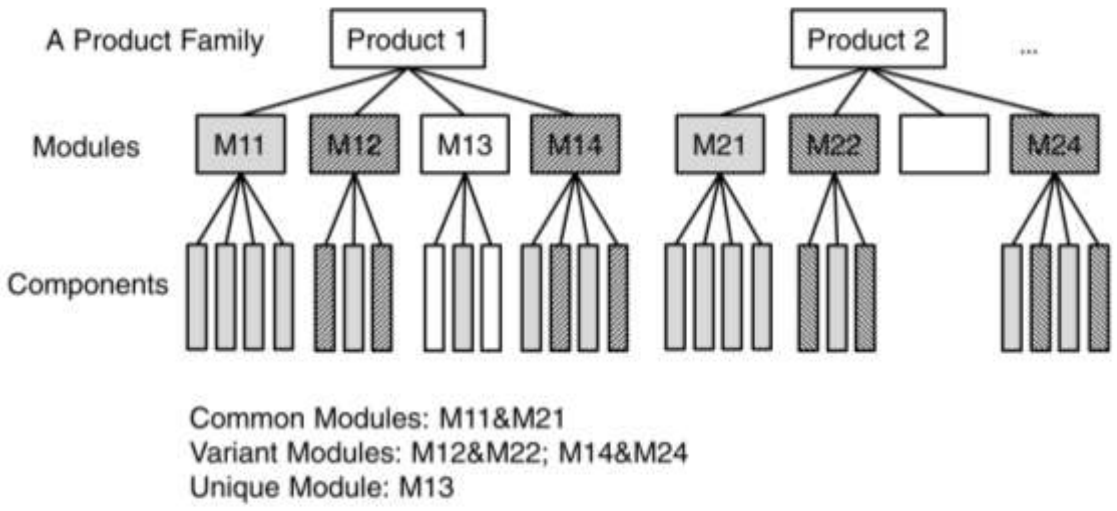

Figure 4-1 A product family architecture (common components are in grey color, variant components are in upward diagonal shape (M12, M14) or downward disgonal shape (M22, M24), unique components are in white color)

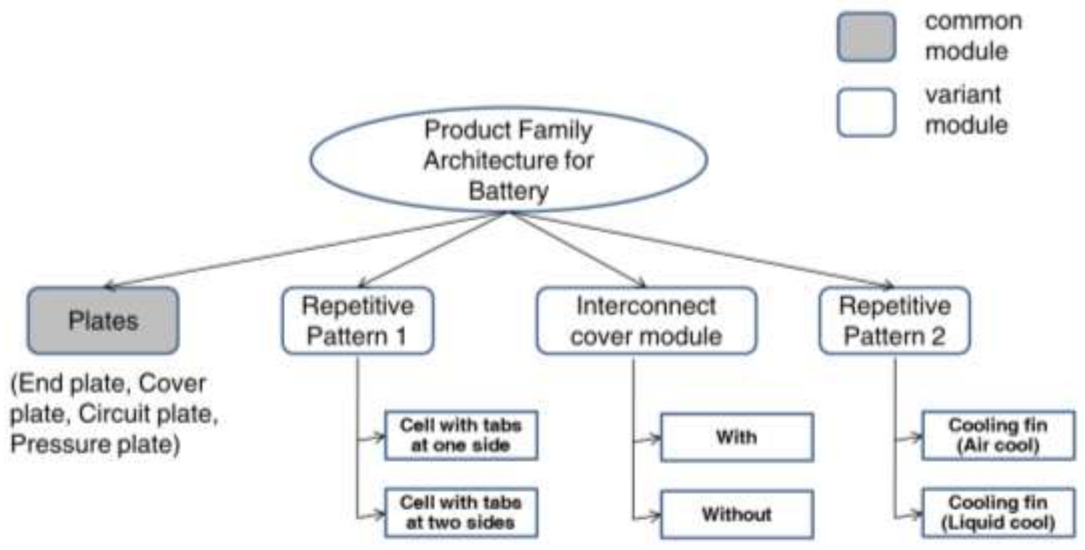
common module
variant module
Product Family Architecture for Battery
Plates
(End plate, Cover plate, Circuit plate, Pressure plate)
Repetitive Pattern 1
Cell with tabs at one side
Cell with tabs at two sides
Interconnect cover module
With
Without
Repetitive Pattern 2
Cooling fin (Air cool)
Cooling fin (Liquid cool)

Figure 4-2 Product family architecture for battery (one common plate module, variant repetitive patterns which differentiate one from the other by either cell tab position or cooling fin structure, one unique interconnect cover module)

Assembly system design requires the representation of assembly hierarchy and components. In addition to the PFA method to represent the relationship among components or modules in an assembly, several methods are available, such as liaison graph, Bill-of-Material (BOM), precedence graph. Liaison graph is a graphical network where nodes represent components and lines between nodes represent relations between components, such as physical contact or joining. The assembly representation methods for both a single product and a product family were reviewed by Hu et al. [11].

A tree type liaison graph is used to represent the topographic patterns for a battery product family. Figure 4-3 shows the generalized liaison graph representation of the battery example, where the grey circle represents common components (e.g. plates) and white circle represents variant components, such as cells with tabs at either one side or two sides, cooling fins with either air cool or liquid cool structure.

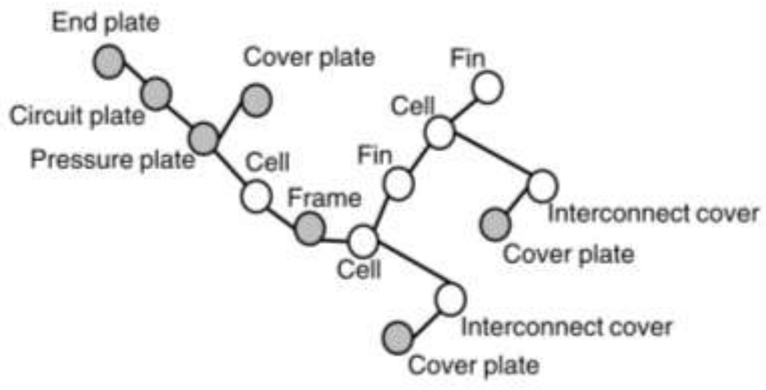

Figure 4-3 A liaison graph representation (grey circle represents common components and white circle represents variant components)

Each product is composed of components or modules that are linked to each other following certain topographic patterns, such as a tree type structure (without loop) as shown in Figure 4-3. This chapter mainly studies the system configuration design method for a family of products with a tree type structure. The method to identify assembly/subassembly grouping given a liaison graph was introduced in Chapter 2.

After representing the relationship among components in a product family, the design of an assembly system often begins with assembly precedence identification and sequence generation [33-34]. Bourjault presented the first algorithm that generated all feasible assembly sequences by a series of "yes" or "no" questions [18]. De Fazio and Whitney built on Bourjault's method, simplified the determination of precedence constraints, and increased the size of the problem to accommodate assemblies with much higher component numbers [19]. Lots of research took advantage of a computer aid for automatic assembly sequence generation and planning [56-59]. Methods were also developed to derive the assembly sequences from the disassembly sequences [24-25]. Those traditional assembly sequence generation methods are based on sequential task sequences generation, i.e. adding one part at a time. Li *et al*. [16] considered concurrent task sequences and adding more than one part at a time in generating all feasible subassemblies. The method utilized a hierarchical subassembly decomposition to facilitate automatic configuration of assembly systems for a single product and can potentially enhance the system throughput.

Based on a set of feasible assembly sequences, the design of an assembly system then creates optimal system configurations and balances the assembly system by assigning tasks to machines and selecting appropriate machine types and quantities. In order to handle a variety of products, different configurations have been designed. Figure 1-6 shows different system configurations: a serial configuration, a parallel configuration, a serial system with parallel machines and a parallel system with serial machines.

After a configuration is chosen, assembly line balancing problem is to search for the optimal assignment of assembly tasks to stations given precedence constraints according to a pre-defined single or multi-objective goal: such as 1) minimize the idle time, 2) minimize number of stations/minimize cost, 3) maximize system productivity/throughput etc [11]. For multiple product assembly lines, two approaches were suggested: 1) a mixed-model line which produces product variants on the same line in an arbitrarily intermixed sequence, 2) a multi-model line which produces product variants in a sequence of batches (Figure 4-4) [60].

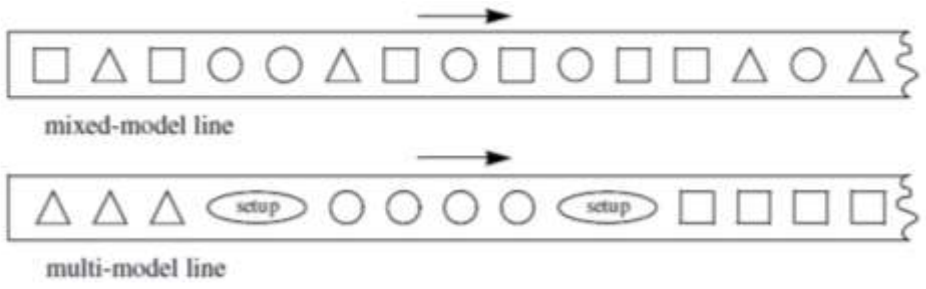

Figure 4-4 Assembly lines for multiple products [60]

For both mixed-model line and multi-model line, because the production of multiple products is executed on the same line, task variations associated with different models cause “drift” in balancing such an assembly line. Drift represents the deviation from the nominal cycle time, where positive drift describes the time exceeding the predefined cycle time regarding one product variant and negative drift describes the time during which no assembly work is needed regarding one product variant (Figure 4-5) [12-13]. The ideal line balancing is to have neither bottleneck station nor idle station. Because of the different assembly process characteristics of different model variants, “drift”, the deviation from nominal cycle time, exists in line balancing for product variety.

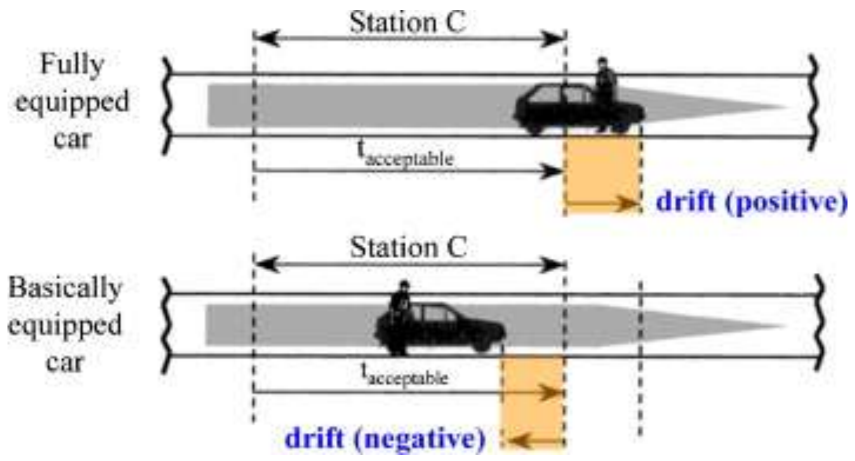

Figure 4-5 Positive and negative drift in accordance with [12] and [13]

The existing research addressing the drift problem focused on serial line balancing [61-65]. To more effectively deal with increased product variety, the assembly system can be set up with more complex, non-serial configurations, e.g., systems with multiple subassembly branches that converge to an assembly line (Figure 4-6). There is a lack of research on non-serial system configuration design and drift analysis for product variety. Furthermore, although drift has been discussed in the previous literature, there is a lack of quantitative measurement of drift. This chapter describes a systematic method for designing assembly system configurations for a family of products: a new mathematical definition for “drift” is introduced; a CUSUM analysis is proposed to model the “drift”; and the “drift” modeling is embedded in the optimal assembly system design problem to minimize cost and drift.

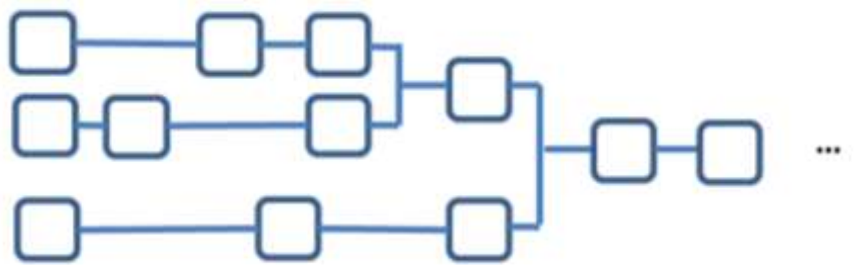

Figure 4-6 Example of non-serial configuration

The remainder of the chapter is organized as follows. Section 4.2 introduces the method of system configuration design for product variety. An overview of method is discussed first and then the mathematical model is introduced. Section 4.3 presents an example of system design given a battery product family configuration. Section 4.4 draws the conclusions.

4.2 System configuration design for product variety

4.2.1 Method overview

The overall procedure for system configuration design for product variety still follows a nested procedure for combinatorial optimization as discussed in Chapter 3. Figure 4-7 shows the procedure highlighting the differences between this work and previous research, and the contributions of this work. The differences and contributions are: 1) Different from past research that focused on assigning tasks to machines in serial configuration, this method considers complex, non-serial configurations for product variety; 2) “Drift”, the deviation of system processing time from the nominal cycle time, is mathematically defined and a CUSUM analysis is adopted to model the “drift”; 3) “drift” modeling is embedded in the optimal assembly system design problem for product variety; 4) Conditions are identified when non-serial configuration with branches outperforms conventional mixed-model line in drift reduction. As shown in Figure 4-7, the algorithm first takes several product designs in a product family as inputs. After identifying the liaison relationship and precedence constraints, a joint liaison graph is generated. Based on the joint liaison graph, the hierarchical subassembly decomposition method as discussed in Chapter 2 (outer loop optimization) is used. The inner loop optimization is formulated to minimize drift under a stochastic product demand mix. At last, discussions are performed to identify conditions when non-serial configuration with branches outperforms conventional mixed-model line.

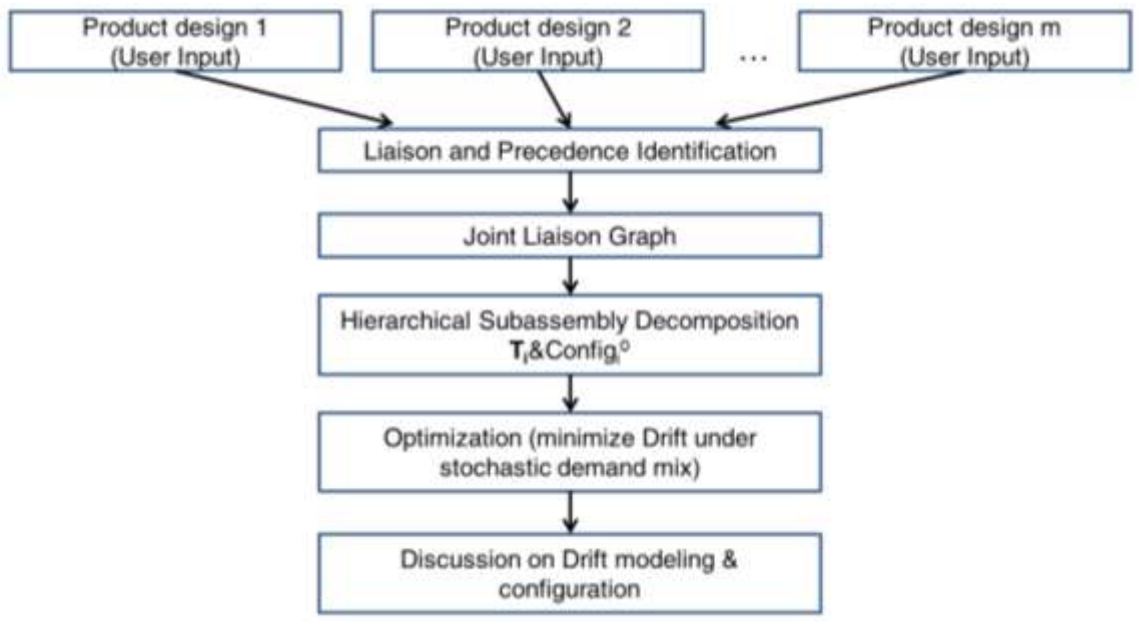
Product design 1 (User Input)
Product design 2 (User Input)
...
Product design m (User Input)
Liaison and Precedence Identification
Joint Liaison Graph
Hierarchical Subassembly Decomposition
T_i&Config_i^o
Optimization (minimize Drift under stochastic demand mix)
Discussion on Drift modeling & configuration

Figure 4-7 Methodology overview for system configuration design for product variety

4.2.2 Mathematical representation of drift

Drift is defined as the deviation of system processing time from the nominal cycle time [12]. Drift exists because of the stochastic changes of product demand mix over time.

Stochastic product demand mix

Because customer preferences may change over time period *l=1 ... L*, the demand of different products in a product family also changes. For example, at one time period, the strategy may be to have a balanced distribution of products; at other time periods, the strategy may be to have one or more primary products. Given the demand percentage of each final product, the required percentage of each component can be calculated correspondingly. For ease of mathematical representation, let $(\alpha_1^l, \alpha_2^l, \ldots, \alpha_s^l, \ldots, \alpha_m^l)$ be the percentage of one variant component at time period *l*, and $(\beta_1^l, \beta_2^l, \ldots, \beta_t^l, \ldots, \beta_n^l)$ be the percentage of another variant component, and so on. For example, as shown in Figure 4-8, A and B are variant components, therefore AB (final product) has four variations. Let Q denote the set of all possible assembly combinations,

$$Q = \{q_l | l = 1, \ldots, L\} \, where \, q_l = \{(\alpha_1^l, \alpha_2^l, \ldots, \alpha_s^l, \ldots, \alpha_m^l), (\beta_1^l, \beta_2^l, \ldots, \beta_t^l, \ldots, \beta_n^l), \ldots\}.$$

Determination of system processing time for different configurations

In order to formulate the mathematical representation of drift, system processing time needs to be determined. System processing time is defined as the maximum processing time among all machines. On each machine, the processing time is a weighted sum of all processing times of different components. For example, in Figure 4-9, two varieties of component A$\{A_1, A_2\}$ are loaded using machine A according to their demand percentages, and two varieties of component B$\{B_1, B_2\}$ are loaded using machine B. The

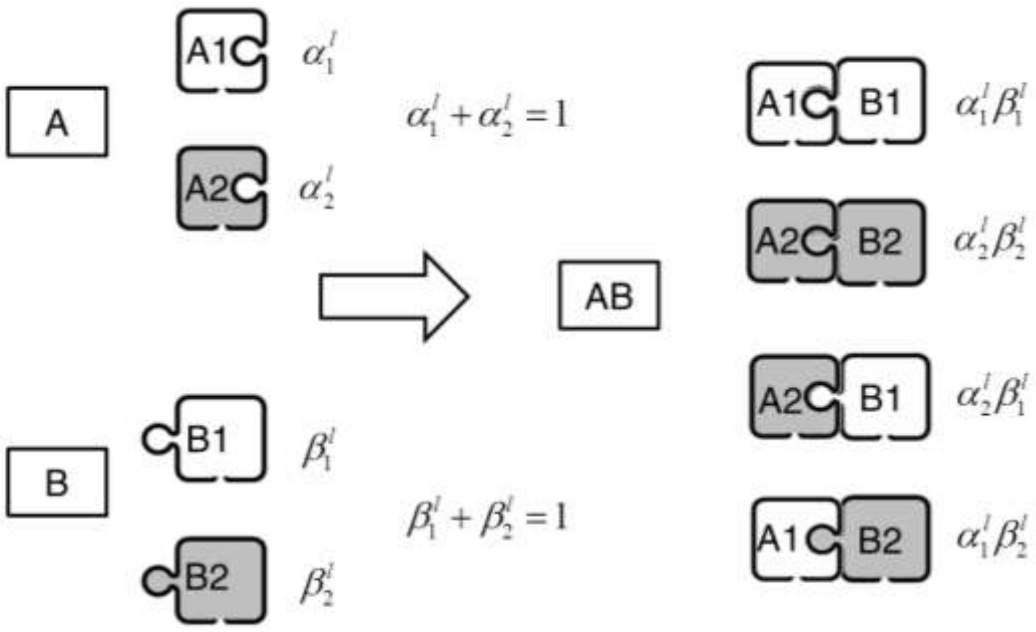

Figure 4-8 Example of possible component and product variations and their demand percentages representation (the percentages of variant component A are A1: α_1^l, A2: α_2^l; variant component B are B1: β_1^l, B2: β_2^l; final products are A1B1: $\alpha_1^l\beta_1^l$, A2B2: $\alpha_2^l\beta_2^l$, A2B1: $\alpha_2^l\beta_1^l$, A1B2: $\alpha_1^l\beta_2^l$)

final stacker (Machine C) assembles component A and B into different final products $\{A_1B_1, A_2B_2, A_2B_1, A_1B_2\}$. The system processing time is calculated as

$$\begin{aligned} t = \max\{&t_{a1,load}\alpha_1 + t_{a2,load}\alpha_2, t_{b1,load}\beta_1 + t_{b2,load}\beta_2, \\ &t_{a1b1,asm}\alpha_1\beta_1 + t_{a2b2,asm}\alpha_2\beta_2 + t_{a2b1,asm}\alpha_2\beta_1 + t_{a1b2,asm}\alpha_1\beta_2\} \end{aligned} \tag{1}$$

In general, the system processing time can be formulated as

$t^{q_l} = \max\{\sum_{s=1}^{m}\sum_{t=1}^{n}...(\alpha_s^l\beta_t^l...)_{(s,t,...)\in i}t_i\}$where

$(\alpha_1^l, \alpha_2^l, ..., \alpha_s^l, ..., \alpha_m^l)$ is the percentage of one variant component at time period *l*,

$(\beta_1^l, \beta_2^l, ..., \beta_t^l, ..., \beta_n^l)$ is the percentage of another variant component at time period *l*; (2)

$(\gamma_1^l, \gamma_2^l, ..., \gamma_u^l, ..., \gamma_o^l)$...

t_i is the task time

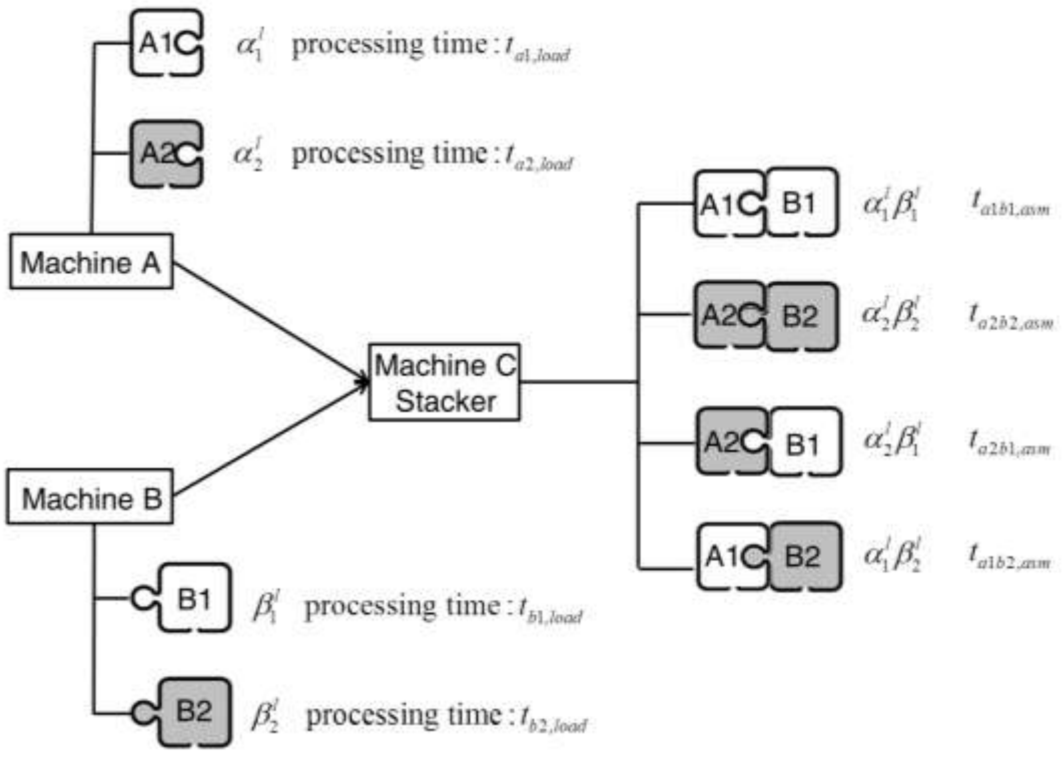

A1
α_1^l processing time : $t_{a1,load}$
A2
α_2^l processing time : $t_{a2,load}$
Machine A
Machine C Stacker
Machine B
B1
β_1^l processing time : $t_{b1,load}$
B2
β_2^l processing time : $t_{b2,load}$
A1 B1 $\alpha_1^l\beta_1^l$ $t_{a1b1,asm}$
A2 B2 $\alpha_2^l\beta_2^l$ $t_{a2b2,asm}$
A2 B1 $\alpha_2^l\beta_1^l$ $t_{a2b1,asm}$
A1 B2 $\alpha_1^l\beta_2^l$ $t_{a1b2,asm}$

Figure 4-9 Example of processing time calculation

Mathematical representation of drift

Drift exists in the system because of the changes of product demand mix. For example, at time period 1 (*l*=1), final products $\{A_1B_1, A_2B_2, A_2B_1, A_1B_2\}$ are produced according to the ratio of {30%, 20%, 20%, 30%}; at time period 2 (*l*=2), final products are produced according to the ratio of {25%, 25%, 25%, 25%} due to customer preference change. This product demand mix continue to change over time period *l=1 … L*. Since drift is defined as the deviation of system processing time from the nominal cycle time and the product demand mix change is a continuous process, drift can be formulated as $C_l = \sum_{m=1}^{l}(t^{q_m} - c_0)$, which is similar to CUSUM analysis in statistical quality control, where t^{q_m} is the processing time at time *m*, c_0 is the nominal cycle time.

The system processing time t^{q_m} is a function of $\alpha, \beta, \gamma, \ldots$, therefore it changes due to the changes of product demand mix. As shown in Figure 4-10, the system processing time sometimes is greater than the nominal cycle time c_0, and sometimes is less than the nominal cycle time.

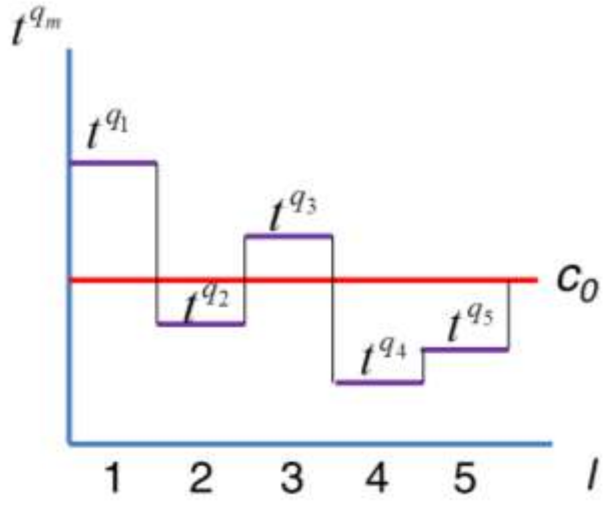

Figure 4-10 System processing time vs planning horizon (time)

C_l is the cumulative sum up to and including time period *l*. C_l incorporates all the information in the sequence of planning horizon. Figure 4-11 plots the positive drift and negative drift from example in Figure 4-10. Ideally, $C_l \sim= 0$ is expected at every different time period *l*.

$$C_l = \sum_{m=1}^{l}(t^{q_m} - c_0) = C_{l-1} + \left(t^{q_l} - c_0\right) \qquad where\ \ C_{l-1} = \sum_{m=1}^{l-1}\left(t^{q_m} - c_0\right) \tag{3}$$

If the process is treated as a deterministic process, i.e. at every time period *l*, the product demand mix is known, the total drifts of the assembly system over time period *l=1 … L,* can be defined as

$$\sum_{l=1}^{L}|C_l| = \sum_{l=1}^{L}\left|\sum_{m=1}^{l}(t^{q_m} - c_0)\right| = |t^{q_1} - c| + |t^{q_1} - c + t^{q_2} - c| + ... + |t^{q_1} - c + t^{q_2} - c + ... + t^{q_L} - c| \quad (4)$$

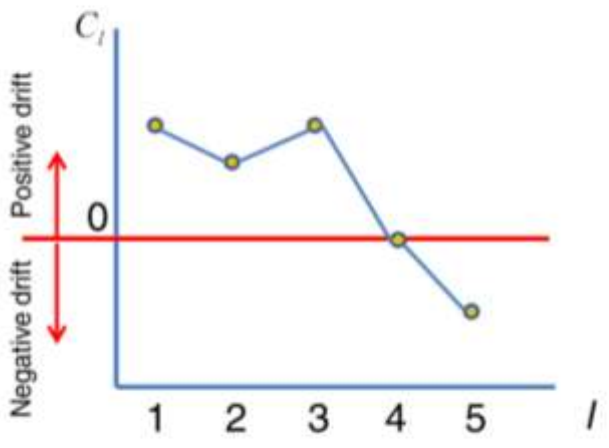

Figure 4-11 Plot of the positive drift and negative drift

The absolute value is used because the imbalance of the assembly line can result from either positive drift or negative drift, where positive drift represents the time exceeding the optimal cycle time and negative drift represents the idle time for one or more of the product variants [11].

The process can also be treated as a stochastic process, i.e. the product demand mix follows a certain distribution, and therefore system processing time t^{q_l} becomes a random variable. Actually at the design stage of an assembly system, the changes of product demand mix are unknown and the objective can only be set to minimize the variation of drift. The detail is discussed in the objective function in section 4.2.4.

4.2.3 Generation of joint liaison graph

Given the liaison graph for each product, a joint liaison graph can be generated according to Thomopoulos's concept of a combined precedence diagram to join the precedence relations of different models on a single diagram [66]. Precedence matrices can be used to construct the joint precedence graph [67]. A precedence matrix is an upper-triangular matrix with the entry to be either 1 or 0: if the processing of column task requires the completion of row task, the entry is 1; otherwise, the entry is 0. Let AB = {a_1b_1, a_1b_2, …, a_mb_n} denotes all the task combination in the precedence matrix. So we have:

$$AB = \begin{array}{c} \\ a_1 \\ a_2 \\ \cdots \\ a_m \end{array} \begin{array}{c} \begin{array}{cccc} b_1 & b_2 & \cdots & b_n \end{array} \\ \begin{bmatrix} a_1b_1 & a_1b_2 & \cdots & a_1b_n \\ a_2b_1 & & & \cdots \\ \cdots & & & \cdots \\ a_mb_1 & \cdots & \cdots & a_mb_n \end{bmatrix} \end{array} \text{ where } a_ib_j = \begin{cases} 1 & \textit{task } b_j \textit{ is an successor of task } a_i \\ 0 & \textit{otherwise} \end{cases}$$

A detailed discussion of combined precedence graph can be found in [66], [68] and [69]. A simple example using a battery product family is shown in Figure 4-12. A, B, C, D, E denotes battery components. One battery has the assembly pattern as B-A-D-A-C-E, and the other battery has the assembly pattern as B-A-A-D-A-C. Numbers 1-6 and T01-T06 denote the assembly tasks. Given the liaison graph for each battery product, their precedence matrices can be generated as shown in Figure 4-12. Therefore, the joint precedence matrix can be constructed according to the rule discussed above. Furthermore, if there are any implied precedence relations, then the related entry in the joint precedence matrix should also be 1. For example, in Figure 4-12, T06 is a successor of T05, therefore T06 is the successor of every preceding tasks of T05. The joint liaison graph can be generated based on the joint precedence matrix.

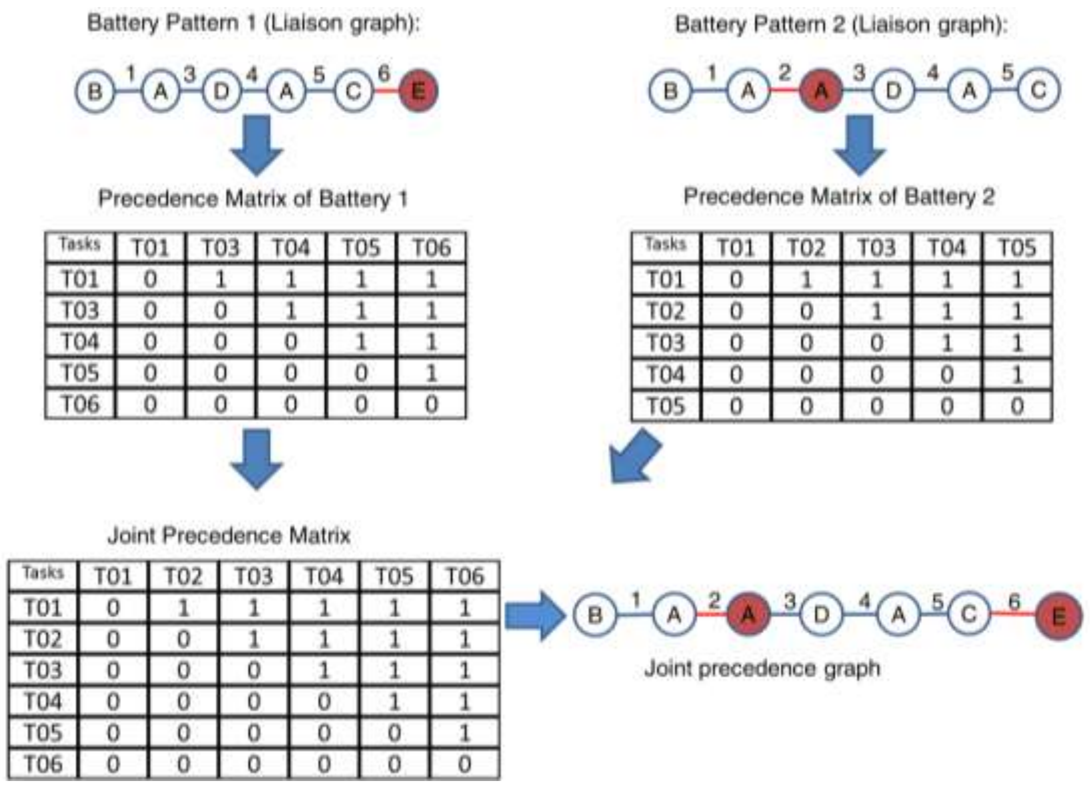
Battery Pattern 1 (Liaison graph):
B 1 A 3 D 4 A 5 C 6 E
Battery Pattern 2 (Liaison graph):
B 1 A 2 A 3 D 4 A 5 C
Precedence Matrix of Battery 1
Precedence Matrix of Battery 2
Joint Precedence Matrix
B 1 A 2 A 3 D 4 A 5 C 6 E
Joint precedence graph

Tasks	T01	T03	T04	T05	T06
T01	0	1	1	1	1
T03	0	0	1	1	1
T04	0	0	0	1	1
T05	0	0	0	0	1
T06	0	0	0	0	0

Tasks	T01	T02	T03	T04	T05
T01	0	1	1	1	1
T02	0	0	1	1	1
T03	0	0	0	1	1
T04	0	0	0	0	1
T05	0	0	0	0	0

Tasks	T01	T02	T03	T04	T05	T06
T01	0	1	1	1	1	1
T02	0	0	1	1	1	1
T03	0	0	0	1	1	1
T04	0	0	0	0	1	1
T05	0	0	0	0	0	1
T06	0	0	0	0	0	0

Figure 4-12 Precedence matrices and joint precedence graph (A-E circles denote the battery components, where the dark circles differentiate batteries in a product family, Numbers 1-6 denote the different assembly tasks)

4.2.4 Assembly system configuration design for product variety

This section describes a mathematical model for the inner loop optimization including decision variables, objective functions and constraints. The optimization problem explains task-machine assignment and workload balancing in assembly systems.

<u>Decision Variables</u>

A task-station assignment variable $x_{i,k}$ is used to represent whether or not a task is assigned to a station.

$$x_{i,k} = \begin{cases} 1 & \text{if task } i \text{ is assigned to the kth station} \\ 0 & \text{otherwise} \end{cases}$$

N_k is the number of machines for station k.

Objective function

The objective in this model is to design an assembly system by minimizing the drift caused by different assembly process characteristics of different products in a family. The main reason that drift exists is that product demand mix changes stochastically. The percentages of variant components $\alpha, \beta, \gamma, ...$ are assumed to be independent and they all follow uniform distribution from 0 to 1, i.e. $\sim U(0,1)$. The system processing time t^{q_m} is a function of $\alpha, \beta, \gamma, ...$, therefore it changes at different time.

The objective is to minimize the variation of drift because of the stochastic nature of system processing time. The objective function is expressed as:

$$\min \ Var(| t^{q_l} - c_0 |)$$

$$\begin{aligned} &Since\ Var(| t^{q_l} - c_0 |) = E[(| t^{q_l} - c_0 |)^2] - [E(| t^{q_l} - c_0 |)]^2 \\ &= E[(t^{q_l})^2] - 2c_0 E(t^{q_l}) + c_0^2 - [E(| t^{q_l} - c_0 |)]^2 \\ &= E[(t^{q_l})^2] - 2c_0 E(t^{q_l}) + c_0^2 - [E(t^{q_l})]^2 + 2c_0 E(t^{q_l}) - c_0^2 \end{aligned}$$

$$Var(| t^{q_l} - c_0 |) = E[(t^{q_l})^2] - [E(t^{q_l})]^2 \tag{5}$$

Constraints

1) Task assignment constraint

This constraint specifies that each task must be assigned to one and only one station.

$$\sum_{k=1}^{K} x_{i,k} = 1 \tag{6}$$

2) Throughput constraint

This constraint ensures that the throughput satisfies the demand of final products and can be represented by

$$\sum_{i=1}^{I} \frac{t_i x_{i,k}}{c_0} \le N_k \tag{7}$$

3) Precedence constraint

This constraint ensures that the precedence relationship can be preserved.

$$\sum_{k=1}^{K} k \cdot x_{i,k} \le \sum_{k=1}^{K} k \cdot x_{j,k}, \quad \forall \, task \;\, j \; and \; i \in \mathbf{P}_j \tag{8}$$
$$\mathbf{P}_j : \; Set \; of \;\; tasks \; that \; must \; precede \; task \; j$$

4) Cost constraint

This constraint requires that total cost including operation penalty cost and amortized annual station cost not to exceed the budget. Penalty cost is incurred due to multiple tasks assigned in one station. If there are more assembly tasks to be processed in one station, the penalty cost is larger. For example, Figure 4-13 explains the penalty cost and station cost. Configuration 1 has one single station (*K*=1) with three parallel machines. Each machine allows loading and assembling all the components (Cell, Fin, Cell, and Frame denoted by C, F, C, Fr) at the same time. Configuration 2 has three stations (*K*=3) with one machine at each station. Only the first station allows assembling two components, and the other two stations only allow assembling one component at a time. The station cost of configuration 2 is higher than configuration 1. The penalty cost of configuration 1 is higher than the penalty cost of configuration 2 at each of its station since more assembly tasks are processed at one station in configuration 1.

$$\sum_{k=1}^{K} N_k (c_k + c) \le G_0 \tag{9}$$

c_k is the penalty cost at the kth station

c is the station cost

G_0 *is the budget*

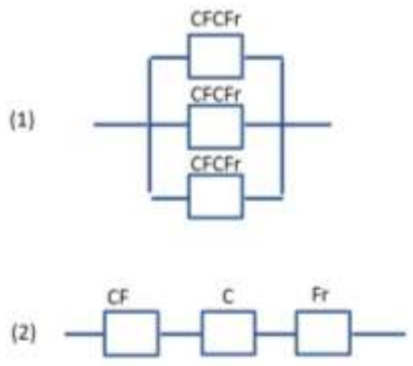

Figure 4-13 Example configuration to explain penalty cost and station cost

5) Zoning constraint:

Some tasks must be assigned to the same station, and the other tasks cannot be assigned to the same station. These constraints are known as positive and negative zoning constraints. For example, tasks requiring similar manufacturing processes or a very expensive machine may be assigned to one station in order to reduce station cost. Tasks requiring different types of manufacturing processes or having certain safety requirements usually cannot be assigned to the same station. The following two equations represent positive and negative constraints, respectively.

$$\begin{aligned} &x_{u,k} = x_{v,k}, (u,v) \in ZS\text{--set of tasks that must be assigned to the same station} \\ &x_{u,k} + x_{v,k} \le 1, (u,v) \in ZD\text{--set of tasks that cannot be on the same station} \end{aligned} \tag{10}$$

<u>Solution Method</u>

The problem is a mixed integer linear programming (MIP) problem that can be solved by any integer programming solvers such as Gurobi.

4.3 Case study

This section demonstrates the configuration generation and line balancing method using a case study of two battery module assemblies. “Drift” is compared between different configurations.

4.3.1 Problem description and results

As shown in Figure 4-14, the repetitive pattern in all of the battery modules is the same: cell-cooling fin-cell-frame. But the types of cell and cooling fin are different depending on the cell tab position (one sided tab/two sided tab) and battery cooling method (air cool/liquid cool), and their repeating time (*N*) is also different. Non-repetitive components are added to the two ends of the repetitive pattern stack to form the module. The whole module pattern is end plate + fin + N*(cell + fin + cell + frame) + end plate.

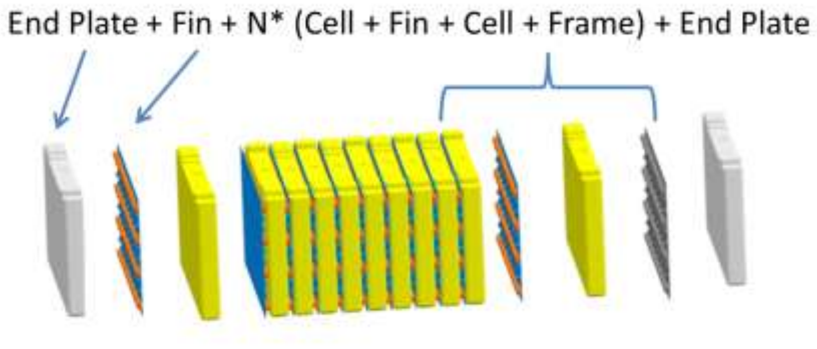
End Plate + Fin + N* (Cell + Fin + Cell + Frame) + End Plate

Figure 4-14 An example of assembly pattern of battery module

Let C, E, F, M denote the cell, end plate, cooling fin and frame respectively. The assembly pattern for the whole module is E + F + N*(C + F + C + M) + E. Table 4-1 shows the enumeration results for the repetitive pattern and Table 4-2 shows the enumeration results for the whole module. If there are no constraints applied, there are a total of 11 possible sequences generated in each case [15].

Table 4-1 Enumeration results for the repetitive pattern

Case#	1	2	3	4
Seq.	((CF)CM)	(((CF)C)M)	((CF)(CM))	(C(FC)M)
Case#	5	6	7	8
Seq.	((C(FC))M)	(C((FC)M))	(CF(CM))	(C(F(CM)))
Case#	9	10	11	
Seq.	((CFC)M)	(C(FCM))	(CFCM)	

Table 4-2 Enumeration results for the battery module ("R" represents repetitive pattern)

Case#	1	2	3	4
Seq.	((EF)RE)	(((EF)R)E)	((EF)(RE))	(E(FR)E)
Case#	5	6	7	8
Seq.	((E(FR))E)	(E((FR)E))	(EF(RE))	(E(F(RE)))
Case#	9	10	11	
Seq.	((EFR)E)	(E(FRE))	(EFRE)	

Given the demand percentage of four final battery modules, the required percentage of components can be calculated correspondingly. For ease of mathematical representation, let $\alpha_1^l, \left(1-\alpha_1^l\right)$ be the demand percentage of cell C1 and C2 at time *l*, $\alpha_2^l, \left(1-\alpha_2^l\right)$ be the percentage of cooling fin F1 and F2 at time *l*, respectively. For example, if the required demand percentage for each product is 1/4 of the total demand, $\alpha_1^l = \alpha_2^l = 0.5$ is needed to achieve the target throughput. Table 4-3 shows the possible product variations and their demand percentages. Among them, the repeating time for product 1 and 4 is N_1=N_4=12; for product 2 and 3 is N_2=N_3=10.

Table 4-3 Product variety representation and demand percentage

Product #	Product Variety	Demand Percentage
Product 1	EF1(C1F1C1M)E or EF1R1E	$\alpha_1^l \alpha_2^l$
Product 2	EF2(C1F2C1M)E or EF2R2E	$\alpha_1^l (1-\alpha_2^l)$
Product 3	EF1(C2F1C2M)E or EF1R3E	$(1-\alpha_1^l)\alpha_2^l$
Product 4	EF2(C2F2C2M)E or EF2R4E	$(1-\alpha_1^l)(1-\alpha_2^l)$

To illustrate the optimization procedure, consider case #2 as the battery assembly repetitive pattern. Table 4-4 lists the assembly tasks for the repetitive pattern. The task sequence is shown in Figure 4-15. Assume the base cost for assembling one task at each machine is \$1M, and proportionally increases as the # of assembly tasks increases at one machine. Zoning constraints require that the assembly tasks cannot all be assigned to one station with parallel machines because of the practical issues, such as redesign of machine tools and reliability issues etc. Amortized annual station cost c= \$0.5M. The task processing time is given in Table 4-5. Given the throughput requirement as 150,000 modules per year ($Th_0 = 30JPH$), the target cycle time (c_0) is 120 second. Table 4-6 shows the optimization results for repetitive pattern case #2. Similarly, perform optimization algorithm to all the repetitive patterns. The results are summarized and shown in Figure 4-16. Under current condition, non-serial configuration with branches (configuration 4) outperforms conventional serial line (configuration 3) in drift reduction given the same cost.

Table 4-4 Assembly tasks description

Task #	Description
L01	Assembly of components C & F (C1F1 or C1F2 or C2F1 or C2F2)
L02	Assembly of components CF & C
L03	Assembly of components CFC & M

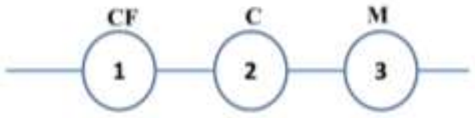

Figure 4-15 Task sequence graph for battery repetitive pattern assembly

Table 4-5 Processing time for the example problem

Loading	$t_{C1} = 2\sec$	$t_{C2} = 3\sec$	$t_{F1} = 2\sec$	$t_{F2} = 3\sec$	$t_{M} = 2\sec$
Assembly (2 components)	$t_{C1,F1} = 3$	$t_{C1,F2} = 4$	$t_{C2,F1} = 4$	$t_{C2,F2} = 5$	$\dots$
Assembly (3 components)	$t_{F1,C1,M} = 8$	$t_{F2,C1,M} = 9$	$t_{F1,C2,M} = 9$	$t_{F2,C2,M} = 10$	$\dots$
Assembly (4 components)	$t_{C1,F1,C1,M} = 10$	$t_{C1,F2,C1,M} = 11$	$t_{C2,F1,C2,M} = 11$	$t_{C2,F2,C2,M} = 12$	$\dots$

Table 4-6 Optimization results for case #2

Configuration	Drift and Cost Calculation
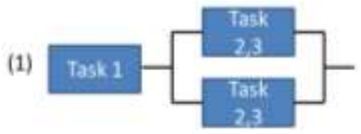	$Drift: Var(\lvert t^{q_l} - c_0 \rvert) = 8143 - (89)^2 = 222(\sec)$ $Cost: \sum_{k=1}^{K} N_k(c_k + c) = 1*(1+0.5) + 2*(2+0.5) = 6.5(\$M)$
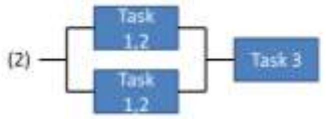	$Drift: Var(\lvert t^{q_l} - c_0 \rvert) = 10208 - (100)^2 = 208(\sec)$ $Cost: \sum_{k=1}^{K} N_k(c_k + c) = 2*(2+0.5) + 1*(1+0.5) = 6.5(\$M)$
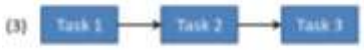	$Drift: Var(\lvert t^{q_l} - c_0 \rvert) = 11817 - (108)^2 = 153(\sec)$ $Cost: \sum_{k=1}^{K} N_k(c_k + c) = 1*(1+0.5) + 1*(1+0.5) + 1*(1+0.5) = 4.5(\$M)$

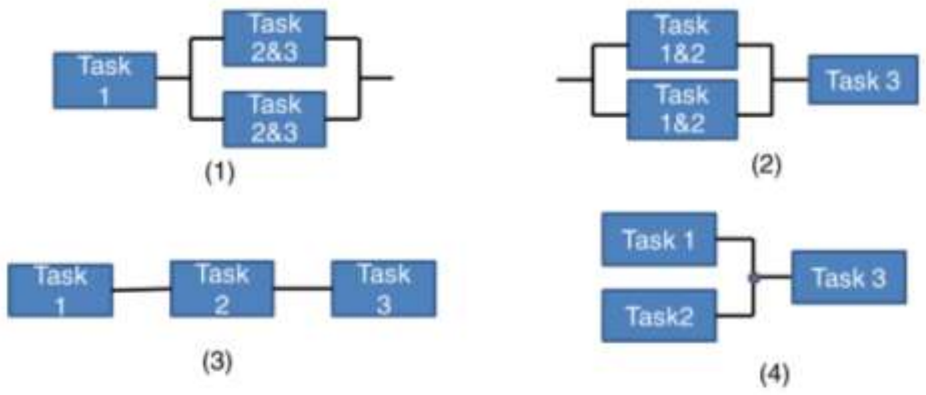

(a) candidate configurations

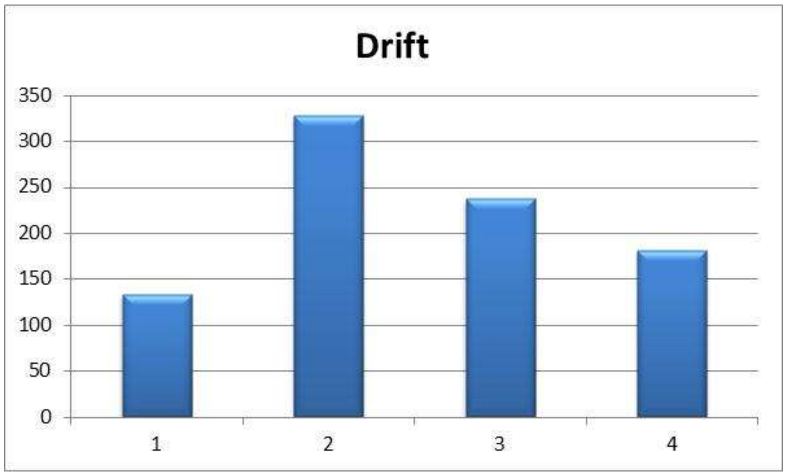

(b) drift comparison among candidate configurations

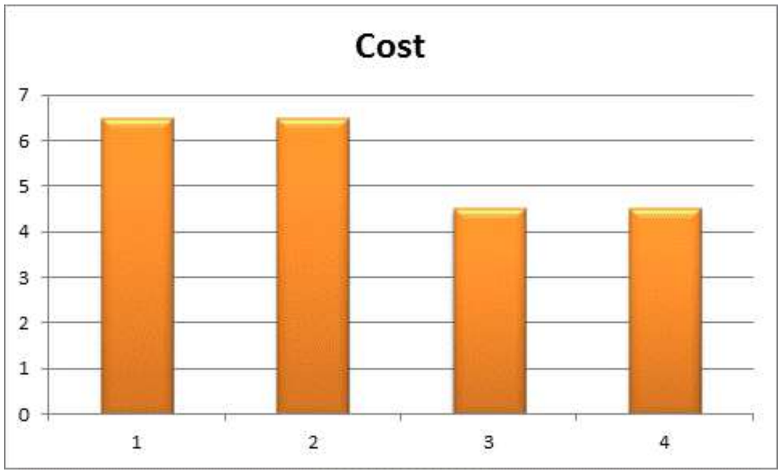

(c) cost comparison among candidate configurations

Figure 4-16 Optimization results for all the repetitive patterns (a) candidate configurations (b) drift comparison (c) cost comparison

4.3.2 Discussion

In the above example, given the processing time as shown in Table 4-5, non-serial configuration with branches outperforms conventional serial line in drift reduction under the same cost. If the assembly time on the bottleneck machine is reduced due to faster machines, and the loading and other assembly times are kept the same as shown in Table 4-7, the drift comparison between conventional serial line and non-serial configuration with branches are shown in Figure 4-17. Under this condition, the conventional serial line (configuration 3) outperforms non-serial configuration with branches (configuration 4) in drift reduction under the same cost.

Table 4-7 Processing time (assembly time on the bottleneck machine is reduced compared with the case study)

Loading	$t_{C1}=2\sec$	$t_{C2}=3\sec$	$t_{F1}=2\sec$	$t_{F2}=3\sec$	$t_M=2\sec$
Assembly (2 components)	$t_{C1,F1}=2$	$t_{C1,F2}=3$	$t_{C2,F1}=3$	$t_{C2,F2}=4$	$\dots$
Assembly (3 components)	$t_{F1,C1,M}=8$	$t_{F2,C1,M}=9$	$t_{F1,C2,M}=9$	$t_{F2,C2,M}=10$	$\dots$
Assembly (4 components)	$t_{C1,F1,C1,M}=10$	$t_{C1,F2,C1,M}=11$	$t_{C2,F1,C2,M}=11$	$t_{C2,F2,C2,M}=12$	$\dots$

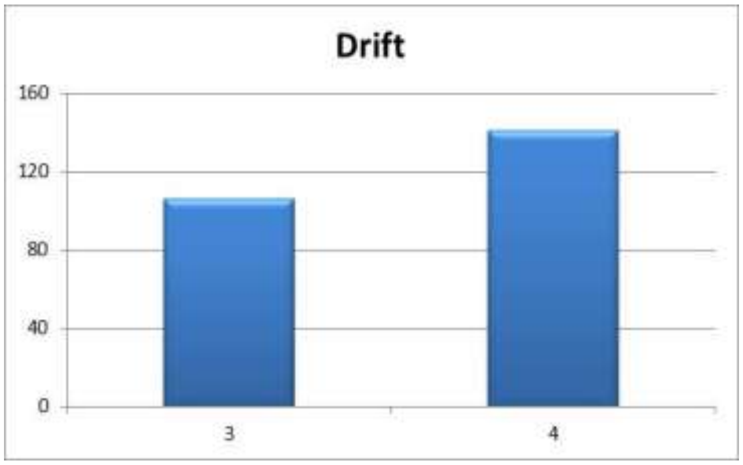

Figure 4-17 Drift comparison between serial line and branched line

An automatic algorithm is implemented in a Graphical User Interface (GUI) as shown in Figure 4-18. In practical, engineers can input a range of task processing times and obtain the optimal configurations with smallest drift and cost.

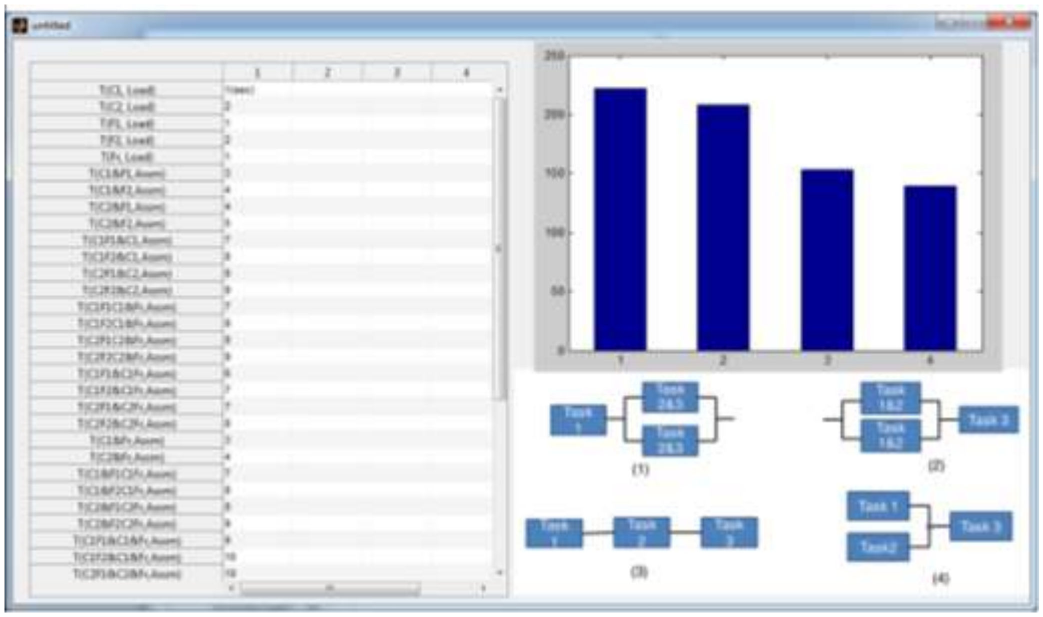

	1	2	3	4
T(C1, Load)	1(sec)			
T(C2, Load)	2			
T(F1, Load)	1			
T(F2, Load)	2			
T(Fc, Load)	1			
T(C1&F1, Assm)	3			
T(C1&F2, Assm)	4			
T(C2&F1, Assm)	4			
T(C2&F2, Assm)	5			
T(C1F1&C1, Assm)	7			
T(C1F2&C1, Assm)	8			
T(C2F1&C2, Assm)	8			
T(C2F2&C2, Assm)	9			
T(C1F1C1&Fc, Assm)	7			
T(C1F2C1&Fc, Assm)	8			
T(C2F1C2&Fc, Assm)	8			
T(C2F2C2&Fc, Assm)	9			
T(C1F1&C1Fc, Assm)	6			
T(C1F2&C1Fc, Assm)	7			
T(C2F1&C2Fc, Assm)	7			
T(C2F2&C2Fc, Assm)	8			
T(C1&Fc, Assm)	3			
T(C2&Fc, Assm)	4			
T(C1&F1C1Fc, Assm)	7			
T(C1&F2C1Fc, Assm)	8			
T(C2&F1C2Fc, Assm)	8			
T(C2&F2C2Fc, Assm)	9			
T(C1F1&C1&Fc, Assm)	9			
T(C1F2&C1&Fc, Assm)	10			
T(C2F1&C2&Fc, Assm)	10			

Figure 4-18 Graphical user interface (taking the processing time as inputs and generating configurations and drift comparison as outputs)

The above results show "on average" under certain condition, which configuration is better in drift reduction given the same cost (e.g. non-serial configuration with branches or conventional serial line). Figure 4-19 shows the drift comparison between two configurations when the process data is changed. When α_1 is fixed, $0 < \alpha_2 < 0.6$, the drift of serial line is bigger than that of the branched line. Same conclusion can be drawn when $\alpha_2 > 0.7$. Otherwise, the drift of branched line is bigger than that of the serial line. Similar conclusions can be summarized and provided as engineering guidelines.

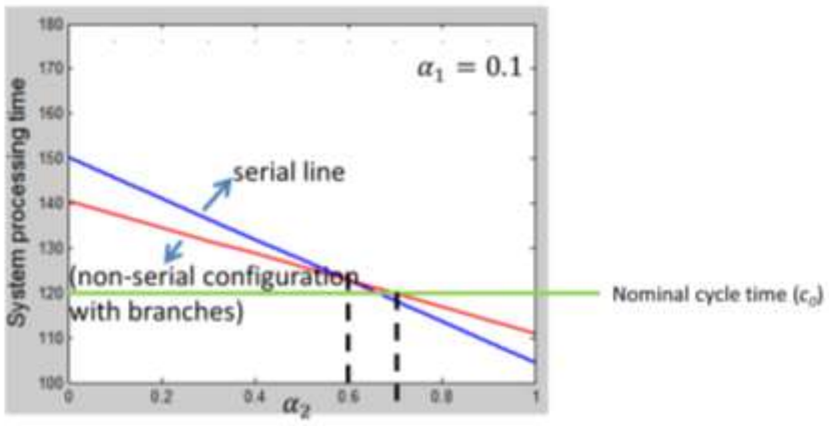

Figure 4-19 Drift comparison between conventional serial line and non-serial configuration with branches (when α1=0.1, and α2 changes from 0-1)

In the assumption, the percentages of variant components $\alpha, \beta, \gamma, \ldots$ are assumed to be independent and they are assumed to follow uniform distribution from 0 to 1, i.e. $\sim U(0,1)$. If the percentages of variant components are not independent, nor they follow uniform distribution, the solution won't change. Since

$$Var(|t^{q_l} - c_0|) = E[(t^{q_l})^2] - [E(t^{q_l})]^2 \tag{5}$$

Where $t^{q_l} = f(\alpha^l, \beta^l, \gamma^l, \ldots)$

$$\begin{aligned} E(t^{q_l}) &= \iint f(\alpha^l, \beta^l, \ldots) p(\alpha^l, \beta^l, \ldots) d\alpha^l d\beta^l \\ &= \iint f(\alpha^l, \beta^l, \ldots) p(\alpha^l) p(\beta^l) d\alpha^l d\beta^l (independence) \\ &= \iint f(\alpha^l, \beta^l, \ldots) d\alpha^l d\beta^l (uniform\ distribution) \\ &\geq \iint f(\alpha^l, \beta^l, \ldots) p(\beta^l \mid \alpha^l) p(\alpha^l) d\alpha^l d\beta^l \end{aligned} \tag{11}$$

Therefore, our solution in calculating the drift is a conservative solution.

4.4 Conclusion

This chapter develops a new approach for designing optimal assembly system configuration when a system processes multiple products in a product family. The stochastic product demand changes cause “drift” in balancing such an assembly system. By considering not only traditional assembly system configurations (serial, parallel stations) but also complex configurations with branches, the method explores the optimal ways of configuration generation and line balancing for a product family in order to minimize the total drift and cost. Compared with the previous research on assembly system configuration generation for a product family, the novel contributions of this work are the generation of complex assembly system configurations with branches, drift definition and modeling, the formulation of guidelines for engineers in practice. Future research includes design of material flow path and control logic based on the generated configuration and manufacturing system reconfiguration.

CHAPTER 5

AN ASSEMBLY SYSTEM CONFIGURATOR FOR AUTOMOTIVE BATTERY PACKS

High power and capacity lithium-ion batteries are being adopted for electrical vehicle applications. The assembly processes for such batteries are influenced by battery cell designs, such as cell type, geometry, tab shape/position, module stack form and repetitive patterns, which require proper assembly equipment for cell handling and joining. Since battery technology is progressing rapidly, a lot of new battery designs are emerging on the market. A math-based tool, *Assembly System Configurator*, is developed for designing reconfigurable battery assembly processes and systems in a cost-effective way. The *Configurator* implements the methods developed in chapter 2-4 by automating the tasks of assembly task generation, sequence planning, equipment selection, assembly line balancing and throughput optimization. The structure of the *Configurator* is introduced and its capabilities are demonstrated using a battery case study.

5.1 Introduction

Lithium-ion batteries are one of the key enabling technologies for the electrification of automobiles because of their advantages over conventional batteries: higher energy density, lighter weight, longer life, and lower toxicity [2]. However, cost-effective manufacturing of lithium-ion batteries for electrical and hybrid electrical vehicles (EV/HEV) has not yet been fully developed. Efficient, flexible, and reliable battery assembly automation is needed for two following reasons: 1) A variety of new battery pack designs and their changing demand rates require the assembly system to be flexible and reconfigurable. The battery designs include variations in cell type, geometry, tab shape/position, module stack form and repetitive patterns; 2) The high current and voltage in battery cells, modules and packs require automatic assembly and material handling.

Systematic approaches do not yet exist for addressing the relationship between battery module/pack configurations and battery assembly processes. Therefore, a math-based tool, *Battery Assembly System Configurator,* is being developed such that the battery assembly systems can be optimally designed by automating the tasks of assembly task generation, sequence planning, equipment selection, assembly line balancing and throughput optimization. By implementing the methods discussed in chapter 2-4, *Configurator* establishes the framework and basis for developing cost-effective manufacturing of vehicle battery, therefore has its practical application.

The *Battery Assembly System Configurator* is programmed in Visual Basic and an Excel-based data structure. With a database of assembly equipment and technology and the product information provided by the user through user interfaces, the Configurator can sort and analyze the data and then report a set of candidate assembly machines with process specifications and performance measures for system configuration designs and optimization.

The remainder of the chapter is organized as follows. Section 5.2 introduces battery module/pack designs and their appropriate assembly processes. Section 5.3 discusses the methodology implemented in the Configurator, including automatic system configuration generation, optimization for task assignment and equipment selection, and throughput analysis. The structure of the Configurator is also presented. Section 5.4 demonstrates the Configurator with an example of system design given a battery configuration. Section 5.5 draws the conclusions and suggests future work.

5.2 Battery module/pack designs and their assembly processes

A lithium-ion battery pack usually has a hierarchical structure consisting of several modules with each module consisting of multiple battery cells and ancillary members, such as frames, cooling fins, and compression foams, as shown in Figure 1-5. Three types of battery cells are commonly seen today: the prismatic cell with a rigid case or container, the prismatic cell with a pouch, and the cylindrical cell with a rigid can. Their shapes and types determine the module/pack configurations and the assembly methods. Battery tab positions (one-sided or two-sided) may also influence the selection of the assembly method. The tab type, stud or foil, mainly influences the methods of joining cells [70].

Figure 5-1 shows the process flow of battery assembly involving four operations: loading, inspection and sorting, stacking, and clamping to module or pack. First, battery cells and auxiliary components are loaded from feeders or crates onto the assembly line.

Then the battery cells are inspected and sorted according to their properties (type, size, tab shape and tab position), conditions (good, damaged, defective, low performance) and different electrochemical characteristics (capacity, voltage) by optical, electrical, ultrasonic, X-ray or mechanical sorting devices. Battery components are assembled and aligned into a stack by appropriate stacking equipment. Each stack is then clamped or strapped with end plates. Upon the completion of these four operations, the cells are welded together into a battery module. Finally several battery modules are mechanically connected to form a battery pack.

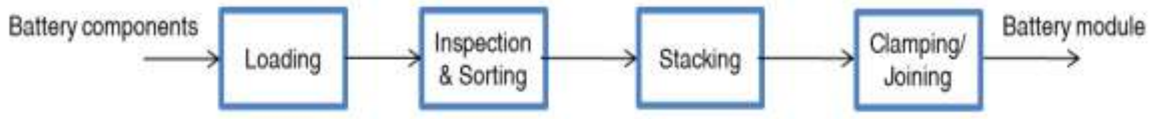

Figure 5-1 Battery module assembly procedures

In the above battery assembly process, stacking and joining are the two most important assembly operations for determining assembly productivity and quality. Meanwhile, they also present major challenges to production automation and flexible system design. Therefore, this chpater will focus on those two critical operations.

5.2.1 Automatic stacking methods

The methods for automatic stacking of components can be categorized into two types: roll and eject; pick and place. This section reviews these two automatic stacking methods and discusses their applications to battery assembly.

Roll and eject

Roll and eject is a fast assembly method using conveyor belt to roll or transport the parts to be stacked and eject them into a stacking bucket with the aid of gravity or an elevator which can move up or down to form a stack (Figure 5-2). Figure 5-2(a) shows the stacking bucket which may have a slightly inclined bottom so that the parts in the bucket can slide to align themselves against the bucket wall. This stacking method is mostly used for stacking non-fragile, light-weight and thin parts, such as newspaper and printing materials [71-74], but not suitable for battery cells which either are too heavy or have tabs with carefully bent geometry for welding.

Roll and eject using an elevator (Figure 5-2(b)) is very robust for extensive stacking applications, like food packaging and video cassette stacking [75]. With little or no falling distance controlled by the elevator, the impact of stacking motion is limited to the edge stopped by the guide of the stack. Prismatic cells should be good candidates for this kind of stacking methods. Still, care needs to be taken to turn the battery cell tabs away from direct contact with the stacking guide of the elevator.

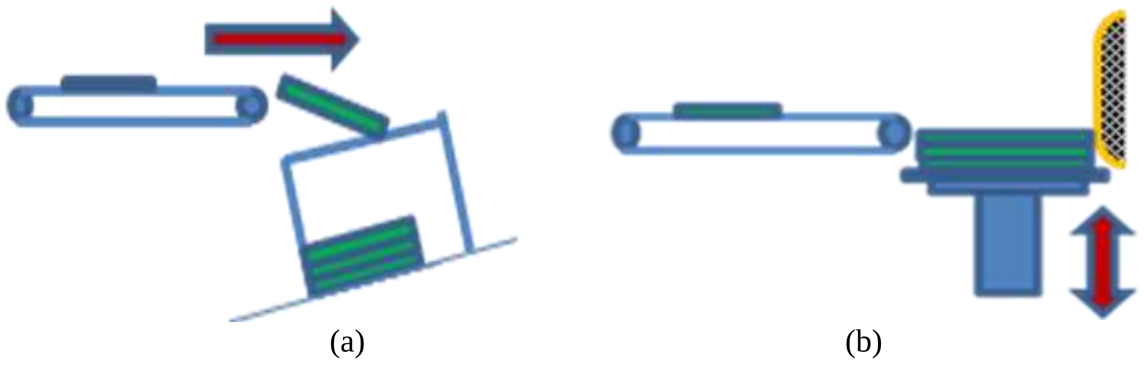
(a) (b)

Figure 5-2 Roll and eject method: (a) into a stacking bucket; (b) using an elevator

Pick and place

The pick and place method uses robots or mechanized grippers to fetch and place individual parts and thereby form a stack. Based on their configurations and degrees of freedom (DOF), four types of robots can be found commercially available, i.e., SCARA (Selective Compliant Assembly Robot Arm) robots (Figure 5-3(a)), PKM (Parallel Kinematic Machine) robot (Figure 5-3(b)), articulate robots (Figure 5-3(c)), and gantry robots (Figure 5-3(d)) [5].

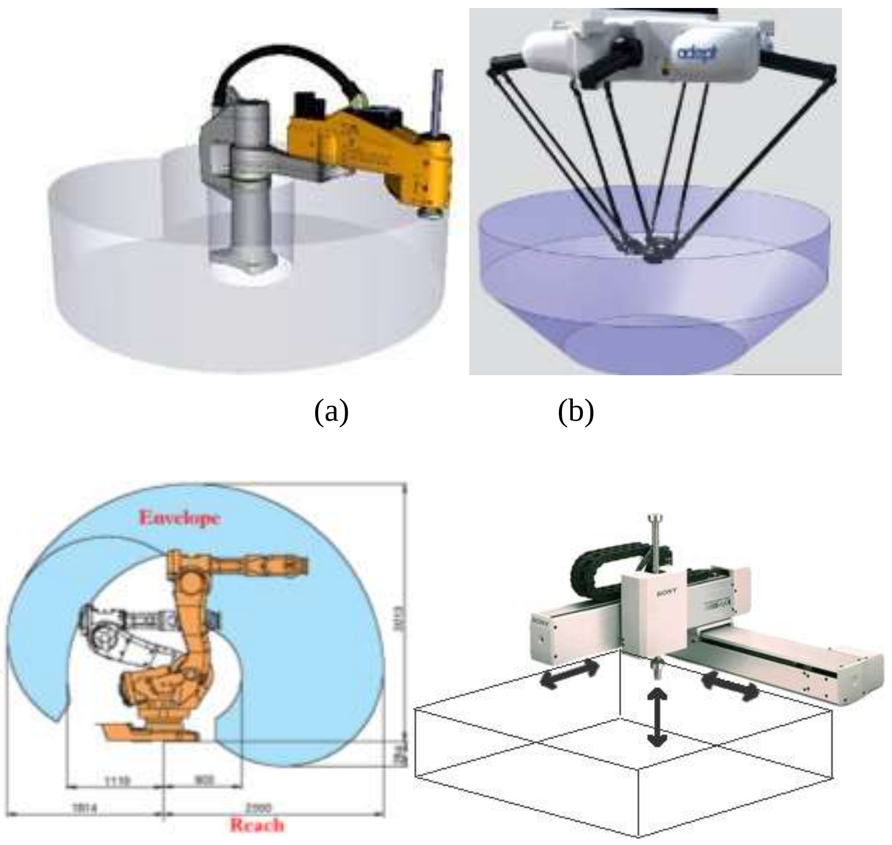

(a) (b)

(c) (d)

Figure 5-3 Pick and place robots [5]

The SCARA robot normally has four DOF with a set of serially jointed and motorized arms that is compliant in the X-Y directions, but stiff in the Z direction. It is particularly suitable for stacking parts that do not need sophisticated manipulation. This type of robots is fast, precise, compact and low cost and thus has been extensively used in the electronics industry.

The relatively new PKM robot has four or more DOF with multiple sets of arms that are connected to a moving platform (end effector). Through coordinated actuation at the base of each arm, the robot can pick and place parts as the conventional robots. Due to its light-weight and non-motorized arms, the robot has the fastest acceleration and speed among all types of robots for applications. For battery assembly, this type of robots may satisfy the speed requirement of stacking; however, its positioning accuracy or repeatability can be a concern.

The articulate robot typically has six DOF with a set of serially articulated and motorized arms. The robot is the most flexible in applications and commercially available with a wide range of reach and payload. It is heavier, slower and more expensive than the SCARA robot, but its flexibility for other applications can be an important consideration in flexible or reconfigurable manufacturing systems.

The gantry robot has three axes that move linearly in the Cartesian or XYZ coordinates. This type of robots usually is the most accurate and customizable to various work range, payload and DOF. In fact, the robot can be scaled down to two DOF, and thus called mechanized module here, for simple pick and place operations. In many applications, the linear movements of the axes afford the gantry robots to relocate parts without the need of an extra rotary axis to adjust part orientation as other types of robots have. The fixed rails of the axes, unfortunately, make this type of robots the poorest in space utilization.

5.2.2 Joining methods

Lee *et al* [70] have conducted a comprehensive review of the state-of-the-art battery joining technologies. In developing the *Configurator*, automatic assembly/stacking methods are our main focus, but the *Configurator* has the capability to handle joining as well.

5.3 Battery assembly system configurator

The overall method implemented in the *Configurator* for the system configuration generation and optimization is shown in Figure 3-4. This method adopts the nested framework proposed in [16] to model the relationship between the product design and system configuration. The detailed method has been introduced in chapter 3.

5.3.1 Configuration generation

Different sequences and system configurations can be used to assemble components for a given stacking pattern in a battery pack. For example, components can be added one at a time, leading to serial sequences. Alternatively, all the components can be assembled at one station with flexible machines, resulting in a parallel operation. Various hybrid assembly sequences can also be obtained by pre-assembling different number of components into subassemblies which in turn are assembled with other components or subassemblies. Webbink and Hu [26] proposed an automated distribution method to enumerate all the possibilities of different combinations of stations which are of serial or parallel configuration. The assembly sequence and configuration generation problem is to enumerate all the non-repetitive ways of hierarchically grouping n elements. A complete description of the algorithm can be found in chapter 2.

5.3.2 Optimization for task assignment and equipment selection

Enumeration in the outer loop generates the candidate assembly tasks/task groups, sequences, and initial configurations. The inner loop changes each initial configuration by assigning the tasks to the selected machines. A mathematical model for the inner loop optimization including task-machine assignment, workload balancing and machine type and number selection in assembly systems is described in chapter 3.

In order to speed up the optimization, the model is simplified to the following: consider the assignment of task to machine type ($x_{i,j}$), and determine the optimized number of machines (N_j) to satisfy the throughput constraint at the same time.

Decision variables

A task-machine assignment variable $x_{i,j}$ is used to represent whether or not a task is assigned to a machine type.

$$x_{i,j} = \begin{cases} 1 & \textit{if task i is assigned to the jth machine type} \\ 0 & \textit{otherwise} \end{cases}$$

N_j is the quantity for machine type j.

Objective function

The objective in this model is to balance an assembly system by minimizing the total equipment investment cost while ensuring the throughput requirement, i.e.,

$$\min \quad G = Th\sum_{i=1}^{I}\sum_{j=1}^{J} c_{ij} h_i x_{ij} + N_j c_j \tag{1}$$

Where $c_{i,j}$ is the operation cost to process task i on machine type j, c_j is the amortized annual cost on machine type j, and h_i is the number of repetition required to produce one unit of the product. *Th* is the actual throughput.

<u>Constraints</u>

(1)Task assignment constraint.

This constraint specifies that each task must be assigned to one and only one type of machine.

$$\sum_{j=1}^{J} x_{i,j} = 1 \tag{2}$$

(2)Task-machine matching constraint

Certain engineering experiences may require a set of tasks not to be assigned to certain machine type, i.e.,

$$x_{m,n} = 0, (m,n) \in TM - set\ that\ task\ m\ cannot\ be\ assigned\ to\ machine\ type\ n \tag{3}$$

(3) Throughput constraint

This constraint ensures that the throughput satisfies the demand of final products and can be represented by

$$\sum_{i=1}^{I} \frac{t_{i,j} x_{i,j}}{c_0} \le N_j \tag{4}$$

Where c_0 is the system cycle time.

(4) Task zoning constraint

There are two types of zoning constraints in the simplified model. The first type of zoning constraint forbids some of the tasks to be assigned to the same machine. Let S={s_1,s_2,…} be a set of task groups. Each task group consists of tasks that are compatible to each other. For any task i∈s and any task i'∈s', s∈S, s'∈S, s≠s', i and i' cannot be assigned to the same machine, i.e., they are incompatible. With such type of constraints, the original optimization problem can be divided to a set of sub-problems. Each sub-problem is to find an optimized configuration for a task group.

The second type of zoning constraint requires tasks within the same group be assigned to the same machine type:

$$x_{u,j} = x_{v,j}, \ j = 1, \ldots J,$$
$$(u, v) \in ZS \text{ --} \mathit{set\ of\ tasks\ that\ must\ be\ assigned\ to\ the\ same\ machine\ type} \quad (5)$$

5.3.3 Software implementation

Figure 5-4 shows the structure of *Assembly System Configurator*, including two engines: process engine and system engine.

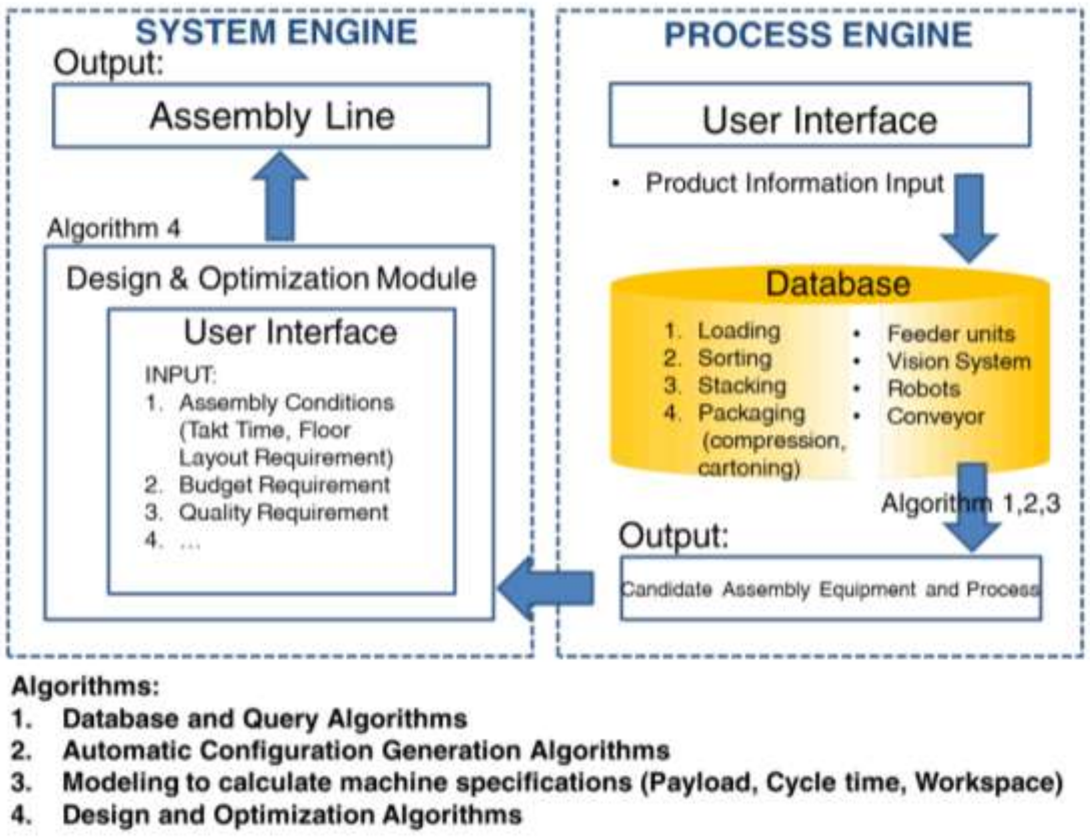
SYSTEM ENGINE
Output:
Assembly Line
Algorithm 4
Design & Optimization Module
User Interface
INPUT:
1. Assembly Conditions (Takt Time, Floor Layout Requirement)
2. Budget Requirement
3. Quality Requirement
4. ...
PROCESS ENGINE
User Interface
• Product Information Input
Database
1. Loading
2. Sorting
3. Stacking
4. Packaging (compression, cartoning)
• Feeder units
• Vision System
• Robots
• Conveyor
Algorithm 1,2,3
Output:
Candidate Assembly Equipment and Process
Algorithms:
1. Database and Query Algorithms
2. Automatic Configuration Generation Algorithms
3. Modeling to calculate machine specifications (Payload, Cycle time, Workspace)
4. Design and Optimization Algorithms

Figure 5-4 Structure of *Assembly System Configurator*

The process engine has 1) user interfaces for inputting battery designs (cells, frames, fins, foams), specifications (size, weight), manufacturing requirements (demand, working days, shifts) etc; 2) database and query algorithms constructed for equipment selection and machine capability calculation; 3) configuration generation algorithms given a hierarchical structure of battery design. The system engine is the design and optimization module in the *Configurator*. The outputs of the process engine (enumeration of the candidate initial configurations, candidate equipment, cycle time and cost) are fed into the system engine to generate the optimal assembly line given several assembly conditions (Takt time, floor layout requirement etc) and the budget.

The process engine of the *Configurator* has an Excel based framework (Figure 5-5). Both the equipment databases and the user interfaces are stored in Excel. While users answer questions in user interfaces, the product information is stored in an Excel spreadsheet and compared with candidate equipment at each stage, and one or several candidate machines are selected. The ID numbers of the potential machines are transferred to Access by Access DLL or Data engine (JET or ACE) to retrieve the full information of candidate machines and thus generate reports. The report is then saved in .pdf format and displayed to the user.

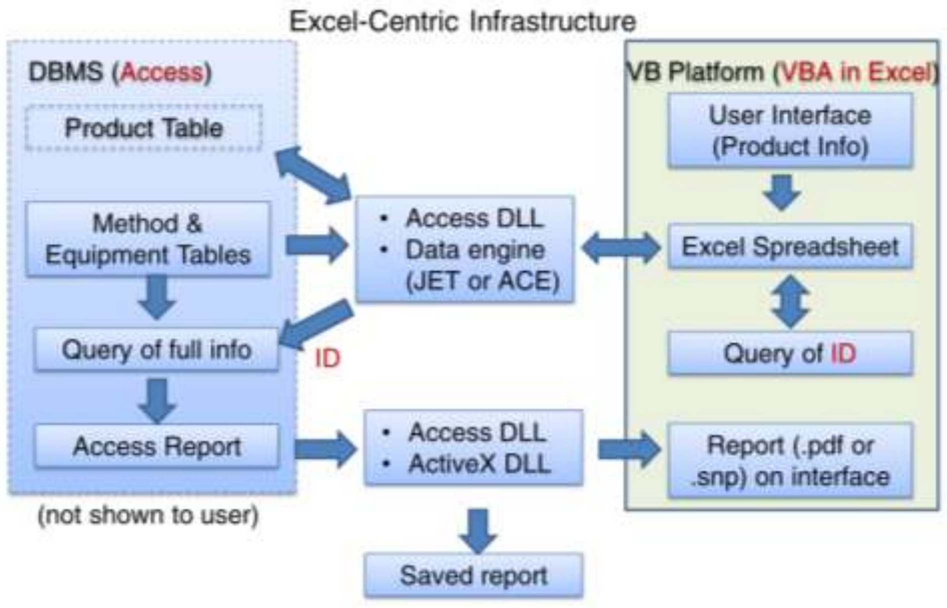
Excel-Centric Infrastructure
DBMS (Access)
Product Table
Method & Equipment Tables
Query of full info
Access Report
(not shown to user)
• Access DLL
• Data engine (JET or ACE)
ID
• Access DLL
• ActiveX DLL
Saved report
VB Platform (VBA in Excel)
User Interface (Product Info)
Excel Spreadsheet
Query of ID
Report (.pdf or .snp) on interface

Figure 5-5 Framework of process engine

5.4 Case study

This section demonstrates the Configurator using a case study of a battery module assembly.

5.4.1 Problem description

The core of a battery module is a stack of battery cells and auxiliary components, such as repeating frames, cooling fins, and compression foams. As shown in Figure 5-6, most of the components are stacked in a repetitive pattern, such as A-B-C-B-D, where A, B, C, D denote the cell and ancillary components. Such a pattern repeats a number of times (N) to form the whole module stack.

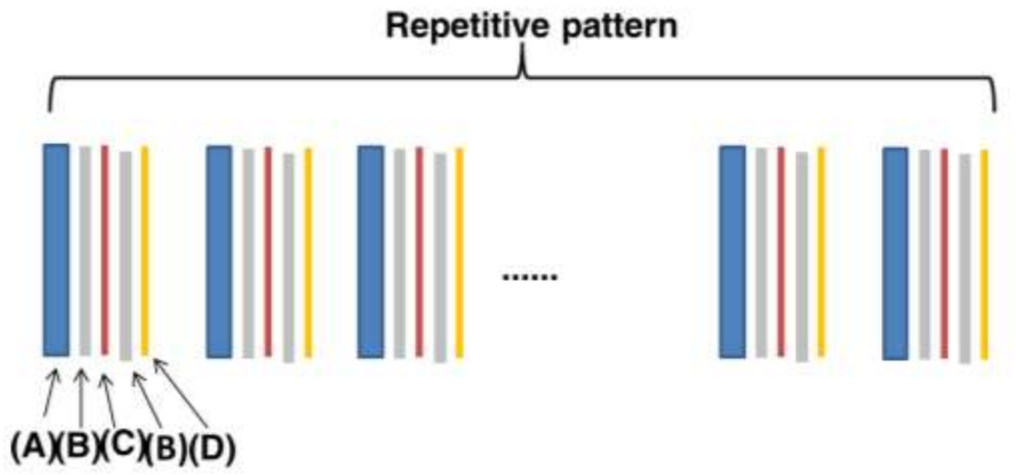

Figure 5-6 An example of assembly of battery module

5.4.2 Configurator demonstration

The Configurator first takes a series of product and process related inputs, such as production rates, working days, battery cell type and specifications, battery tab shape and position etc. (Figure 5-7) in order to generate a report with candidate assembly equipment selection, and specifications of machines (payload, work space, reach and cycle time). (Figure 5-8)

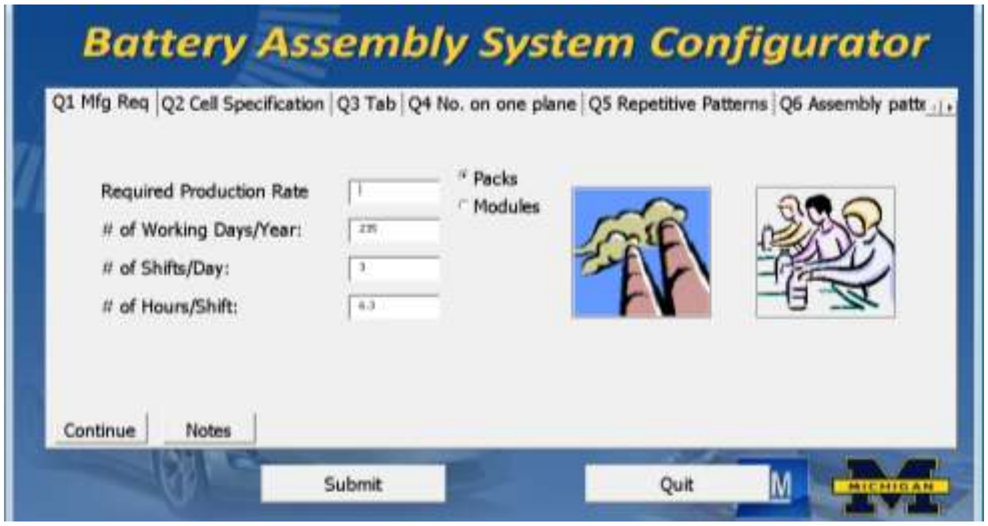

Required Production Rate	1
# of Working Days/Year:	235
# of Shifts/Day:	3
# of Hours/Shift:	6.3

[✓ Packs] Modules

Figure 5-7 Configurator interface 1

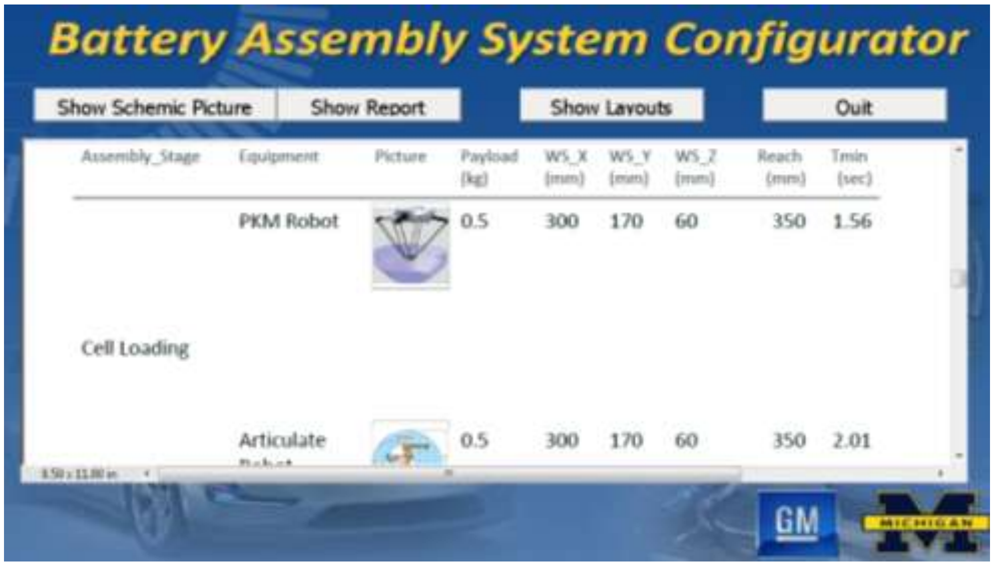

Assembly_Stage	Equipment	Picture	Payload (kg)	WS_X (mm)	WS_Y (mm)	WS_Z (mm)	Reach (mm)	Tmin (sec)
	PKM Robot		0.5	300	170	60	350	1.56
Cell Loading								
	Articulate Robot		0.5	300	170	60	350	2.01

Figure 5-8 Configurator output report

The Configurator can generate all the candidate system initial configurations and sequences for the repetitive pattern with the user input as shown in Figure 5-9. Up to four different repetitive patterns can be input by the user, albeit this battery example needs only one.

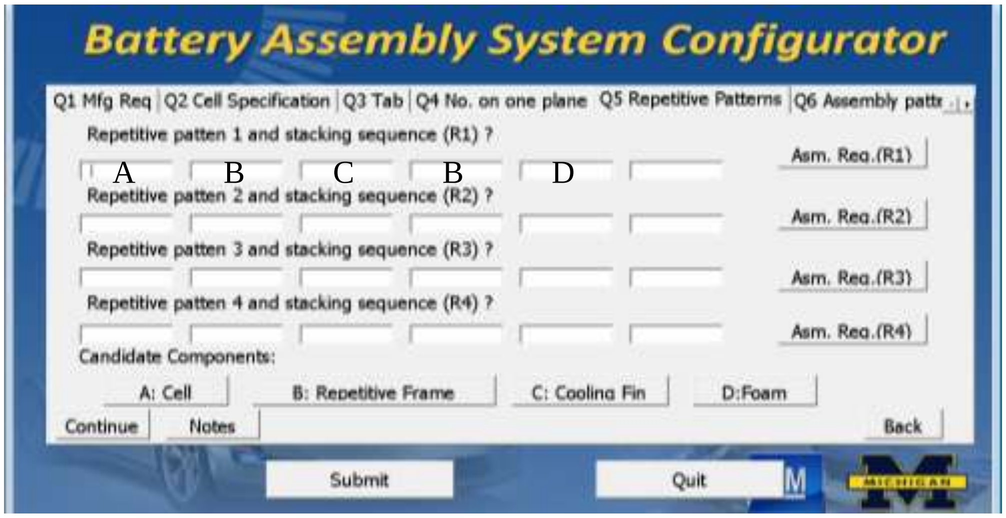

Battery Assembly System Configurator

Q1 Mfg Req | Q2 Cell Specification | Q3 Tab | Q4 No. on one plane | Q5 Repetitive Patterns | Q6 Assembly patt

Repetitive patten 1 and stacking sequence (R1) ?

A B C B D

Asm. Req.(R1)

Repetitive patten 2 and stacking sequence (R2) ?

Asm. Req.(R2)

Repetitive patten 3 and stacking sequence (R3) ?

Asm. Req.(R3)

Repetitive patten 4 and stacking sequence (R4) ?

Asm. Req.(R4)

Candidate Components:

A: Cell | B: Repetitive Frame | C: Cooling Fin | D:Foam

Continue | Notes | Back

Submit | Quit

Figure 5-9 User input of repetitive patterns

Figure 5-10 shows the configuration output of the Configurator. Without any assembly constraints, there are 45 candidate system configurations, which are all represented in alphanumerical characters and parentheses. The symbolic representation can then be displayed in a graphical layout as shown in Figure 5-10. The blue icons represent loading equipment and the green icons represent stacking equipment.

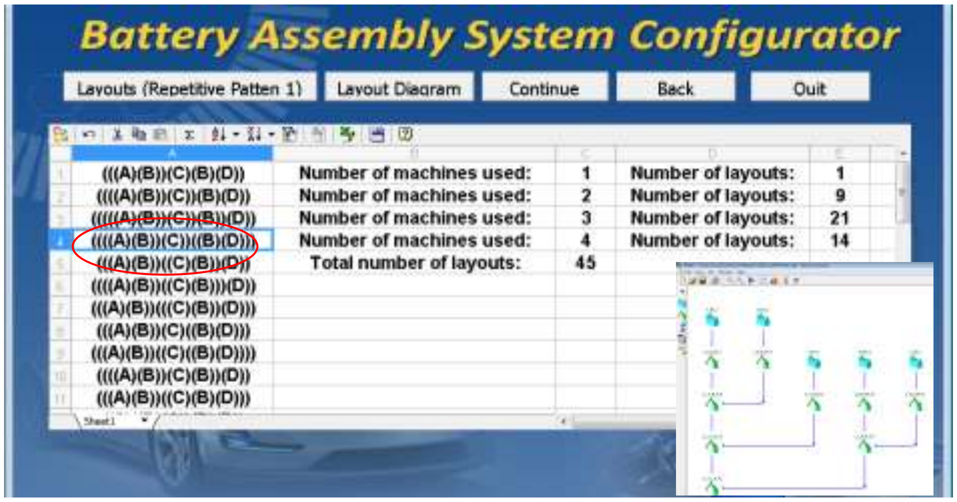

Battery Assembly System Configurator

Layouts (Repetitive Patten 1) | Layout Diagram | Continue | Back | Quit

	A	B	C	D	E
1	(((A)(B))(C)(B)(D))	Number of machines used:	1	Number of layouts:	1
2	((((A)(B))(C))(B)(D))	Number of machines used:	2	Number of layouts:	9
3	(((((A)(B))(C))(B))(D))	Number of machines used:	3	Number of layouts:	21
4	((((A)(B))(C))((B)(D)))	Number of machines used:	4	Number of layouts:	14
5	(((A)(B))((C)(B))(D))	Total number of layouts:	45		
6	((((A)(B))((C)(B)))(D))				
7	(((A)(B))(((C)(B))(D)))				
8	(((A)(B))(C)((B)(D)))				
9	(((A)(B))((C)((B)(D))))				
10	((((A)(B))(C)(B))(D))				
11	(((A)(B))((C)(B)(D)))				

Sheet1

Figure 5-10 Automatic generation of initial configurations and sequences

The design and optimization module of the Configurator has interfaces for selecting machines from the candidate lists (Figure 5-11), inputting zoning constraints (Figure 5-12), and revising cycle time and cost data if necessary (Figure 5-13). The candidate machine lists, cycle time and cost data are taken from the previous selection and calculation. The optimal assembly line is generated in a report with appropriate task assignment and equipment selection (Figure 5-14).

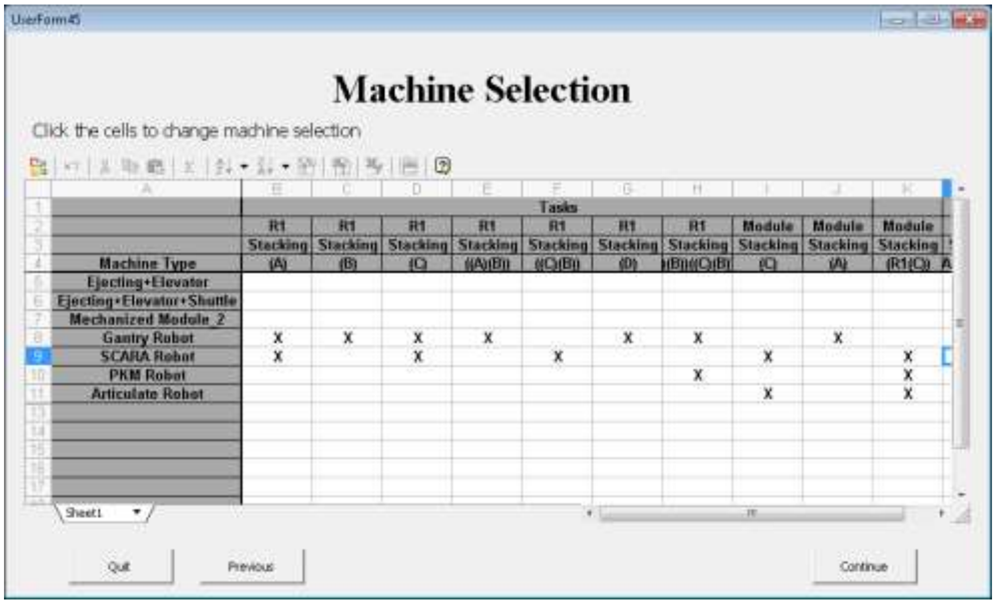

Machine Selection

Click the cells to change machine selection

	Tasks									
Machine Type	R1 Stacking (A)	R1 Stacking (B)	R1 Stacking (C)	R1 Stacking ((A)(B))	R1 Stacking ((C)(B))	R1 Stacking (D)	R1 Stacking (B))((C)(B)	Module Stacking (C)	Module Stacking (A)	Module Stacking (R1(C))
Ejecting+Elevator										
Ejecting+Elevator+Shuttle										
Mechanized Module_2										
Gantry Robot	X	X	X	X		X	X		X	
SCARA Robot	X		X		X			X		X
PKM Robot							X			X
Articulate Robot								X		X

Figure 5-11 Machine selection

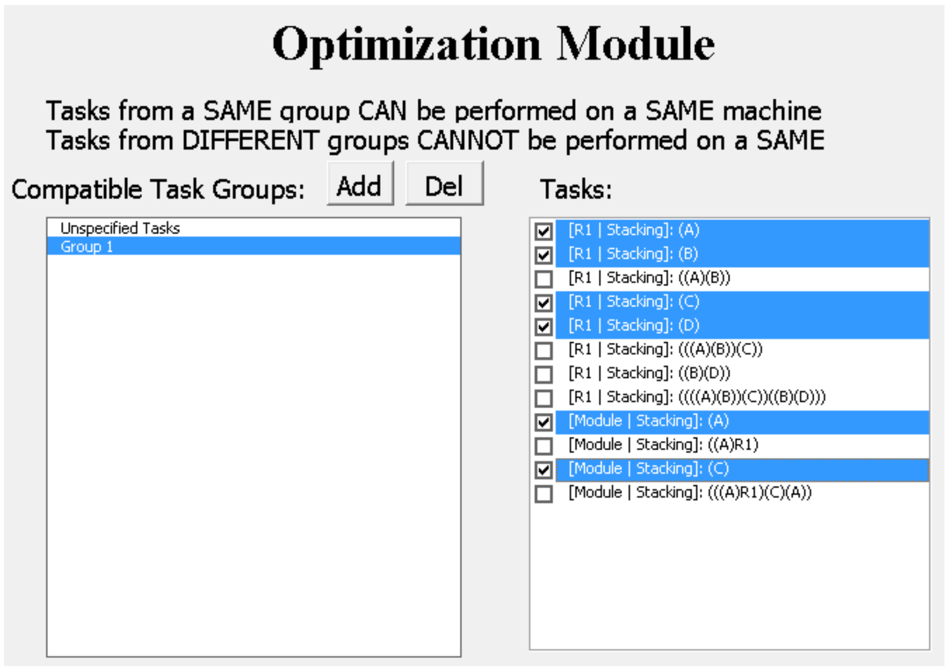
Optimization Module

Tasks from a SAME group CAN be performed on a SAME machine
Tasks from DIFFERENT groups CANNOT be performed on a SAME

Compatible Task Groups: Add Del

Unspecified Tasks
Group 1

Tasks:

- [x] [R1 | Stacking]: (A)
- [x] [R1 | Stacking]: (B)
- [ ] [R1 | Stacking]: ((A)(B))
- [x] [R1 | Stacking]: (C)
- [x] [R1 | Stacking]: (D)
- [ ] [R1 | Stacking]: (((A)(B))(C))
- [ ] [R1 | Stacking]: ((B)(D))
- [ ] [R1 | Stacking]: ((((A)(B))(C))((B)(D)))
- [x] [Module | Stacking]: (A)
- [ ] [Module | Stacking]: ((A)R1)
- [x] [Module | Stacking]: (C)
- [ ] [Module | Stacking]: (((A)R1)(C)(A))

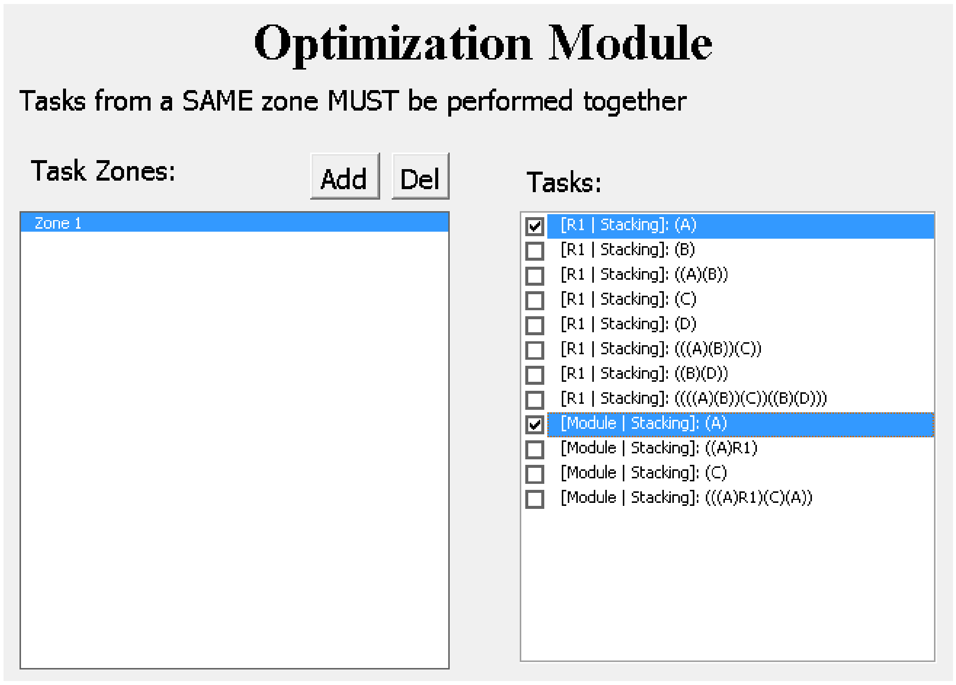
Optimization Module

Tasks from a SAME zone MUST be performed together

Task Zones: Add Del

Zone 1

Tasks:

- [x] [R1 | Stacking]: (A)
- [ ] [R1 | Stacking]: (B)
- [ ] [R1 | Stacking]: ((A)(B))
- [ ] [R1 | Stacking]: (C)
- [ ] [R1 | Stacking]: (D)
- [ ] [R1 | Stacking]: (((A)(B))(C))
- [ ] [R1 | Stacking]: ((B)(D))
- [ ] [R1 | Stacking]: ((((A)(B))(C))((B)(D)))
- [x] [Module | Stacking]: (A)
- [ ] [Module | Stacking]: ((A)R1)
- [ ] [Module | Stacking]: (C)
- [ ] [Module | Stacking]: (((A)R1)(C)(A))

Figure 5-12 Zoning constraints

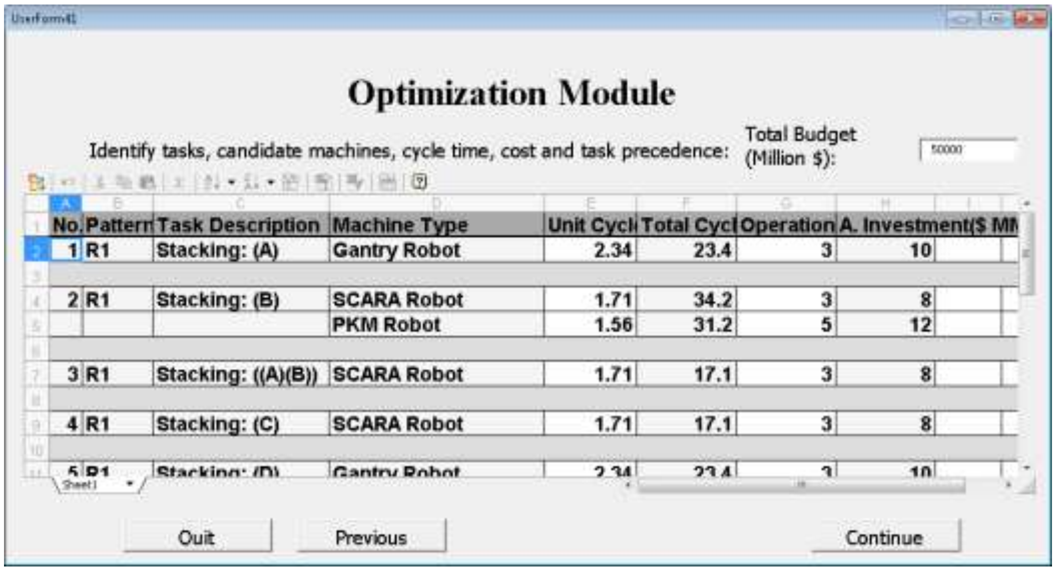

Optimization Module

Identify tasks, candidate machines, cycle time, cost and task precedence:

Total Budget (Million $): 50000

No.	Pattern	Task Description	Machine Type	Unit Cycl	Total Cycl	Operation	A. Investment($ MN
1	R1	Stacking: (A)	Gantry Robot	2.34	23.4	3	10
2	R1	Stacking: (B)	SCARA Robot	1.71	34.2	3	8
			PKM Robot	1.56	31.2	5	12
3	R1	Stacking: ((A)(B))	SCARA Robot	1.71	17.1	3	8
4	R1	Stacking: (C)	SCARA Robot	1.71	17.1	3	8
5	R1	Stacking: (D)	Gantry Robot	2.34	23.4	3	10

Figure 5-13 Cycle time and cost data

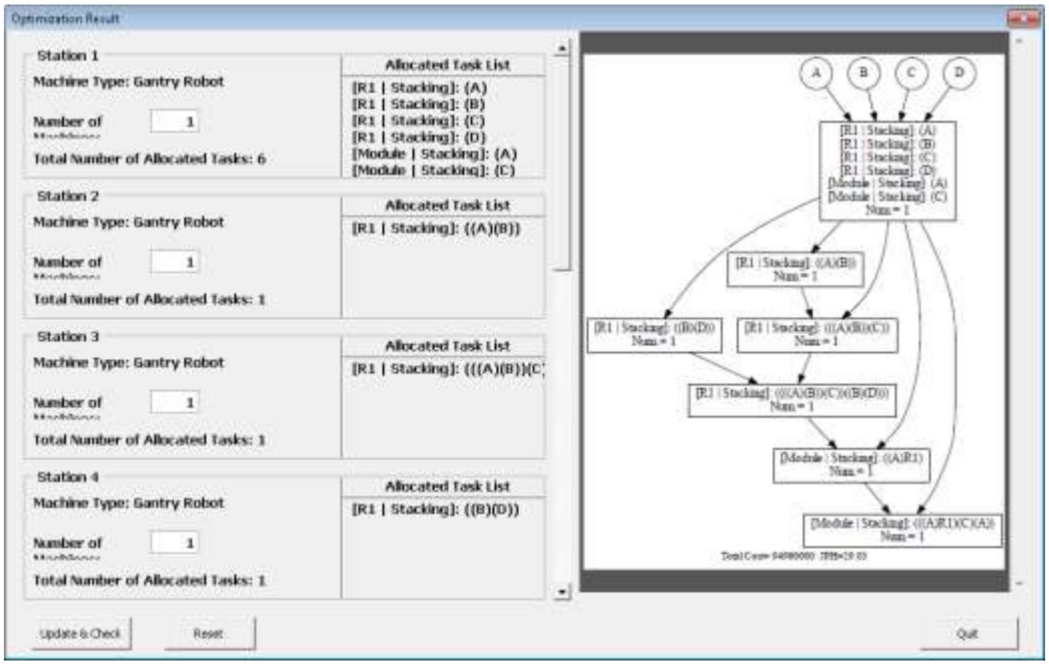

Station 1
Machine Type: Gantry Robot
Number of Machines: 1
Total Number of Allocated Tasks: 6

Allocated Task List
[R1 | Stacking]: (A)
[R1 | Stacking]: (B)
[R1 | Stacking]: (C)
[R1 | Stacking]: (D)
[Module | Stacking]: (A)
[Module | Stacking]: (C)

Station 2
Machine Type: Gantry Robot
Number of Machines: 1
Total Number of Allocated Tasks: 1

Allocated Task List
[R1 | Stacking]: ((A)(B))

Station 3
Machine Type: Gantry Robot
Number of Machines: 1
Total Number of Allocated Tasks: 1

Allocated Task List
[R1 | Stacking]: (((A)(B))(C

Station 4
Machine Type: Gantry Robot
Number of Machines: 1
Total Number of Allocated Tasks: 1

Allocated Task List
[R1 | Stacking]: ((B)(D))

Figure 5-14 Report for optimal assembly line

5.4.3 Performance evaluation

The output of the Configurator is input to a throughput simulation model as shown in Figure 5-15. The purpose of using a simulation model for performance evaluation is to explore the most effective production control and production line layout for the assembly operations [76-77]. The optimal assembly line configuration with task assignment and machine cycle time is needed to build the simulation model in Witness as shown in Figure 5-16. Seven machines are used (green icons in Figure 5-16) with some machines for loading components, some machines for stacking cells and ancillary components, the last machine for final stacking all the components together.

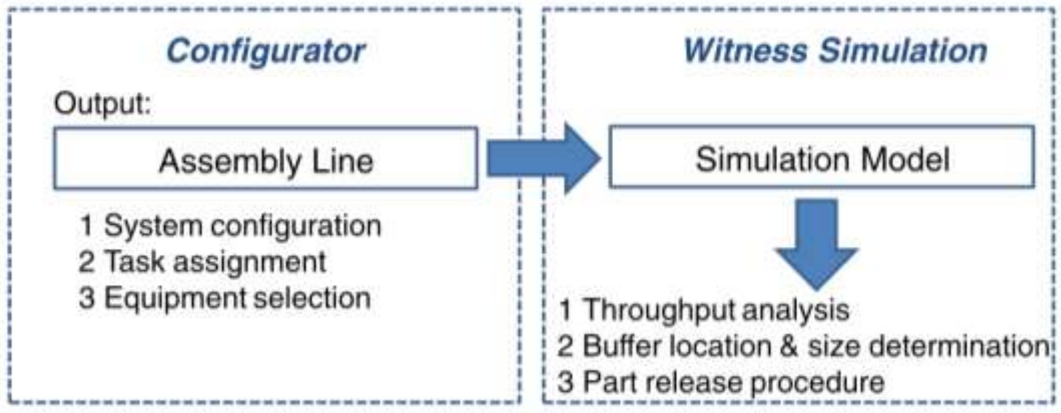

Figure 5-15 Flowchart of configurator and simulation model

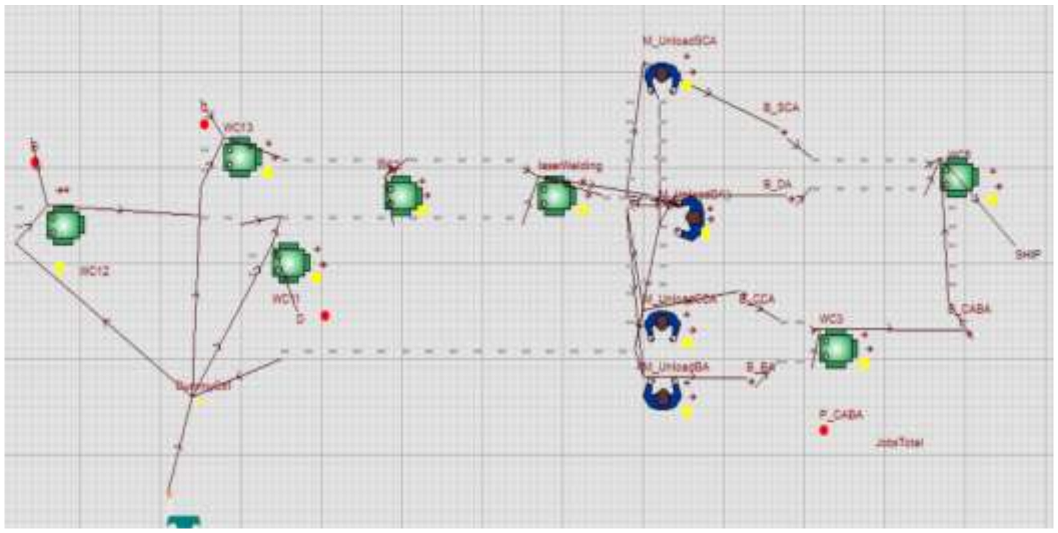

Figure 5-16 Simulation model in Witness

The performance measures studied in this research include the system throughput, the work-in-process level, the buffer size deployments, and the system robustness to uncertainties such as machine failures and part scraping rates. Some critical control issues and their impacts on the overall system performance are explored. These control issues include: different production line layouts and the number of independent conveyors for material handling required in the system, the pull and push production mechanisms and their impact on the system throughput and the WIP.

Figure 5-17 shows the throughput results when one of the control procedures is changed: control the re-allocation of the tasks from an expensive machine (final stacker) to other machines. From the simulation model, a significant throughput improvement can be observed and proper re-allocation level can also be concluded: Case 2 in this example, since further re-allocation cannot change the throughput.

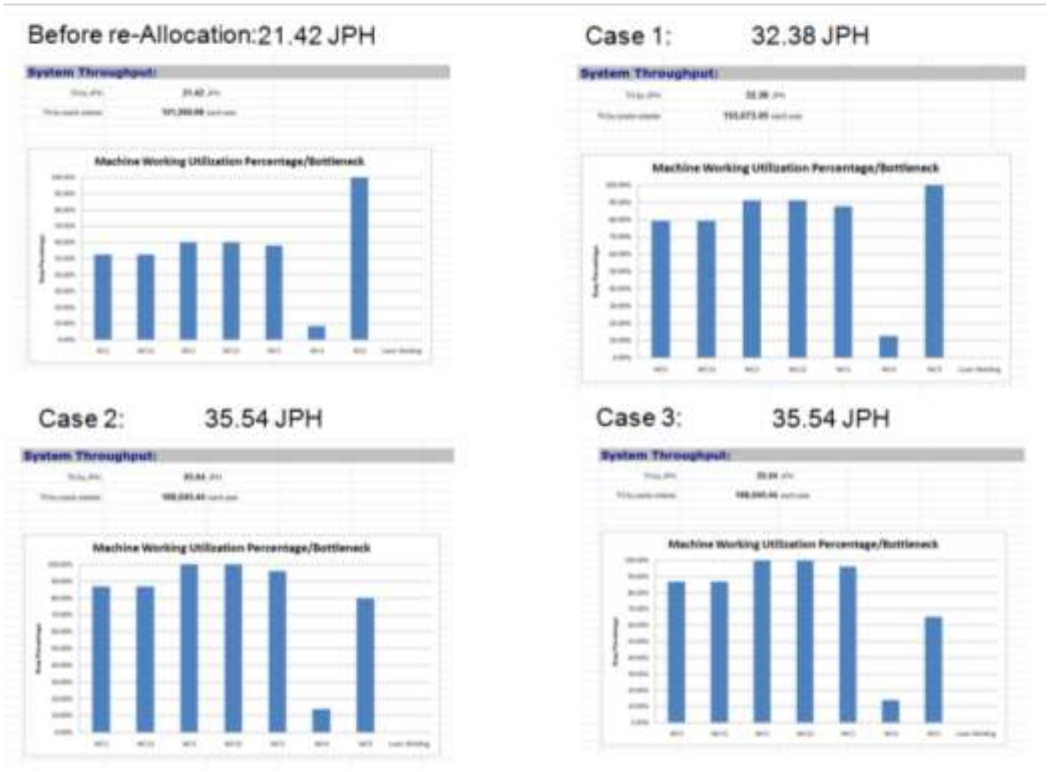

Figure 5-17 Throughput results when control procedure is changed

5.5 Summary and future Work

This chapter presents the methodology and implementation of a math-based tool, an *Assembly System Configurator* for automotive battery packs. The *Assembly System Configurator* integrates functions of process planning and optimal system configuration generation given the current and possible future generations of products.

Future work for continuous improvement of Configurator includes: test running of more product design cases in *Battery Assembly Configurator* and attempts to calibrate the modeling and decision making.

5.6 Nomenclature

i	Index of tasks; i=1, 2...I;
j	Index of machine types; j=1, 2...J;
$x_{i,j}$	Decision variable;
N_j	Decision variable;
$t_{i,j}$	Processing time of each task i for the jth machine type;
c_{ij}	Operating cost of performing task i on machine type j;
c_j	Amortized annual cost on machine type j;
h_i	The number of repetition required by the throughput requirement;
Th	Actual throughput;
c_0	System cycle time;
ZS	Set of task pairs for type two zoning constraint;

CHAPTER 6

CONCLUSIONS AND FUTURE WORK

6.1 Summary and conclusions

Motivated by the battery assembly problem, several research opportunities in manufacturing system design have been addressed and the related literature and the state of the art of battery module/pack designs and their assembly processes are reviewed. Compared with the previous research on assembly system design and configuration generation, this work has the following novel contributions:

- A new approach for assembly sequence generation is developed by exploiting the product design patterns and identifying assembly hierarchies and sequences. Unlike previous algorithms of assembly sequence generation, the method identifies assembly hierarchies that enable parallel assembly sequences or tasks. Such a characterization of the assembly hierarchy is the key to designing system with the complex configuration with subassembly branches. The efficient, exhaustive computational subassembly decomposition method ensures a truly optimal system can be identified and provides enough candidate systems for special considerations.
- A new method is developed to jointly consider product design, configuration generation, line balancing and equipment selection. Conventional manufacturing system balancing mainly focuses on serial configurations. Our

method deals with balancing of systems with various configurations along with process planning and equipment selection. The results show that non serial configurations with subassembly branches outperform serial configurations, resulting in enhanced system performance (throughput and cost).

- A novel method is developed to design system configurations under stochastic product demand mix. The “drift” problem is mathematically defined and incorporated into the optimization. The method is unique in delivering a system with subassembly branches through joint decision making over possible configurations and all subassembly branches.
- All these methods are implemented in a software package for system configuration, “*Assembly System Configurator*,” developed to integrate functions of process planning and optimal system configuration generation given the current and possible future generations of products.

6.2 Future work

The future research goal is to develop a reconfigurable battery assembly system with hybrid configurations under product variety and uncertainty. Figure 6-1 shows the research accomplishments (Chapter 2-5) and future work or research plan (bolded) which is described below.

- *Novel algorithm of system reconfiguration with known product evolution*: Given information on product design changes, a method is needed to identify system reconfiguration solutions. As shown in Figure 6-2, as the new product type P_{N+1},P_{N+2}…etc are considered, assembly system that was designed for products $P_1 \dots P_N$ will need to be reconfigured by adding/removing/reconnecting machines, reselecting equipment, or adding/changing buffers. An appropriate reconfiguration will be able to reduce reconfiguration cost while ensuring system performances.

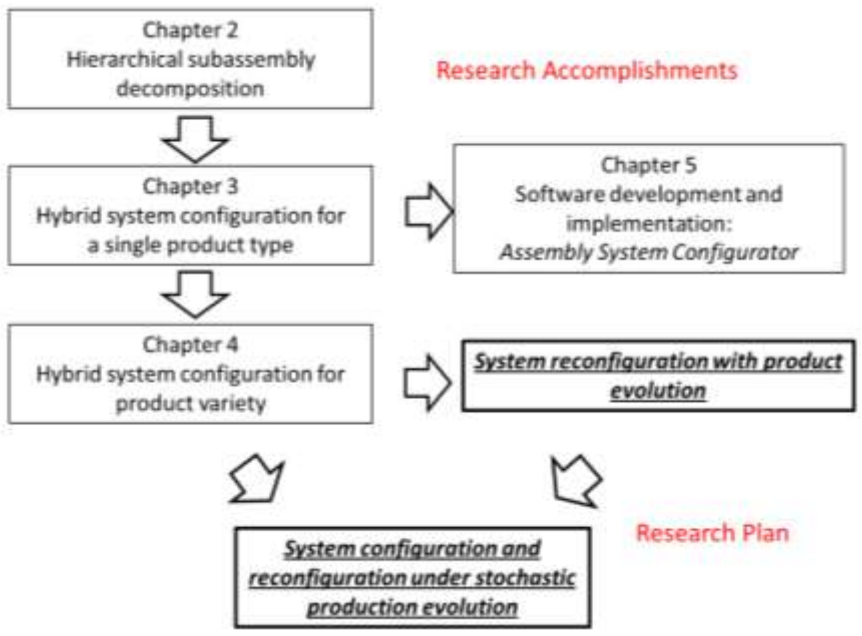
Chapter 2
Hierarchical subassembly decomposition
Research Accomplishments
Chapter 3
Hybrid system configuration for a single product type
Chapter 5
Software development and implementation:
Assembly System Configurator
Chapter 4
Hybrid system configuration for product variety
System reconfiguration with product evolution
System configuration and reconfiguration under stochastic production evolution
Research Plan

Figure 6-1 Research accomplishments and research plan

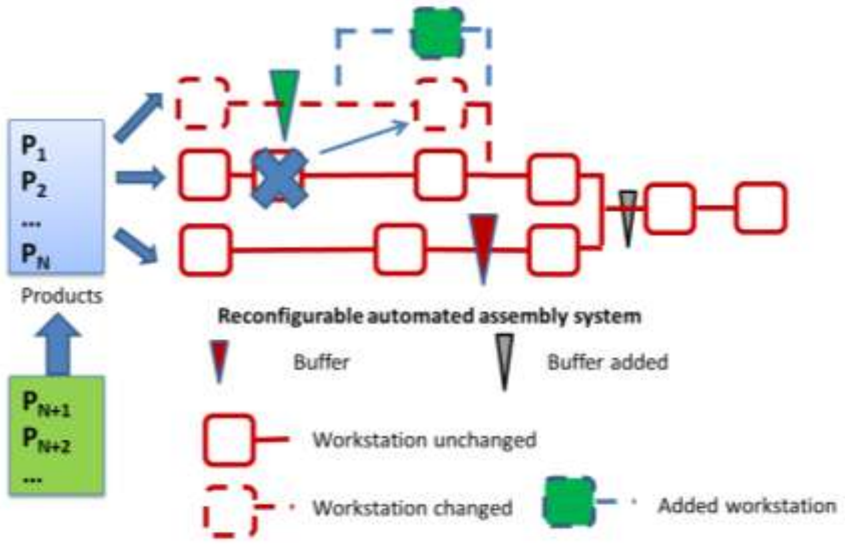

Figure 6-2 System reconfiguration under product evolution

- *New method of system configuration and reconfiguration under stochastic product evolution*: Product design changes are rarely deterministic because of unpredictable market environments, customer orders, and technological advancement. A new method is needed to minimize the total configuration and reconfiguration cost considering the product evolution uncertainty.

BIBLIOGRAPHY

1. K. Aleklett and C.J. Campbell, "The peak and decline of world oil and gas production", Uppsala 2003, www.peakoil.net

2. D. Linden and T.B. Reddy, *Handbook of Batteries*, 2002, McGraw-Hill, New York

3. Y. Koren and M. Shpitalni, "Design of reconfigurable manufacturing systems", *Journal of Manufacturing Systems*, Vol 29, Issue 4, Oct 2010, pp 130-141

4. G. Berdichevsky, K. Kelty, J.B. Straubel and E. Toomre, "The Tesla Roadster Battery System", *Tesla Motors*, Aug 16, 2006

5. S. Li, H. Wang, S. J. Hu, Y.T. Lin and J. Abell, "Review of high capacity battery module/pack designs for electric vehicles and their implications to assembly process automation", *Proceedings of ASME (American Society of Mechanical Engineers) – MSEC 2010 Manufacturing Science Engineering Conference (MSEC)*, Oct 12-15, 2010, Erie, PA

6. Http://gm-volt.com/2010/03/26/gm-exec-gen-3-voltec-battery-to-have-shortened-lifespan-simpler-shape-and-be-offered-in-smaller-ranges/, GM Exec: Gen 3 Voltec Battery to Have Shortened Lifespan, Simpler Shape, and be Offered in Smaller Ranges, Accessed July 16th, 2012

7. http://www.batteryuniversity.com/parttwo-34.htm, Accessed July 16th, 2012

8. http://www.prba.org/, The rechargeable battery association, Accessed July 16th, 2012

9. J. Kurfer, M. Westermeier, and G. Reinhart, “Cell stacking process of high-energy lithium-ion cells”, *Proceedings of the 4th CIRP conference on assembly technologies and systems*, May 20-22, 2012, Ann Arbor, MI

10. A. Tornow and A. Raatz, “Conceptual DFA method for electric vehicle battery systems”, *Proceedings of the 4th CIRP conference on assembly technologies and systems,* May 20-22, 2012, Ann Arbor, MI

11. S.J. Hu, J. Ko, L. Weyand, H.A. ElMaraghy, T.K. Lien, Y. Koren, H. Bley, G. Chryssolouris, N. Nasr, and M. Shpitalni, “Assembly System Design and Operations for Product Variety”, *CIRP Annals–Manufacturing Technology*, 2011.05.004

12. W. Eversheim, I. Abels, “Simulationsgestützte Personaleinsatzplanung in Der Pkw-Endmontage (Simulation-Based Staff Planning in the Field of Final Assembly of Cars)” in J. Bayer (Ed.) et al., *Simulation in Der Automobilproduktion*, Springer, 2003, pp. 61–70

13. L. Weyand, “Risikoreduzierte Endmontageplanung Am Beispiel Der Automobilindustrie (Risk-Reduced Final Assembly Planning in the Automotive Industry)”, Dr. -Ing. Dissertation. Universität des Saarlandes, Germany

14. S. Li, H. Wang, S.J. Hu, “Assembly system configuration design for a product family with tree type assembly liaisons,” submitted to *ASME Journal of Manufacturing Science and Engineering*, 2012

15. Y.T. Lin, H. Wang, C.H. Shao, S. Li, S.J. Hu, “Computational assembly task and sequence generation for battery stack assembly system with hybrid

configurations," submitted to *IEEE Transactions on Automation Science and Engineering*, 2012

16. S. Li, H. Wang, S.J. Hu, Y.T. Lin, J. Abell, "Automatic generation of assembly system configuration with equipment selection for automotive battery manufacturing," *Journal of Manufacturing Systems*, Volume 30, Issue 4, Oct 2011, Pages 188-195
17. S. Li, Y.T. Lin, H. Wang, S. Yang, C. Chen, S.J. Hu, J. Abell, "An assembly system configurator for automotive battery packs," *the 10th International Conference on Frontiers of Design and Manufacturing*, June 10-12, 2012, Chongqing, China
18. A. Bourjault, "Contribution a nue approche methodologique de l' assemblage automatise: Elaboration automatique des sequences operatiores", Thesis to obtain Grade de Docteur es Sciences Physiques at L' Universite de Franche-Comte, 1984
19. T.L. De Fazio and D.E. Whitney, "Simplified generation of all mechanical assembly sequences", *IEEE J. Robot. Autom.*, 3, 640-658, 1987
20. L.S. Homem de Mello and A.C. Sanderson, "Representations of mechanical assembly sequences", *IEEE Trans Robotic Autom*, 7, 211-227, 1991
21. M. Santochi and G. Dini, "Computer aided planning of assembly operations: the selection of assembly sequences", *Robot CIM-Int Manuf*, 9, 439-446, 1992
22. T. Gu, Z. Xu and Z. Yang, "Symbolic OBDD representations for mechanical assembly sequences", *Comput Aided Des*, 40, 411-421, 2008

23. F. Demoly, X.T. Yan, B. Eynard, L. Rivest and S. Gomes, “An assembly-oriented design framework for product structure engineering and assembly sequence planning”, *Robotics and Computer-integrated manufacturing*, 27, 33-46, 2011

24. Y.Q. Lee and S.R.T. Kumara, “A scheme for mechanical assembly design and assembly line layout conceptualization”, *Computers in Industrial Engineering*, 27, 261-264, 1994

25. U. Roy, P. Banerjee and C.R. Liu, “Design of an automated assembly environment”, *Computer-Aided Design*, 21, 561-569, 1989

26. F. Webbink and S.J. Hu, “Automated Generation of Assembly System-Design Solutions,” *IEEE Transactions on Automation Science and Engineering*, Vol. 2, pp. 32-39, 2005

27. H. Wang, J. Ko, X. Zhu, and S.J. Hu, "A Complexity Model for Assembly Supply Chains and Its Application to Configuration Design," *ASME Transactions on Journal of Manufacturing Science and Engineering*, 13, doi:10.1115/1.4001082, 2010

28. J.A. Abell, "Generating Production Sequences for an m-Machine Robotic Workcell," *Proceedings of Autofact '98*, Society of Manufacturing Engineers, September 1998

29. D.E. Knuth, *The Art of Computer Programming, Volume 4, Fascicle 3: Generating All Combinations and Partitions*, Addison Wesley Professional, 2005

30. R.P. Stanley, *Enumerative Combinatorics*, Vol. 1, Cambridge Press, 1997

31. D.E. Knuth, *The Art of Computer Programming, Volume 4, Fascicle 4: History of Combinatorial Generation*, Addison Wesley Professional, 2005

32. T.H. Cormen, C.E. Leiserson, R.L. Rivest, and C. Stein, *Introduction to Algorithms*, Second Edition. MIT Press and McGraw-Hill, 2001. ISBN 0-262-03293-7. Section 22.3: Depth-first search, pp. 540–549.

33. R.G. Askin, C.R. Standridge, *Modeling and Analysis of Manufacturing System*, Wiley, New York, 1993

34. D.E. Whitney, *Mechanical Assemblies: Their Design, Manufacture, and Role in Product Development*, Oxford University Press, New York, 2004

35. Y. Koren, S.J. Hu and T.W. Weber, "Impact of manufacturing system configuration on performance", *CIRP Annals-Manufacturing Technology*, 47, 369-372, 1998

36. R.G. Askin and M. Zhou, "A parallel station heuristic for the mixed-model production line balancing problem", *International Journal of Production Research*, 35, 3095-3105, 1997

37. J. Bukchin and J. Ruvinovitz, "A weighted approach for assembly line design with station paralleling and equipment selection", *IIE Transactions*, 35, 73-85, 2003

38. T. Freiheit, M. Shpitalni, and S.J. Hu, "Throughput of paced parallel-serial manufacturing lines with and without crossover", *Journal of Manufacturing Science and Engineering-Transactions of the ASME*, 126, 361-367, 2004

39. M.K. Jeong, M. Perry and C. Zhou, "Throughput gain with parallel flow in automated flow lines", *IEEE Transactions on Automation Science and Engineering*, 2, 84-86, 2005

40. P. Pinto, D.G. Dannenbring and B.M. Khumawala, “A branch and bound algorithm for assembly line balancing with paralleling”, *International Journal of Production Research*, 13, 183-196, 1975

41. D.S. Cochran, D.C. Dobbs, “Evaluating manufacturing system design and performance using the manufacturing system design decomposition approach”, *Journal of Manufacturing Systems*, 20, 390-404, 2002

42. J. Ko, S.J. Hu, “Balancing of manufacturing systems with complex configurations for delayed product differentiation”, *International Journal of Production Research*, 46, 4285-4308, 2006

43. I. Baybars, “A survey of exact algorithms for the simple assembly line balancing problem”, *Management Science* 32, 909-932, 1986

44. P.A. Pinto, D.G. Dannenbring, B.M. Khumawala, “Assembly line balancing with processing alternatives: an application”, *Management Science* 29, 817–830, 1983

45. S.C. Graves, B.W. Lamar, “An integer programming procedure for assembly system design problems”, *Operations Research* 31, 522-545, 1983

46. S.C. Graves, C. Holmes Redfield, “Equipment selection and task assignment for multiproduct assembly system design”, *International Journal of Flexible Manufacturing Systems* 1, 31-50, 1988

47. J. Bukchin, M. Tzur, “Design of flexible assembly line to minimize equipment cost”, *IIE Transactions* 32, 585-598, 2000

48. A. Agnetis, A. Ciancimino, M. Lucertini, M. Pizzichella, “Balancing flexible lines for car components assembly”, *International Journal of Production Research*, 33, 333-350, 1995

49. R. Rachamadugu, B. Talbot, "Improving the equality of workload assignments in assembly lines", *International Journal of Production Research*, 29, 619-633, 1991

50. P.M. Vilarinho and A.S. Simaria, "A two-stage heuristic method for balancing mixed-model assembly lines with parallel workstations", *International Journal of Production Research*, 40,1405-1420, 2002

51. T.W. Simpson, Z. Siddique, and J.X. Jiao, "*Product platform and product family design: methods and applications*," Boston, MA: Springer Science & Business Media, LLC. 2006

52. M.H. Meyer and A.P. Lehnerd, "*The power of product platforms: building value and cost leadership*," Free press, New York, NY. 1997

53. X.F. Zha and R.D. Sriram, "Platform-based product design and development: knowledge support strategy and implementation," *Intelligent knowledge-based systems*, Volume I., 3-35, 2005

54. S. Sanderson and M. Uzumeri, "Managing product families: The case of the Sony Walkman," *Research Policy,* 24(5): 761-782, 1995

55. K. Sabbagh, "*Twenty first century jet – The making and marketing of the Boeing 777*," Scribner, New York, NY, 1996

56. D.F. Baldwin, T.E. Abell, M. Lui, T.L. De Fazio, and D.E. Whitney, "An Integrated Computer Aid for Generating and Evaluating Assembly Sequences for Mechanical Products," *IEEE Transactions on Robotics and Automation,* Volume 7, number 1, pp. 78–94, 1991

57. C.K. Choi, X.F. Zha, T.L. Ng, and W.S. Lau, "On the Automatic Generation of Product Assembly Sequences," *International Journal of Production Research*, Volume 36, number 3, pp. 617–633, 1998

58. S. Kanai, H. Takahashi, and H. Makino, "ASPEN: Computer-Aided Assembly Sequence Planning and Evaluation System Based on Predetermined Time Standard," *CIRP Annals – Manufacturing Technology*, Volume 45, number 1, pp. 35–39, 1996

59. P.K. Khosla and R. Mattikali, "Determining the Assembly Sequence from a 3-D Model," *Journal of Mechanical Working Technology*, Volume 20 Journal Article, pp. 153–162, 1989

60. C. Becker and A. Scholl, "A survey on problems and methods in generalized assembly line balancing," *European Journal of Operational Research*, 168 (2006) 694-715, 2006

61. J. Bautista, J. Cano, "Minimizing Work Overload in Mixed-Model Assembly Lines", *International Journal of Production Economics*, 112 (1) (2008), pp. 177–191

62. S. Matanachai, C.A. Yano, "Balancing Mixed-Model Assembly Lines to Reduce Work Overload", *IIE Transactions*, 33 (1) (2001), pp. 29–42

63. P.Y. Tambe, "*Balancing Mixed-Model Assembly Line to Reduce Work Overload in a Multi-Level Production System*", master's thesis, 2005

64. W. Xu, T. Xiao, "Mixed Model Assembly Line Balancing Problem with Fuzzy Operation Times and Drifting Operations", *Winter Simulation Conference (WSC 2008)*, Miami, Florida, USA, 7–10 December (2008), pp. 1752–1760

65. X. Zhao, K. Ohno, and H.S. Lau, “A Balancing Problem for Mixed Model Assembly Lines with a Paced Moving Conveyor”, *Naval Research Logistics*, 51 (3) (2004), pp. 446–464

66. N. T. Thomopoulos, “Mixed-model line balancing with smoothed station assignments”, *Management Science*, 16, 1970, 593-603.

67. H. Gokcen and E. Erel, “Binary integer formulation for mixed-model assembly line balancing problem”, *Computers and Industrial Engineering*, Vol. 34, No. 2, pp. 451-461, 1998

68. J. L. C. Macaskill, “Production line balances for mixed-model lines”, *Management Science*, 19, 1972, 423-433

69. A. K. Chakravarty and A. Shtub, “Balancing mixed model lines with in-process inventories”, *Management Science*, 31, 1985, 1161-1174

70. S. Lee, T.H. Kim, and S.J. Hu, Joining technologies for automotive lithium ion battery manufacturing: a review, *ASME 2010 International Manufacturing Science and Engineering Conference*, 2010, pp 541-549

71. M.C. Bethesda and B.B. Potomac, Method of treating printed computer paper, US4573409, 1986

72. R. Dufour, Automatic Stacking Machine, US3593624, 1971

73. J.B. Cole, Split-Stream Collating Apparatus, US3421758, 1969

74. H. Hansen, Paper Accumulating Device, US2697388,1954

75. P.L. McGilvery, Automatic Cassette Wrapping and Assembly Machine, US 6186208 B1, 2001

76. S., Yang, S. Li, H. Wang, C. Chen, S.J. Hu, Y.T. Lin, Analysis and control of the Li-ion battery assembly line based on simulation models, Manuscript in preparation

77. A. Law, *Simulation modeling and analysis*, McGraw-Hill Publishing Co., 4th edition, 2006